

1066

Reference Commercial High-Level Waste Glass and Canister Definition

S. C. Slate
W. A. Ross
W. L. Partain

September 1987

Prepared for the U.S. Department of Energy
under Contract DE-AC06-76RLO 1830

Pacific Northwest Laboratory
Operated for the U.S. Department of Energy
by Battelle Memorial Institute



PNL 8888

This report was prepared as an account of work sponsored by the United States Government. Neither the United States nor the Department of Energy, nor any of their employees, nor any of their contractors, subcontractors, or their employees, makes any warranty, express or implied, or assumes any legal liability or responsibility for the accuracy, completeness or usefulness of any information, apparatus, product or process disclosed, or represents that its use would not infringe privately owned rights.

The views, opinions and conclusions contained in this report are those of the contractor and do not necessarily represent those of the United States Government or the United States Department of Energy.

PACIFIC NORTHWEST LABORATORY
operated by
BATTELLE
for the
UNITED STATES DEPARTMENT OF ENERGY
Under Contract DE-AC06-76RGO 1830

Available from
National Technical Information Service
5285 Port Royal Road
Springfield, Virginia 22151

Microfilm \$3.00

	NTIS
	Springer-Verlag
001-075	\$3.00
072-050	\$2.50
073-007	\$2.50
074-104	\$2.00
075-123	\$2.50
076-151	\$2.50
077-113	\$2.00
078-200	\$3.00
079-123	\$3.25
080-150	\$3.50
081-123	\$10.75
082-150	\$11.00

REFERENCE COMMERCIAL HIGH-
LEVEL WASTE GLASS AND
CANISTER DEFINITION

S. C. Slate
W. A. Ross
W. L. Partain (a)

September 1981

Prepared for
the U.S. Department of Energy
under Contract DE-AC06-76RLO 1830

Pacific Northwest Laboratory
Richland, Washington 99352

(a) Sage Technical Associates, Richland, Washington

ABSTRACT

This report presents technical data and performance characteristics of a high-level waste glass and canister intended for use in the design of a complete waste encapsulation package suitable for disposal in a geologic repository. The borosilicate glass contained in the stainless steel canister represents the probable type of high-level waste product that will be produced in a commercial nuclear-fuel reprocessing plant. Development history is summarized for high-level liquid waste compositions, waste glass composition and characteristics, and canister design. The decay histories of the fission products and actinides (plus daughters) calculated by the ORIGEN-II code are presented.

CONTENTS

ABSTRACT	iii
INTRODUCTION	1
CONCLUSIONS	3
HIGH-LEVEL LIQUID WASTE DESCRIPTION	7
BACKGROUND OF FUEL REPROCESSING PLANT FLOWSHEETS	7
The PUREX Process	8
The HLLW Stream	8
The ILLW Stream	9
Fuel-Reprocessing Gaseous Effluents	9
Potential Variations in FRP Flowsheets	10
FUEL EXPOSURE HISTORY	13
REFERENCE HLLW DESCRIPTION	15
HIGH-LEVEL WASTE GLASS DESCRIPTION	19
GLASS FORMULATION	20
Waste Composition	20
Waste Loading Considerations	20
Alumino-Silicate Waste Glasses	21
Borosilicate Waste Glasses	22
EFFECTS OF PROCESSING CONDITIONS	23
Processing Temperature and Melter Residence Time	23
Volatility During Melting	24
Corrosion During Melting	24
Oxidation-Reduction During Melting	24

PROPERTIES OF RADIOACTIVE WASTE IN CANISTERS	25
Physical and Mechanical Properties of Waste Glass	25
THERMAL EFFECTS AND DEVITRIFICATION	30
Volatility	30
Devitrification	31
Phase Separation	35
LEACHING	36
RADIATION EFFECTS	38
Stored Energy	40
Density Change	40
Radiation Effects on Devitrification and Metamictization	40
Radiation Effects on Leach Rates	41
Helium Behavior	42
Transmutation	43
HIGH-LEVEL WASTE CANISTER DESCRIPTION	47
BACKGROUND	47
TYPE OF GLASS VITRIFICATION PROCESS	48
MATERIAL REQUIREMENTS	49
Process Temperature	50
Creep Properties	50
Canister Oxidation	50
Corrosion from Molten Glass	51
Stress Corrosion Cracking	52
Residual Stress	53
Surface Decontamination	55

Lid Welding	56
Impact Damage	56
Retention of Geometry	56
Cost	57
Reference Material	57
DESIGN DESCRIPTION	57
Size	57
Closure	59
Design Parameters	60
THERMAL ANALYSIS	60
RADIATION ANALYSIS	67
REFERENCES	73
ACKNOWLEDGMENTS	77
APPENDIX A--ORIGEN-II CALCULATIONS	A.1

FIGURES

1	Viscosity of Typical Waste Glass	26
2	Effect of Impact Velocity on Fraction of Respirable Particles Formed	28
3	Thermal Conductivity of Waste Glasses	29
4	Volatility of Waste Constituents	31
5	Photomicrographs of Vitreous and Devitrified Waste Glass 77-260 .	33
6	Leach Behavior as a Function of Devitrification for Three Representa- tive Borosilicate Waste Glasses	34
7	Comparison of Static and IAEA (Simulated Flow) Leach Test Results for a 72-68 Glass	38
8	Radiation-Induced Density Change in Waste Glass	41
9	Isothermal Helium Release from Glass	42
10	Potential Helium Pressure in Waste Glass Containers	44
11	Isochronous Stress-Strain Curves for 304L Stainless Steel at 1050°C	51
12	Isochronous Stress-Strain Curves for Inconel 601 at 1050°C . . .	52
13	Comparison of Material Oxidation Rates at 1000°C	53
14	Corrosion Rate of AISI 304L in PW-4b Glass as a Function of Temperature	54
15	Time-Temperature-Sensitization for Stainless Steel with Various Car- bon Contacts	55
16	Schematic of the Reference HLW Canister	58
17	Schematic of the Twist-Lock Canister Closure	59
18	Canister Emplacement Model for a Salt Repository	64
19	Thermal Response as a Function of Time for a Salt Repository with the Canister Emplacement Model of NWTS-3 (1980)	65
20	Maximum Temperature Profile for a Canister Emplacement in a Salt Repository with the Maximum Isolation Package Model	66

21	Thermal Response as a Function of Time for a Salt Repository with the Maximum Isolation Emplacement Package Model	67
22	Profile of High-Level Waste Canister Dose Rate, mrem/h	71

TABLES

1	Example of the Extremes Possible in HLLW/ILLW from a Fuel Reprocessing Plant	14
2	Composition of Combined HLLW and ILLW Wastes	16
3	Combined HLLW and ILLW in Calcine Form	17
4	Listing of Individual Fission Products and Actinides (Plus Daughters) At Time of Reprocessing	18
5	Typical Waste Glass Compositions	21
6	Typical Thermal Expansion Coefficients of Glasses	30
7	Factors Affecting Leach Rate Measurements	36
8	Leach Rates of Waste Glasses Based on Cesium, Strontium and Europium in a Modified IAEA Test at 25°C	37
9	Time Distribution of Alpha Decay in a Representative Waste Glass	39
10	Radioactive Decay Transmutations That Occur in Waste	45
11	Design Parameters of the HLW Canister	61
12	Canister Decay Heat	61
13	Gamma Source Terms	68
14	Energy Flux at Canister Surface Versus Decay Time	69
15	Dose Rate at Canister Surface Versus Decay Time	69
16	Direct Beam Gamma Spectrum Versus Decay Time	70

INTRODUCTION

This report was written as part of the U.S. Department of Energy's (DOE) Long-Term High-Level Waste Technology Program, which is coordinated by Savannah River Laboratory. The information here is provided as support to the DOE's National Waste Terminal Storage Program administered by Battelle Memorial Institute's Office of Nuclear Waste Isolation. The latter program requires a description of a commercial high-level waste (HLW) canister, which will be used as a reference in the conceptual design of a HLW canister package system suitable for disposal in a geologic repository.

The report is organized into three major sections:

- High-Level Liquid Waste Description--The potential variations in the high-level liquid waste (HLLW) composition are described, and the bases for the selected reference composition are explained.
- Waste Glass Description--The choice of a borosilicate-glass system for waste immobilization is discussed. Physical characteristics and performance data of a HLW glass compatible with the reference HLLW composition are presented.
- High-Level Canister Description--Candidate alloys for the canister are compared. Physical characteristics and performance data for the primary alloy candidates are discussed. In addition, the glass-filled canister is described, and the results of a preliminary thermal analysis and radiation flux analysis of the canister are given.

In the Conclusions section following this Introduction, all technical data that describe the reference commercial-HLW canister are listed for easy reference. Finally, an appendix includes a description of the fission products and actinides (plus daughters) assumed to be in the HLW as calculated by the ORIGEN-II computer code.

CONCLUSIONS

Laboratory research has indicated the practicality of reprocessing fuel for the efficient recovery of uranium and plutonium along with a minimal addition of nonradioactive chemicals. However, a fuel reprocessing plant (FRP) has not demonstrated such a process on a production basis. Since the Allied General Nuclear Services (AGNS) FRP is the most modern United States commercial-fuel reprocessing plant, the HLLW composition described here is based on the flowsheet from this plant. Additional assumptions made in estimating the HLLW composition include 99% recovery of the uranium and plutonium and the combination of the HLLW with the intermediate-level liquid waste (ILLW).

The reference HLW glass chosen for this study is a borosilicate-based composition suitable for the immobilization of the reference HLLW. The reference composition is very similar to a commercial-HLW borosilicate glass (code number 77-260) developed at Pacific Northwest Laboratory (PNL) in 1977. Therefore, the physical and performance data derived for the 77-260 glass is quoted in this study as reference technical data.

Extensive research on canister materials over the past 5 years at PNL indicates that either stainless steel or a high-nickel alloy can serve satisfactorily as the canister material under examined conditions. In this study, stainless steel 304L has been chosen as the reference material since it satisfies the performance criteria of the HLW glass production process and is a lower cost alternative to Inconel, which was also found to be acceptable. (Inconel 601 proved to have better performance in all of the categories evaluated and should be seriously considered if the glass-making process is the in-can melter.) Material characteristics and performance data are summarized for both stainless steel 304L and Inconel 601.

The canister size is primarily determined by the decay heat rate. A thermal analysis indicates that a canister 30 cm in dia and 3 m tall, when filled 90% with glass formed from 5-year-old HLW, will have a maximum centerline temperature of $\sim 150^{\circ}\text{C}$ when stored in a water basin or $\sim 380^{\circ}\text{C}$ when stored in an air-cooled vault. Two different emplacement models were analyzed assuming the repository had an average areal heat loading of 25 W/m^2 (100 kW/acre). The

more complex emplacement model having the objective of maximum isolation yields the highest glass centerline temperature. A maximum glass temperature of $\sim 430^{\circ}\text{C}$ is predicted for 10-year-old waste (after reactor discharge). The maximum temperature occurs shortly after emplacement and falls to $\sim 150^{\circ}\text{C}$ at 100 years. The maximum temperature is acceptable for the glass waste form. The maximum wall temperature for this case is 355°C . Evaluation of the effects resulting from maximum temperatures calculated for overpack and backfill materials was beyond the scope of this document. However, the information in this document can be used in more detailed studies that address these components of the total waste emplacement package.

A radiation flux profile of the filled canister is presented, including sufficient data to permit calculation of radiation dose profiles for various overpack systems and geologic repository configurations.

To simplify use of this document as a reference for a commercial-HLW canister, a summary of the technical data is presented in tabular form below. A detailed list of radionuclides and their decay histories, as calculated by ORIGEN-II, are given in the appendix. Many of the parameters are normalized to the amount of HLW generated due to the reprocessing of spent fuel containing one metric tonne of uranium (MTU).

High-Level Liquid Waste

Composition	HLLW and ILLW are combined. The reference concentration is 620 L/MTU. The complete compositions are given in the HLLW Description Section (Tables 2, 3 and 4).
Activity	4.476×10^5 Ci/MTU; 722 Ci/L (at 5 yr after reactor discharge)
Decay Heat	1624 W/MTU; 2.62 W/L (at 5 yr after reactor discharge)

	<u>Constituents</u>	<u>Oxide Form, kg/MTU</u>
Calcine (Some Vitrification Processes have a Separate Calcination Stage) TOTAL	Fission Products	34.7
	Actinides Plus Daughters	12.36
	Nonradioactive Chemicals	39.81
		<u>86.87</u>

High-Level Waste Glass

PNL Identification

The reference glass is very similar to HLW glass 77-260 developed for the AGNS FRP flowsheet

Composition

<u>Constituents</u>	<u>wt%</u>
SiO ₂	36
B ₂ O ₃	9
P ₂ O ₅	2
Alkali Metal Oxides	13
Alkaline Earth Oxides	1
Fe ₂ O ₃ , Cr ₂ O ₃ , NiO	1
Al ₂ O ₃	2
TiO ₂	6
CuO	3
Gd ₂ O ₃	10
Fission Product Oxides	12
Actinide Oxides	5

Waste Loading

The oxides from the HLLW constitute 31 wt% of the glass

Quantity

277 kg/MTU; 89 L/MTU

Activity

1616 Ci/kg; 5029 Ci/L (at 5 years after reactor discharge)

Decay Heat

5.9 W/kg; 18.3 W/L (at 5 years after reactor discharge)

Density

3.1 g/c³

Process Melting Temperature

1050° to 1150°C

Softening Temperature

575° to 650°C (viscosity = 4 x 10⁷ poise)

Transition Temperature

500° to 550°C (viscosity = 10¹³ poise)

Temperature Limit to Prevent Devitrification

500°C

Leach Rate

1.0-2.0 x 10⁻⁶ g/cm²-d (25°C water)

Thermal Conductivity

0.8-1.3 W/m-°K from 0° to 500°C

Heat Capacity

700 to 800 J/kg-°C (estimated)

Thermal Expansion

1 x 10⁻⁵/°C

Compressive Tensile Strength	4×10^7 Pa
Young's Modulus	7×10^{10} Pa (estimated)
<u>HLW Canister</u>	
Material	Stainless Steel 304L
Dimensions	3-m high by 31.1-cm-ID cylinder; 6.35-mm wall thickness (12-in. Schedule 20 Pipe)
Bottom	Slightly reversed dished flanged tank end
Top	Flanged only tank head
Closure	PNL "twist-lock"
Fins (internal)	Required for ICM process but not for JHGM process. Capacities given below assume no fins.
Empty weight	160 kg \pm 5%
Fill height	90%
Glass content	200 L; 630 kg; 2.28 MTU HLW (all \pm 5%)
Weight when filled	790 kg \pm 5%
Activity	1.02×10^6 Ci (at 5 years from reactor discharge) 6.58×10^5 Ci (at 10 years from reactor discharge)
Decay Heat	3.71 kW (at 5 years from reactor discharge) 2.2 kW (at 10 years from reactor discharge)
Maximum Canister Centerline Temperature in a Repository	430°C (at 10 years from reactor discharge)

HIGH-LEVEL LIQUID WASTE DESCRIPTION

The development of solid HLW forms has been complicated by the many possible variations in the composition of the HLLW. HLLW accumulated during the processing of fuel from defense reactors is quite different from the HLLW expected in a commercial fuel-reprocessing plant. Defense fuel has a much lower exposure and, consequently, has lower concentrations of fission products, lower radiation levels, and less decay heat per tonne of fuel. Also, defense fuel has been neutralized before storage by the addition of sodium hydroxide which increases the sodium loading in the HLLW. Also contained in the HLLW is the fuel cladding that has been chemically dissolved. Dissolution of Zircaloy cladding requires the use of a fluoride compound. A substantial amount of aluminum was added to HLLW during one of the early reprocessing methods that employed aluminum nitrate as a salting agent. Finally, much of the defense waste has been stored for over 10 years, which has resulted in a decline in radioactivity and decay heat.

On the other hand, only the PUREX process is used in the reprocessing of commercial fuel. Thus, the fuel cladding is separated out as a solid, intermediate-level waste. At one extreme, the PUREX process can be modified to produce an HLLW that contains essentially only the fission products, unrecovered uranium/plutonium losses and the other actinides. At the other extreme, the PUREX process can require the addition of chemicals to the HLLW for oxidation-state control and neutron poisoning, and the HLLW can be combined with the ILLW for solidification as a combined high-level waste form. However, even in this latter case where the addition of nonradioactive chemicals increases the amount of waste to be solidified (which in effect dilutes the radioactivity), the commercial HLW has many times the decay heat and radioactivity of the defense waste on a volume or mass basis.

BACKGROUND OF FUEL REPROCESSING PLANT FLOWSHEETS

The HLLW composition depends strongly on the particular variation of the PUREX process used to dissolve the fuel and recover the uranium and plutonium.

A summary of variations in process flowsheets is given here primarily to give researchers in waste-form development a practical view of the potential variations in HLLW composition.

The PUREX Process

The PUREX process is one of several solvent extraction processes for separating the uranium and plutonium products from the fission products and other actinides. The process is characterized by the use of a solution of tributylphosphate (TBP), usually 30 vol% in a hydrocarbon diluent, as the solvent, and the use of nitric acid as the salting agent. Several cycles are required to achieve adequate decontamination (removal of other actinides and fission products) and separation of the uranium and plutonium products. The solvent is reused and a substantial fraction of the nitric acid is recovered by a denitration/ NO_x absorption process.

The PUREX process has many variations, and the most important factors in the subsequent HLW treatment process are:

- the fraction of uranium and plutonium recovered during reprocessing
- type of chemical additives used to adjust plutonium valence states
- need for soluble neutron poison for prevention of criticality.

The HLLW Stream

The HLLW stream consists of the 2 to 3 M HNO_3 aqueous stream from the first separation column of the PUREX process. This aqueous stream normally contains 99% of both the fission products and actinides other than the uranium and plutonium. Approximately one percent or less of the uranium and plutonium from the fuel will normally be unrecovered and contained in the HLLW.

In addition to the fission products and actinides, the HLLW stream will contain small amounts of zirconium shear fines, activated corrosion products, phosphates from degraded solvent, and potentially large amounts of a neutron poison (gadolinium or cadmium).

Typically, 5% to 10% of the cations expected to be in the HLLW may actually exist in an insoluble form. These solids would consist of the zirconium cladding shear fines and alloys formed by noble metal fission products with some of the actinides.

The HLLW stream is normally sent through a concentration step that may increase the molarity to a range of 5 to 7 M HNO_3 . The stream is then stored in tanks until it is sent through the HLLW solidification process.

As part of preprocessing before solidification, the HLLW may undergo denitration by the addition of a reducing agent (e.g., formic acid) to reduce the volatilization of ruthenium during the solidification process.

The ILLW Stream

The ILLW stream consists of aqueous waste from the second and third uranium and plutonium cleanup cycles, aqueous waste from the solvent regeneration, and process vessel flushes.

The amount of ILLW generated increases during process startup and shutdown. Decontamination flushes in preparation for maintenance will introduce additional chemicals into the ILLW stream.

The ILLW stream composition is generally concentrated before its transfer to the storage tank. The ILLW is generally stored with a nitric acid molarity of 1 to 3 M.

The chemical composition of the ILLW is determined principally by the amount of uranium loss to this stream, the sodium nitrite introduced for Pu valence control, and the chemicals (e.g., sodium carbonate, sodium hydroxide, hydrazine carbonate, potassium permanganate, and manganese dioxide) used to clean up the solvent.

Fuel-Reprocessing Gaseous Effluents

Several radionuclides are released to the process offgas during fuel reprocessing and waste solidification. Under currently proposed regulations, essentially all of these gaseous or volatile radionuclides will have to be trapped in the offgas cleanup system. Some waste-treatment flowsheets call for immobilizing the various adsorber/reaction bed materials by combining them with

the HLW during solidification. Examples of these adsorber beds are silver zeolite for iodine trapping, silica gel or ferric oxide for ruthenium tetroxide adsorption, molecular sieves for krypton and carbon dioxide (C-14), calcium carbonate for carbon dioxide (C-14), and desiccant for water vapor (H-3 in a fuel voloxidation step).

It would be difficult to melt most of these adsorber/reaction beds in the glass without releasing the volatiles, with the possible exceptions of the ruthenium adsorber beds. Therefore, the reference flowsheets developed in this study assume that these adsorber/reaction beds will be encapsulated separately and disposed of as intermediate-level solid wastes.

Potential Variations in FRP Flowsheets

The descriptions of the HLLW stream and the ILLW stream have indicated many of the process alternatives that have been developed for the PUREX process. A list of the major alternatives with a brief description of each is given here:

1. Dissolution of wire baskets containing sheared fuel segments. The Western New York Nuclear Service Center (WNYNSC) FRP transported the sheared fuel segments to the dissolvers in wire baskets that were dissolved with the fuel. This contributed a significant amount of iron to the HLLW stream.
2. Type of fuel cladding--Zircaloy or stainless steel. All of the domestic light-water reactor (LWR) cores are currently utilizing Zircaloy cladding. However, some of the early cores now in storage utilized stainless steel cladding. A fraction of the stainless steel will dissolve, resulting in an addition of iron to the HLLW, as well as some chromium and nickel.
3. Use of a soluble neutron poison (gadolinium or cadmium). Both the Allied-General Nuclear Services (AGNS) plant and the conceptual FRP design by E. I. duPont Nemours Co. (1978) require the use of gadolinium for criticality control. The concentration of gadolinium required by these designs ranges from 10 to 25 wt% of the cations in

the HLLW plus ILLW. The Exxon Nuclear Co. (1977) design used a criticality safe dissolver and avoided the need for chemical additives.

4. The uranium-plutonium recovery efficiency. FRP flowsheet specifications generally guarantee 99% recovery of the uranium and plutonium. In practice, higher recoveries are expected and 0.5% entrainment is commonly used in HLLW flowsheet assumptions. Uranium and plutonium can also be entrained in the ILLW.
5. The chemicals used to oxidize and reduce the plutonium during the uranium-plutonium product separation stage and in subsequent cleanup stages. Ferrous sulfamate has commonly been used to reduce the plutonium in the partitioning column at defense reprocessing plants and at WNYNSC. This introduces both iron and sulfate to the waste stream and, therefore, its use has not been considered in recent designs. Two alternatives to the use of ferrous sulfamate are: 1) the use of U(IV), which is prepared by electro-reduction (either in-situ or externally), and 2) the use of hydroxylamine nitrate. Adoption of either of these alternatives would substantially lower the amount of nonradioactive chemicals in the HLLW and ILLW.

Sodium nitrite has been commonly used to oxidize the plutonium from Pu(III) nitrate to Pu(IV) nitrate. Use of the sodium nitrite introduces the sodium into the ILLW stream. There are alternatives to the use of sodium nitrite that do not add inerts to the waste streams. These are NO_2 gas or electrolytic oxidation.

6. The combination of HLLW and ILLW before solidification. The Technology for the Management of Commercially Generated HLLW (U.S. DOE 1979) and the Final Environmental Impact Statement on Commercial HLLW (U.S. DOE 1980) were based on solidification of separate HLLW and ILLW streams. However, the ILLW is a transuranic (TRU) waste (contains greater than 10 nanocuries of alpha-emitting actinides other than uranium per gram of waste) and will have to be disposed of at a

repository even if solidified separately. Therefore, some HLLW flow-sheets call for the combination of ILLW with HLLW for waste solidification.

7. Chemicals used to wash the PUREX solvent. TBP and the hydrocarbon diluent are slowly degraded by a combination of acid hydrolysis and radiolytic reaction; the latter is the predominant mode. Higher burnup of the fuel and reprocessing at shorter cooling periods increase the rate of degradation. The acidic breakdown products of TBP are usually removed by washes with an alkali such as sodium carbonate and sodium hydroxide. The disadvantage of these wash solutions is the introduction of the sodium into the ILLW. Hydrazine carbonate is a possible alternate that introduces no solid residue. Potassium permanganate is sometimes used to oxidize the fission products and actinide complexants that have formed in the presence of degraded solvent and diluent. Manganese dioxide beds are then used to filter out these complexants. This practice introduces the potassium ion and manganese dioxide to the ILLW stream.
8. Solvent and phosphate in the ILLW. The ILLW will contain the degraded products of the TBP solvent and diluent after they have been separated in the solvent cleanup process. The presence of these organics must be considered in any concentration step since there is a potential for formation of explosive complexants consisting of nitrated organics and heavy metals. The end product of solvent oxidation is a phosphate.
9. Detergent in the ILLW. Detergent is introduced into the ILLW as part of vessel decontamination. Sodium and phosphate are the principal ions introduced to the final waste form by the use of detergent.
10. Zircaloy fines in the HLLW. In the fuel-rod shearing process Zircaloy fines are generated. The Zircaloy cladding hulls are separated from the HLLW, but the small fines will normally be entrained in the HLLW stream.

11. Corrosion products (iron, chromium, and nickel). The HLLW and ILLW nitric acid solutions have a small corrosive effect on the stainless steel piping and storage vessels. The corrosion products are assumed to be typical of a 70% iron, 20% chromium, and 10% nickel stainless steel composition.
12. Fluoride in HLLW and ILLW. In general, the use of fluoride is not anticipated in a commercial LWR fuel reprocessing plant. It has been used in a defense reprocessing plant to dissolve a Zircaloy cladding on the metal fuel and the use of hydrofluoric acid may be required to dissolve either LWR fuel or LMFBR fuel having a significant fraction of PuO_2 . If the purified uranium is processed to the UF_6 form at the FRP, some fluoride waste may be sent to the ILLW.
13. Aluminum in the HLLW and ILLW. Aluminum is commonly used to complex the free fluoride if it is present in either the HLLW or ILLW.

As indicated, many of these potential variations in the HLLW and ILLW composition can be controlled by modifying the chemistry of the PUREX process and by changes in the design of the process equipment. Most of the processing experience with the PUREX process has been with defense fuels, and there has not been a great deal of emphasis on reducing the amount of nonradioactive chemicals added to the HLLW in defense fuel reprocessing. The design of a commercial FRP can be expected to strike a balance between the demonstrated defense PUREX technology with its high loading of nonradioactive chemicals in the HLW, and the newer techniques that have been developed in the laboratory that give a very "clean" HLW that contains essentially only fission products, unrecovered U/Pu, and the other actinides. Table 1 lists the extremes that could be expected, which depend upon the process variations discussed above.

FUEL EXPOSURE HISTORY

The fuel that is received for processing at an FRP will have a varying content of radionuclides, which depends primarily on burnup and decay history. In addition, the length and diameter of the fuel pins will vary from one model of reactor to another. For example, the dimensions of BWR fuel and PWR fuel

TABLE 1. Example of the Extremes Possible in HLLW/ILLW from a Fuel-Reprocessing Plant

<u>HLW Constituents, kg of Oxides/MTU</u>			
<u>"Clean" HLLW Only</u>		<u>HLLW/ILLW Combined With Many Chemical Additions to Process</u>	
Fission Products	27.8	Fission Products	27.8
Actinides Plus Daughters	1.9	Actinides Plus Daughters	12.7
Nonradioactive Chemicals	<u>3.6</u>	Nonradioactive Chemicals	<u>83.5</u>
TOTAL	33.3		124.0

are significantly different. These variations in physical dimension complicate the fuel bundle (assembly) disassembly and the fuel shearing operations, but do not greatly affect the fuel dissolution and separation processes.

Fuel with low burnup comes from the initial cores of reactors where fuel is removed when it is only approximately one-third exposed. Other low-burnup fuel is that in fuel pins or fuel assemblies removed early because of damage. Early commercial LWR fuel has been in storage for up to 20 years and has undergone a significant reduction in radioactivity due to radionuclide decay. However, the bulk of stored fuel has a much shorter decay period because of the growth in nuclear electric-power generation.

The maximum burnups currently achieved are ~33,000 to 35,000 MWD/t, with the exception of burnups in some specific tests that are carrying fuel to burnups approaching 50,000 MWD/t. The projected decay time before reprocessing depends on the growth of the reprocessing industry. A single 2000 MTU/yr plant is not sufficient to reduce the fuel backlog and keep up with the discharged fuel from the projected nuclear-power generating plants. Realistically, it appears that spent fuel will have undergone a significant decay period before reprocessing. On the other hand, it is desirable to base HLW package designs on a conservatively short-decay period to avoid underestimating the decay heat. As a compromise, the reference fuel history chosen for this report assumes that the fuel will be reprocessed 5 years after discharge from the reactor and that the HLLW will be solidified at approximately the same time. However, a new FRP design should be based on a system study to determine what the minimum age and

burnup of spent fuel to be handled will be at time of reprocessing. If the HLLW is solidified at approximately the same time it is produced (as opposed to interim tank storage), the waste form may have to take into account the higher activity.

For the purpose of this study, a pressurized-water reactor fuel typical of a current generation Westinghouse reactor (~1180 MWe) was used as input to the ORIGEN-II code (Croff 1980) in order to calculate the yields, activity, decay heat, gamma flux, and neutron flux from the spent fuel.

The fuel was assumed to be irradiated at a specific power of 38.4 MW/MTU for three equal periods of 284 days each, interrupted by two equal cooling (reactor downtime) of 106 days each. This is equivalent to an 80% availability factor. The fuel was specified as 3.1% enriched with a 20 ppm N₂ contamination (important for carbon-14 calculations).

At the time of reprocessing, (assumed to be 5 years after discharge for the purpose of this study), the He, C, N, Ne, Ar, Kr, Xe, Rn, and H are removed from the main ORIGEN-II tables and the decay histories calculated by the code in separate tables. Likewise, 99% of the uranium, plutonium, and iodine are removed from the main tables and the decay histories calculated by the code in separate tables.

REFERENCE HLLW DESCRIPTION

The specific FRP flowsheet chosen as the reference is essentially that of the AGNS FRP at Barnwell, South Carolina. The flowsheet reflects a combined HLLW and ILLW that tends to overestimate the ILLW in steady-state conditions, but which is representative of early plant operation or plant operation with frequent process interruption.

The composition of the combined HLLW and ILLW is given in Table 2. The concentration should be considered as a process variable. A listing of the fission products, actinides (plus daughters), and inert chemicals is given in Tables 3 and 4 on an elemental basis and an oxide basis as they would appear after calcination.

TABLE 2. Composition of Combined HLLW and ILLW Wastes

<u>Composition</u>	<u>Elemental or Ion Bases, kg/MTU</u>
Fission products (less Xe, Kr, I)	24.46
Uranium (0.5% in HLLW plus 0.5% in ILLW)	9.57
Plutonium (0.5% in HLLW plus 0.5% in ILLW)	0.09
Other transuranics	0.88
Soluble poison (gadolinium)	22.40
Iron (estimated corrosion product)	0.8
Chromium (estimated corrosion product)	0.2
Nickel (estimated corrosion product)	0.1
Manganese	0.14
Zircaloy shear fines	0.25
Chloride	0.11
Phosphate	6.70
Sulfate	0.03
Iodine (estimated as 0.5% in HLLW)	0.002
Sodium	5.0
Nitrates (5 <u>M</u> HNO ₃ and 2.2 <u>M</u> salts)	275.9
Hydrogen ion (HNO ₃ is 7 <u>M</u> in HLLW and 2.5 <u>M</u> in ILLW)	3.1
Estimated insolubles (included in above constituents)	12.0
 <u>Characteristics</u>	
Combined waste volume (L/MTU)	620
Total decay heat per MTU (W)	1624
Heat load (W/L)	2.62
Activity level (Ci/L)	722

TABLE 3. Combined HLLW and ILLW in Calcine Form

<u>Compostion</u>	<u>Oxides</u> <u>kg/MTU</u>
Fission products	34.703
Actinides plus daughters	12.360
Nonradioactive chemicals:	
Gd ₂ O ₃	25.827
Fe ₂ O ₃	1.143
Cr ₂ O ₃	0.292
NiO	0.127
MnO ₂	0.221
ZrO ₂	0.338
P ₂ O ₅	5.007
NaSO ₄	0.037
NaCl	0.181
Na ₂ O	6.634
Total Solids	<u>39.807</u> <u>86.870</u>

TABLE 4. Listing of Individual Fission Products and Actinides (Plus Daughters) At Time of Reprocessing

<u>Fission Products</u>	<u>Element, kg/MTU</u>	<u>Oxide(a) kg/MTU</u>
SeO ₂	0.055	0.077
Rb ₂ O	0.339	0.371
SrO	0.800	0.946
Y ₂ O ₃	0.444	0.564
ZrO ₂	3.496	4.723
MoO ₃	3.292	4.938
Tc ₂ O ₇	0.761	1.196
RuO ₂	2.180	2.871
Rh ₂ O ₃	0.464	0.572
PdO	1.402	1.613
Ag ₂ O	0.078	0.085
CdO	0.112	0.128
SnO ₂	0.091	0.116
TeO ₂	0.479	0.599
I	0.002	---
Cs ₂ O ₃	2.472	2.621
BaO	1.578	1.762
La ₂ O ₃	1.200	1.407
CeO ₂	2.327	2.859
Pr ₆ O ₁₁	1.100	1.329
Nd ₂ O ₃	3.968	4.628
Pm ₂ O ₃	0.037	0.044
Sm ₂ O ₃	0.829	0.961
Eu ₂ O ₃	0.143	0.166
Gd ₂ O ₃	<u>0.110</u>	<u>0.127</u>
	27.759	34.703
<u>Actinides Plus Daughters</u>		
U ₃ O ₈	9.566	11.278
NpO ₂	0.438	0.497
PuO ₂	0.087	0.093
Am ₂ O ₃	0.423	0.465
Cm ₂ O ₃	<u>0.025</u>	<u>0.027</u>
	10.539	12.360

(a) Converted to oxide form in a calcination process.

HIGH-LEVEL WASTE GLASS DESCRIPTION

Radioactive waste glasses are formulated by combining a preselected mixture of glass-making additives with the waste. The glass-making additives usually comprise 65 to 85 wt% of the product waste glass. Because of the many different potential formulations possible, waste glass cannot be thought of as a single substance with set properties. It is possible, however, to consider waste glass as belonging to just a few general types, whose properties have a generic similarity, notwithstanding the compositional variations.

The composition selected for a given radioactive waste glass is governed by three factors:

- the constituents of the radioactive waste to be immobilized;
- the vitrification process to be used for the immobilization;
- the properties desired for the immobilized waste product.

A wide range of radioactive wastes are candidates for immobilization as glasses. For this reason, the innate flexibility of glass is a definite advantage. It permits a large number of components to be accommodated in varying concentration ratios.

The major formulation requirement imposed by the vitrification process is that the viscosity of the glass be less than a specified value at the melting temperature. The viscosity of the glass melt is formulated to be less than 200 poise at the operating temperature. The processes can impose certain additional requirements on the glass; for instance, if the process utilizes joule-heating by passage of electric current through the molten glass, then electrical conductivity-versus-viscosity relationships become important. Other process-related considerations include high-temperature volatility, corrosion, and melt homogeneity.

Of the three factors listed above, the most difficult to define is the third. There is general agreement that the properties of the immobilized waste should form an ultimate barrier to release of the contained radioactivity. This is achieved by developing a glass that has a low leach rate, little devitrification, and minimum cracking. However, many of these attributes require

an optimization decision with regard to melting temperature, percent waste loading, volatiles loss during melting, and process complexity.

GLASS FORMULATION

Waste Composition

The HLLW composition is discussed in the preceding section.

Waste Loading Considerations

The variable with the greatest influence on the properties of waste glass is waste loading. Waste loading is the weight percent of the glass product composed of waste components. Obviously, by decreasing the waste loading sufficiently, the concentration of radioactive atoms could be diluted until those atoms were only inconsequential contaminants, without effect on the parent material. Such low waste loadings are inherently undesirable because of increased costs and the multiplication of hazards that would be associated with handling the much larger volumes. Therefore, development has emphasized waste glass with a relatively high waste loading.

Factors that limit the upper waste loading include:

- maximum solubility of waste components in the glass;
- viscosity increase of the molten glass resulting from excess waste loading;
- leach rate increase in the product glass because of excess waste loading;
- excessive glass centerline temperatures during waste canister storage resulting from the presence of too much heat-generating waste;
- excessive canister wall temperatures during waste storage because of the presence of too much heat-generating waste.

When these factors are taken into account, the maximum waste loading in low-melting waste glasses (processing temperature of 950° to 1150°C) is in the range of 25 to 45 wt%. The specified waste loading is typically maintained in the range of 15 to 35 wt to allow processing flexibility.

Contrary to what might be expected, low-melting glasses permit higher waste loadings than do high-melting glasses. High-melting (~1300°C) glasses, including about 95% of commercial glass, and the long-lasting natural rhyolytic obsidians and tektites, contain over 70 wt% SiO₂. This immediately limits waste loading to less than 30 wt%. The limits are actually much lower because of the poor solubility of many waste components in SiO₂. Although only limited investigations have been made, waste loading is probably restricted to 5% to 15% in high-melting glasses.

Alumino-Silicate Waste Glasses

Some of the first waste-glass formulations investigated were of the alumino-silicate type (Goldman 1958). Of particular interest is the Canadian nepheline syenite glass (Table 5). Blocks of this glass were prepared in 1960 and buried a few feet below ground level as bare glass in a swampy area on the Chalk River Atomic Energy Establishment. Leaching of ⁹⁰Sr from these

TABLE 5. Typical Waste Glass Compositions

Oxide	Pyrex	Waste Glass Composition, wt%		
		Borosilicate	Alumino-Silicate	77-260 Study Reference
SiO ₂	81	25-50	33-40	36
B ₂ O ₃	13	9-22		9
P ₂ O ₅		0-2		2
Alkali metal oxides	4	8-19	18-22	13
Alkaline earth oxides		0-6	13-16	1
Fe ₂ O ₃ , Cr ₂ O ₃ , NiO		1-20		1
Al ₂ O ₃	2	0-10	26-30	2
TiO ₂		0-6		6
ZnO		0-22		--
CuO		0-3		3
PbO		0-50		--
Gd ₂ O ₃		0-12		10
Fission products		15-30	5	12
Actinides		2-10	1	5

alumino-silicate glass blocks has been monitored by removing water from nearby test holes (Merritt and Parsons 1964). By 1968 the leach rate had reached a steady-state value of 5×10^{-11} g of glass/cm²-day, a very low rate (Merritt 1977).

An apparent advantage of alumino-silicate waste glasses is their excellent chemical durability. The disadvantages include higher process temperature (1350°C) and lower waste loading.

Borosilicate Waste Glasses

Throughout the world, most of the radioactive waste glasses that are developed to the point of process application are borosilicate formulations (IAEA 1977). Borosilicate glass has long been used industrially and commercially. Pyrex is a borosilicate glass, although Table 5 shows it has quite a different composition from that of typical borosilicate waste glasses. Boron serves two major and desirable purposes in borosilicate waste glasses: 1) it lowers viscosity, and hence, processing temperature; and 2) it increases the solubility of many waste constituents in silica-based glass. For these reasons, most waste glasses, as shown in Table 5, contain from 5 to 15 wt% B₂O₃.

Before 1977, a series of waste glasses was developed for various potential commercial high-level wastes. Four of these glasses, 72-68, 76-68, 76-107, and 77-260, were extensively characterized for some of their properties (Ross et al. 1978). Glass 77-260, which was developed for the waste PW-7c, has been selected as a reference glass for this study since the reference wastes are similar in composition. The composition of 77-260 is shown in Table 5. Considerable data have been generated on the 77-260 composition, and its characteristics will be reported and compared to data on other waste glasses, most notably 76-68. From a review of the characteristics, it would appear that some improvements to this glass are possible and may be desirable if it appears probable that a commercial FRP will produce a HLLW similar to the reference composition given in this report.

EFFECTS OF PROCESSING CONDITIONS

Although waste loading is the factor that most controls glass properties, properties will also be affected significantly by processing parameters. Therefore, any consideration of glass properties must include information on how the glass was made or processed. Significant process parameters include:

- degree of mixing of constituents prior to melting;
- processing temperature;
- degree of melt agitation;
- time at processing temperature;
- materials of construction for melt containment;
- rate of cooling from processing temperature to storage temperature.

Processing Temperature and Melter Residence Time

The liquidus temperature is defined as the maximum temperature at which equilibrium exists between the molten glass and its primary crystalline phase; i.e., at temperatures above the liquidus temperature, the primary crystalline phase is completely soluble in the melt. Waste glasses are usually raised to a temperature of 100°C or more above the liquidus temperature. In a composition as complex as that of waste glasses, there may be minor crystalline phases whose liquidus temperature is not exceeded at the operating temperature. Examples of crystalline phases that may exist in minor concentrations (total less than 5 vol%) at the melting temperature are RuO₂, or ruthenium metal, palladium metal, spinel and CeO₂. All of these are inert crystalline phases and do not affect the quality of the solidified waste glass. Raising the operating temperature as much as 300° to 400°C does not dissolve any of these phases, except CeO₂, which is usually completely dissolved in waste glasses melted above 1200°C.

Waste glasses have relatively low viscosities (5 to 200 poise) at the operating temperature. The low viscosity assists in establishing equilibrium conditions quickly. Experience has shown that a residence time of 2 to 4 hours at the operating temperature is sufficient to produce good-quality waste glass.

Volatility During Melting

Although volatility is minimized by the low melting temperatures used in waste vitrification, some waste constituents do have a significant vapor pressure in the melter. This means that some constituents of HLLW will not be incorporated in the waste glass but will exit with the offgas. In particular, volatiles that could later cause pressurization of the canisters that contain the product glass are removed. The product glass contains less than 0.001 wt% nitrate and 0.2 wt% H₂O.

Another significant constituent that is volatilized is the long-lived fission product ¹²⁹I. It is estimated that about 0.5% of the ¹²⁹I in spent fuel will be in the HLLW. This constituent will be volatilized entirely during vitrification, and the volatilized ¹²⁹I will be scrubbed from the offgas and disposed of separately. Most chloride present in the HLLW will also volatilize during vitrification. Fluoride exhibits a lower volatility and can be incorporated in waste glass; a small fraction may volatilize but it can be recycled. The cesium and ruthenium that are volatilized during melting will be trapped in the offgas system and either recycled in the melter feed or encapsulated separately.

Corrosion During Melting

Waste glass is melted either in ceramic refractory melters or in the metallic canister. The ceramic refractory melters are designed for a lifetime of several years. The corrosion rates are ~0.001 mm/h. The corrosion product concentration is too low to have any effect on waste glass properties. Minor effects on the glass have been noted from corrosion of the metal canister during in-can melting.

Oxidation-Reduction During Melting

Normally, waste glass is in a highly oxidized state because of the nitrate in HLLW. In some situations, it may be desirable to reduce the oxidation potential in waste glass. For instance, at high fission-product loading, liquid-liquid phase separation of a mixed alkali-alkaline earth molybdate salt can occur in borosilicate waste glasses. Reducing the molybdenum to a tetravalent or lower state, or to the metal, prevents phase separation of the

water-soluble molybdate salt. It has been demonstrated that silicon metal added to the melt batch can affect the desired reduction of molybdenum (Ross, Patent 1978). Small amounts of some other constituents of the waste glass melt may also be reduced to the metal when silicon is added. The reduced metal then appears as globules, usually less than 2 mm in diameter, suspended in the solidified glass. The metal globules are alloys, often rich in tellurium, that do not affect the overall properties of the waste glass (Ross et al. 1978).

PROPERTIES OF RADIOACTIVE WASTE IN CANISTERS

Physical and Mechanical Properties of Waste Glass

The physical and mechanical properties of radioactive waste glass are innate properties that may be treated generically. The properties are relatively independent of composition and are of much the same magnitude for most waste glasses.

Viscosity and Softening Point

Waste glasses are generally formulated to have a viscosity ~200 poise at the processing (melting) temperature, which is usually within the range of 1050° to 1150°C. The viscosity of waste glasses as contrasted with that of commercial glasses is shown in Figure 1. The viscosity of the reference glass is the upper limit of the range shown for waste glasses.

Some important properties of waste glass can be related to viscosity. The softening temperature (Littleton softening temperature) of glasses is defined as the temperature at which the viscosity is 4×10^7 poises. This is the temperature above which the glass cannot support its own weight and begins to slump. Cracks in the glass will heal rapidly at the softening temperature, which is about 575° to 650°C for most waste glasses. The glass transition temperature is the temperature at which the viscosity is about 10^{13} poise. For waste glasses, this temperature usually is in the range of 500° to 550°C. As described earlier, glass is plastic above the glass transition temperature and thus is not susceptible to fracture.

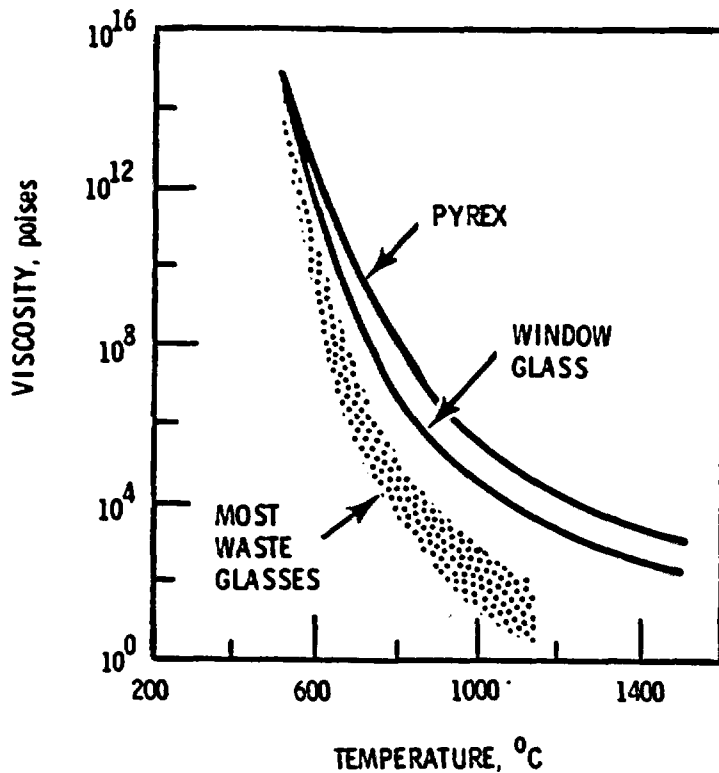


FIGURE 1. Viscosity of Typical Waste Glass

Density

The density of glass is an additive function of the constituents (Elliot 1945). Within limits, the density of a glass can be predicted from empirically derived density factors for each constituent. The density factors are related to atomic weight. Thus, waste glasses containing high loadings of fission products that have higher atomic weights than most usual glass constituents will be more dense than those with low loadings of fission products. Certain special glass constituents, such as zinc or lead, also markedly increase density.

Common commercial soda-lime-silica glass has a density of about 2.5 g/c^3 . Depending on waste composition and waste loading, radioactive waste glass densities are usually in the range of 2.5 to 3.3 g/c^3 . The density of 77-260 is 3.1 to 3.2 g/c^3 .

For a given glass composition, the density of the final product may vary over 0.1 g/c^3 depending on the time-temperature curve of its cooling through the transformation range.

Mechanical Properties

The strength properties of glass are more a function of surface condition and previous glass thermal history than they are of composition. Specific mechanical property data for 77-260 glass have not been determined. It is possible, however, to use data obtained from other glasses to obtain reasonable estimates. Tensile strengths determined by a diametral compression test for two different waste glasses have been found to be 51 MPa (Chick et al. 1980) and 37 MPa (Bunnell 1979). The latter measurement reported a standard deviation of 7 MPa. Theoretical calculations of tensile strength of glasses give values of ~7000 MPa. The significant difference between measured and theoretical values demonstrates the effects of surface condition and internal defects on glass strength.

Young's modulus is generally insensitive to composition or surface condition and is found to be about 7×10^4 MPa for glass (Shand 1958). Other moduli values can be calculated from this value.

Impact Behavior

Fractures increase the surface area, and the amount of activity released in a leaching situation may be proportional to the exposed surface area. However, this exposed area is less than the total geometric area of all the glass pieces. Also, the fractures may produce a small fraction of less than 10- μ m-dia particles, which are respirable.

Impact tests of waste glass are usually either a weight dropped on a glass specimen, or the glass specimen itself dropped onto an unyielding surface. The most comprehensive impact tests on waste glass yet performed are described by Smith and Ross (1975). In these tests, the glass was cast in stainless steel canisters either 5-cm in dia by 10 cm long or 16.8 cm in dia by 132 cm long. The large canisters were dropped onto a concrete pad from heights up to 9 m (maximum impact velocity equalled 13.4 m/s). The smaller canisters were released in the path of a 35-kg granite block mounted on a rotating arm. Impact velocities up to 35.7 m/s (80 mph) were achieved in this apparatus. None of the large canisters failed in the impact tests. Some of the small canisters had small cracks after impacts at 22.9 and 35.7 m/s, but weight loss

measurements showed that no glass escaped through the cracks. After the tests, each of the canisters was opened and the particle size of the contained glass was determined. Figure 2 shows the amount of particles smaller than 10 μm in diameter that are formed as a function of impact velocity.

Impact behavior is relatively independent of glass composition. Impact tests that compare waste glasses and commercial soda-lime-silica glasses yielded similar results. A comparison of vitreous and devitrified 77-260 also indicated identical behavior (Bunnell 1979).

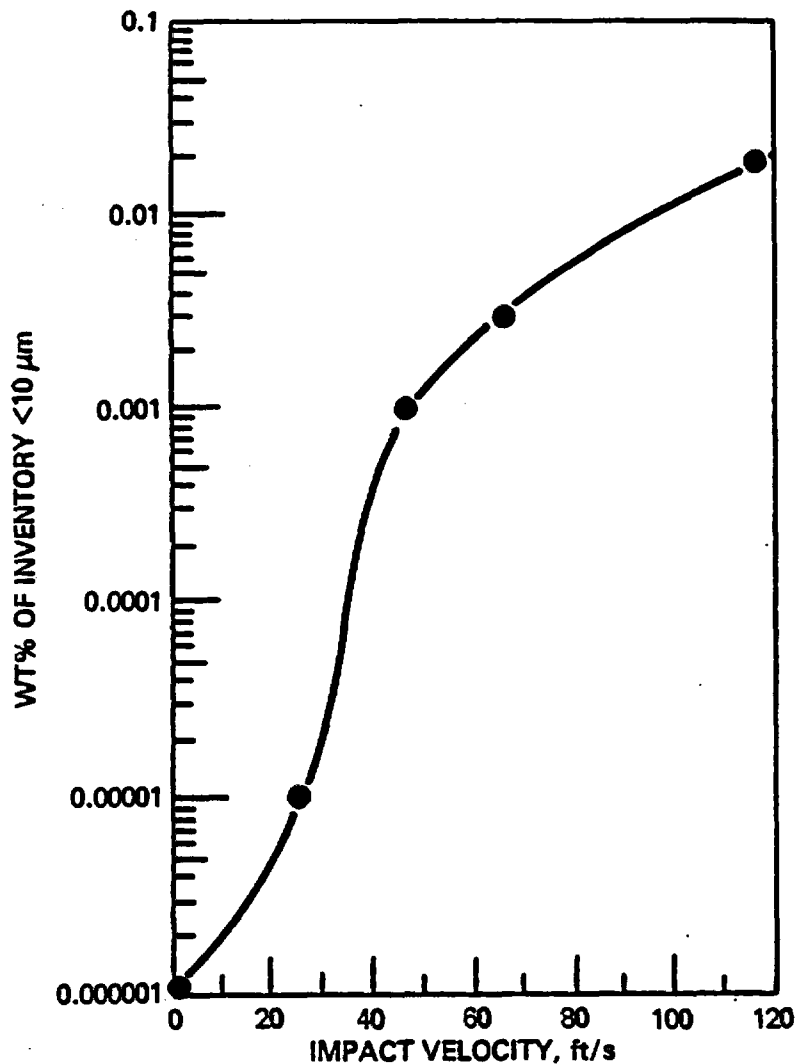


FIGURE 2. Effect of Impact Velocity on Fraction of Respirable Particles Formed

Thermal Conductivity

Thermal conductivity is another physical property of waste glass that is relatively independent of glass composition. The thermal conductivity of most waste glasses falls within the limits shown in Figure 3. The thermal conductivity increases gradually with temperature until the softening point of the glasses is reached. Above the softening point, the increase in the thermal conductivity as a function of temperature is more rapid. Specific data on 77-260 are not available.

Thermal Expansion Coefficient

The thermal expansion coefficients of waste glasses are similar to those of commercial soda-lime-silica glasses. Representative thermal expansion coefficients of glass are shown in Table 6. The thermal expansion coefficients are relatively independent of composition, with the exception of the alkali

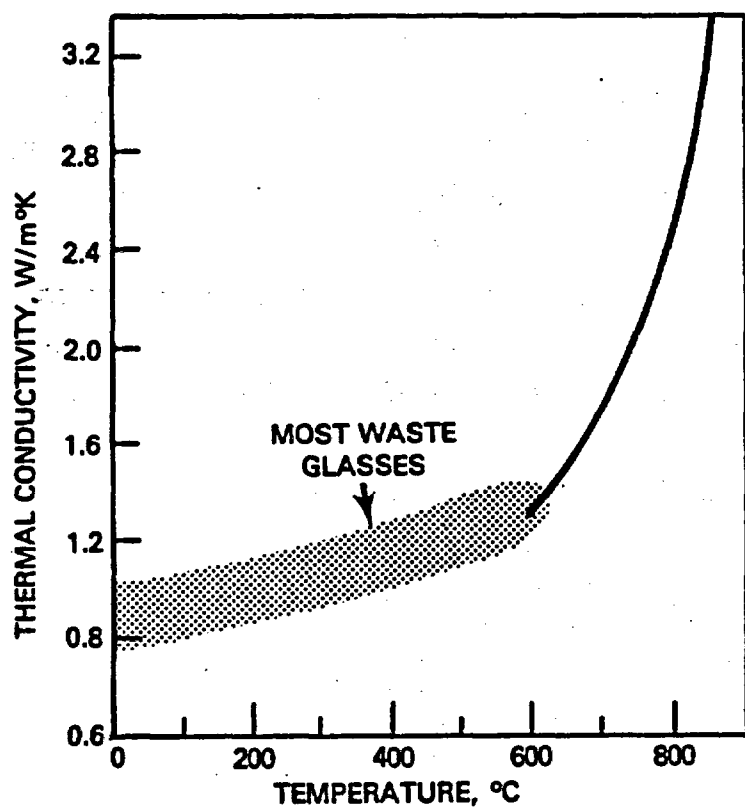


FIGURE 3. Thermal Conductivity of Waste Glasses

constituents. Sodium probably has the greatest effect on thermal expansion of any of the waste constituents. Decreasing sodium content usually decreases the thermal expansion coefficient.

A low thermal expansion coefficient gives increased thermal shock resistance and decreases the time required to anneal a block of glass, and thus would appear to be a desirable characteristic. On the other hand, a low thermal expansion coefficient will further increase the mismatch in thermal expansion coefficient between the waste glass and its canister, and thus will increase the strain in the canister wall. The thermal expansion coefficients of waste glass as shown in Table 6 represent a good compromise between the opposing requirements.

THERMAL EFFECTS AND DEVITRIFICATION

Volatility

After manufacture, volatility from waste glass is a factor only in accident analyses. Waste glass manufacturing temperatures are several hundred degrees above the maximum design storage temperatures, which assures that any volatiles that might pressurize the canisters during storage have been removed. However, accidents can be postulated, involving external heat sources or clusters of uncooled waste canisters, in which the temperature rises far above normal storage or handling temperatures. Volatility data are available for analysis of these postulated accidents. An example of such data is shown in

TABLE 6. Typical Thermal Expansion Coefficients of Glasses

<u>Glass Type</u>	<u>Thermal Expansion Coefficient x 10⁻⁷ / °C</u>
Waste glasses	80-100
77-260	100(a)
Commercial Na-Ca-Si	92(b)
Pyrex	32(b)

(a) Ross et al. (1978).
 (b) Shand (1958).

Figure 4. The data demonstrate that volatility is very temperature dependent and that cesium is the most volatile radioisotope. Although ruthenium often exhibits significant volatility in radioactive processes, its volatility from waste glasses is less than that of cesium. Specific data on 77-260 glass are not available.

Devitrification

Devitrification is the formation of crystals caused by the ordering of certain atoms in the glassy matrix. Crystals form because their ordered structure has a lower free energy. This ordered structure is more thermodynamically stable than the random network of the glass. The amount and identity of the crystals formed depends on the initial composition of the glassy matrix. The

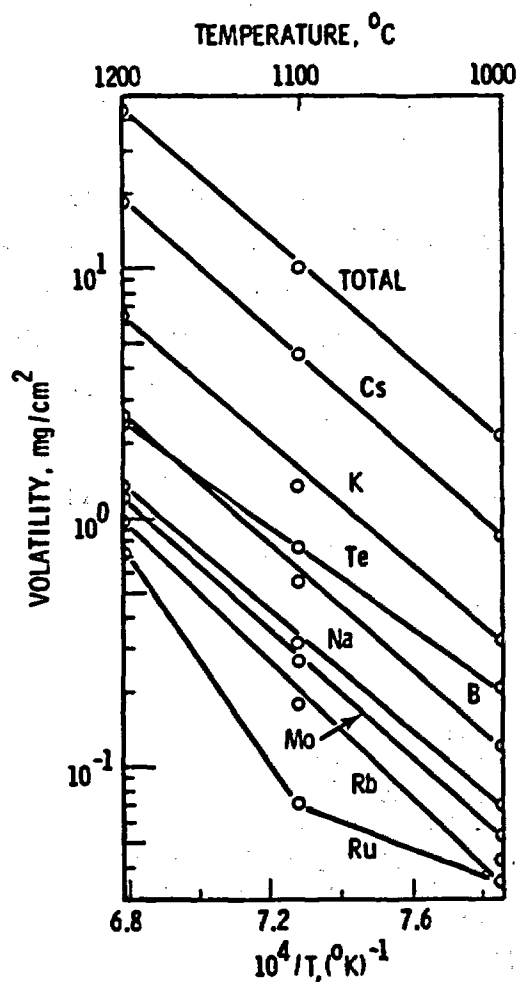


FIGURE 4. Volatility of Waste Constituents (Gray 1976)

rate of crystal formation is time and temperature dependent. Measurable devitrification of waste glasses generally occurs only from 950° to 500°C. Above 950°C, the crystals redissolve.^(a) Below 500°C, the viscosity of the glassy matrix is so high that crystallization is diffusion-limited to extremely low rates. At lower temperatures, the rate of formation decreases, but the equilibrium yield of crystals increases. It is possible to define approximate equilibrium yields at 700°C in experimentally practical times (1 year). At lower temperatures, the experiments cannot be completed in practical times. But the temperature effect above 700°C exhibits Arrhenius behavior and can be extrapolated to lower temperatures. Extrapolation shows the kinetics are extremely slow at geologic storage temperatures. Below approximately 200°C, measurable crystallization (anhydrous) would require millions of years (Turcotte and Wald 1978). The existence of natural glasses millions of years old is an indication that the extrapolation is justified.

It is important to understand what devitrification does to waste glass. Figure 5 shows photomicrographs of 77-260 waste glass before and after devitrification. It is only on the microscopic scale that the effects are truly apparent. Even "totally devitrified" waste glass usually includes only 30 to 40 vol% crystals, as compared to 95 vol% in commercial glass-ceramics. The 77-260 waste glass contains 44% crystalline material after two months at 600°C (Ross 1979). To the naked eye, the devitrified waste glass is unchanged except that its luster is dulled and the color may change.

Devitrification usually increases the overall leach rate of waste glasses. The increase may occur in the residual glass phase (because of depletion of silica) or in one of the crystalline phases that is formed, like strontium

(a) There are some exceptions to this. Fission products ruthenium and palladium are insoluble in waste glass at all temperatures. Also, the fission product oxide CeO_2 does not completely dissolve in waste glass until a temperature of about 1200°C is reached. Spinel, having the general formula A_2BO_4 , where A can be Fe or Cr, and B can be Ni, Zn, Fe(II), etc., apparently may even exhibit a retrograde solubility above 950°C in certain waste glass compositions. Regardless of their high temperature behavior, the effects of these species are indistinguishable from the other devitrification species at the handling and storage temperatures of concern here.

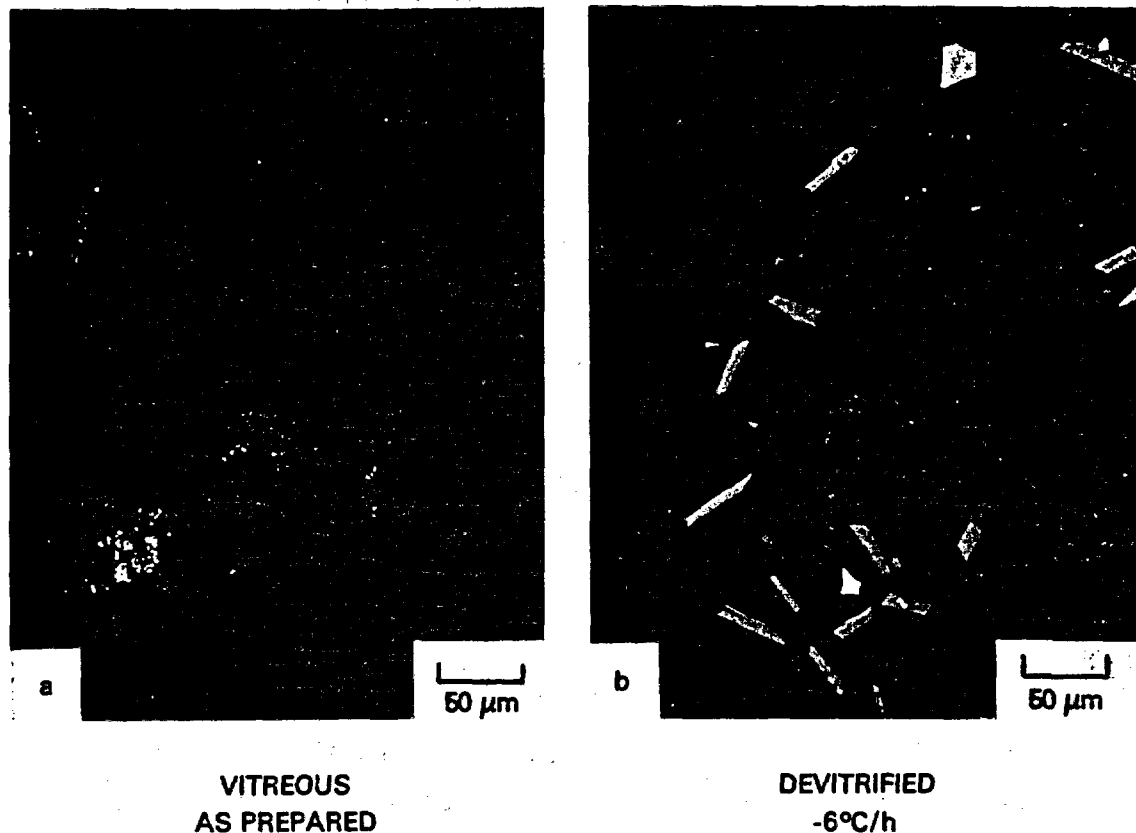


FIGURE 5. Photomicrographs of Vitreous and Devitrified Waste Glass 77-260

molybdate (Malow and Schiewer 1972). The increase in leaching of borosilicate waste glasses after devitrification is usually no more than a factor of 2 to 5, although in some instances an increase up to a factor of 10 has been observed in waste glass after maximum devitrification at 750°C as shown in Figure 6. The behavior of 77-260 shows a factor of 5 or less increase. Figure 6 also demonstrates that there can be considerable variation in the leach rate of non-devitrified waste glass.

Because the amount and identity of the crystalline species formed during devitrification are so dependent on composition, a large amount of work has been done to identify the various species that may form in specific waste glasses. A review of that work is beyond the scope of this report; however, some general observations may be made:

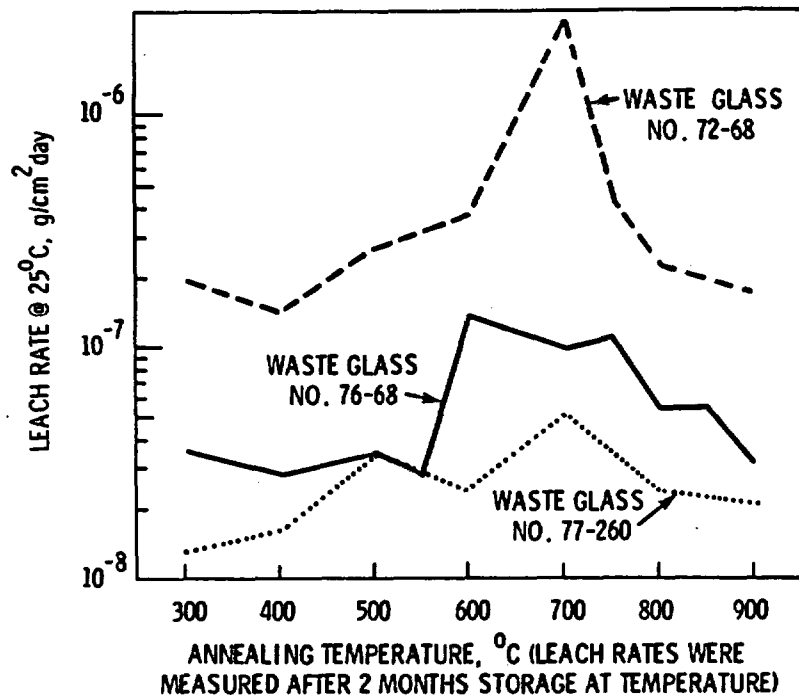


FIGURE 6. Leach Behavior as a Function of Devitrification for Three Representative Borosilicate Waste Glasses

- The species formed on devitrification of borosilicate waste glasses are often crystalline silicates; boron usually remains in the glass matrix. The end result is a boron-rich residual glassy phase, which has a somewhat higher leach rate than the initial glass because of its higher boron content.
- A larger proportion of the high-valence, high-atomic-weight cationic constituents tends to appear in the crystalline silicate species. Sodium, potassium, and calcium, etc., are relatively absent from the crystalline silicate devitrification species. In general, however, other anions that may be present in the glass, such as molybdate, phosphate, or fluoride, exhibit a strong tendency to form crystalline devitrification species which, in contrast to the silicates, usually preferentially contain alkalis and alkaline earths. The identities of the exact crystalline compounds that will form from a given glass composition cannot yet be predicted with confidence; they must be determined empirically.

- Secondary devitrification reactions have also been observed in which a rapidly formed crystalline species is slowly converted into another crystalline species.
- At optimum devitrification conditions, crystals may form several hundred micrometers in the longest dimension. Microcracking in the surrounding glass matrix may occur as the result of mismatching thermal expansion coefficients.

Tests on 77-260 have shown that the major crystals that form on devitrification are $Gd_2Ti_2O_7$, $Ca_3Gd_7[(SiO_4)]_5(PO_4)O_2$, and CeO_2 . Crystals of RuO_2 , $NiFe_2O_4$ and Pd metal have been observed in as-melted waste glass (Wald and Westsik 1979). Reduction of the gadolinium and titanium contents of the glass would appear to be helpful in reducing devitrification.

Phase Separation

Phase separation is another time-temperature-dependent phenomenon involving atomic rearrangement and it is a liquid-phase separation. Borosilicate glasses are particularly susceptible to phase separation and form a boron-rich and a silica-rich phase (Doremus 1973). There is evidence that some borosilicate waste glasses are phase-separated as formed.

Phase separation is difficult to study because the dimensions of the separated phases are usually less than 500 Å. Two types of phase separation are known to borosilicate glasses. In one, the borate-rich phase is distributed as discrete disconnected globules in the silica-rich phase. In the other, the borate-rich globules are connected to form a continuous network. It may be postulated that the former type of phase separation occurs in waste glasses, since if the borate-rich phase was continuous, higher leach rates would be expected than those actually observed.

Molybdenum and sulfate also exhibit phase separation in borosilicate waste glasses. A molybdenum-rich salt phase that also contains sodium, cesium, and strontium separates. As is typical of phase separation phenomena, the molybdenum-rich phase is completely miscible in waste glasses above about 1150°C. At lower temperatures, the phase separation is composition dependent.

If the concentration of molybdenum and sodium is high enough in borosilicate waste glasses, the molybdenum-rich phase will separate out on a macroscale and float to the surface of the molten glass. As noted earlier, reducing conditions can be used to avoid the separation of the molybdenum salt phase. This phase separation behavior has not been observed with 77-260.

LEACHING

The factors that can significantly affect the value for the leach rate obtained in a given leach test are shown in Table 7. Some of these factors are intrinsic, related only to the waste glass itself and its condition. Others are extrinsic and can vary independently of the waste glass. The factors in Table 7 are interrelated. Understanding the leaching of waste glass rests on knowing the type of influence each factor has in relation to the others.

For example, a set of leach data for representative HLW is shown in Table 8. These data were obtained by Wald and Westsik (1979) and indicate little difference in the leach rate between simulated and fully loaded waste glass samples. The data also indicate that leach rates vary as a function of glass composition, element of interest and thermal history of the sample and that a difference of a factor of two may represent the combination of all these parameters as well as the uncertainty in the analysis.

For an estimation of the long-term leach rates, it is very important to know the flow conditions. The data in Figure 7 obtained by J. Westsik (Ross, Turcotte, Mendel and Rusin 1979) show a major change in behavior at longer times between static and fresh leachates. Leach rates for powdered specimens

TABLE 7. Factors Affecting Leach Rate Measurements

<u>Intrinsic</u>	<u>Extrinsic</u>
Glass composition	Temperature
Thermal history	Pressure
Radiation effects	Composition of leachant (including pH and Eh)
Physical form	Flow rate of leachant
Surface character	

TABLE 8. Leach Rates of Waste Glasses Based on Cesium, Strontium and Europium in a Modified IAEA Test at 25°C

	Cesium		Strontium, Simulated	Europium, Radioactive
	Simulated	Radioactive		
72-68				
As Prepared	9.0×10^{-6}	2.3×10^{-5}	6.9×10^{-6}	3.1×10^{-6}
Devitrified	3.2×10^{-5}	4.3×10^{-5}	1.5×10^{-5}	4.2×10^{-6}
76-68				
As Prepared	2.7×10^{-6}	3.0×10^{-6}	2.8×10^{-6}	1.3×10^{-6}
Devitrified	3.0×10^{-6}	2.6×10^{-6}	3.3×10^{-6}	1.3×10^{-6}
77-107				
As Prepared	6.4×10^{-6}	6.5×10^{-6}	6.5×10^{-6}	2.2×10^{-6}
Devitrified	8.0×10^{-6}	4.4×10^{-6}	6.0×10^{-6}	7.7×10^{-7}
77-260				
As Prepared	9.1×10^{-7}	1.8×10^{-6}	1.4×10^{-6}	8.1×10^{-7}
Devitrified	9.8×10^{-7}	1.8×10^{-6}	1.2×10^{-6}	5.7×10^{-7}

(a) The leach rates in $\text{g/cm}^2\text{-d}$ are average rates covering 8 through 24 days of testing.

in the static solution have decreased to 3 to 5×10^{-9} $\text{g/cm}^2\text{-day}$, which is 100 times lower than leach rates for the first 10 days (Ross, Turcotte, Mendel and Rusin 1979). This apparently results from a saturation or approach to saturation of the leachate with species from the waste form. Saturation does not occur to the same degree in a solution that is changed regularly.

Measurements of canisters of simulated waste glass have shown that surface areas are increased by a factor of 10 to 20 over the external geometric surface areas from thermal shock during processing (Slate et al. 1978). Conservative calculations have previously used this surface area increase in calculating the increase in leaching from cracking. Data that have been obtained by comparing powdered and slab samples of 76-68 glass have indicated differences of up to two orders of magnitude in leach rate when total surface area is considered (Ross et al. 1978). More recent data (Perez and Westsik 1980) indicate that tight cracks in waste forms do not leach. These data indicate that the degree of thermal-mechanical fracture may not be strongly related to the quantity of material leached from the waste form.

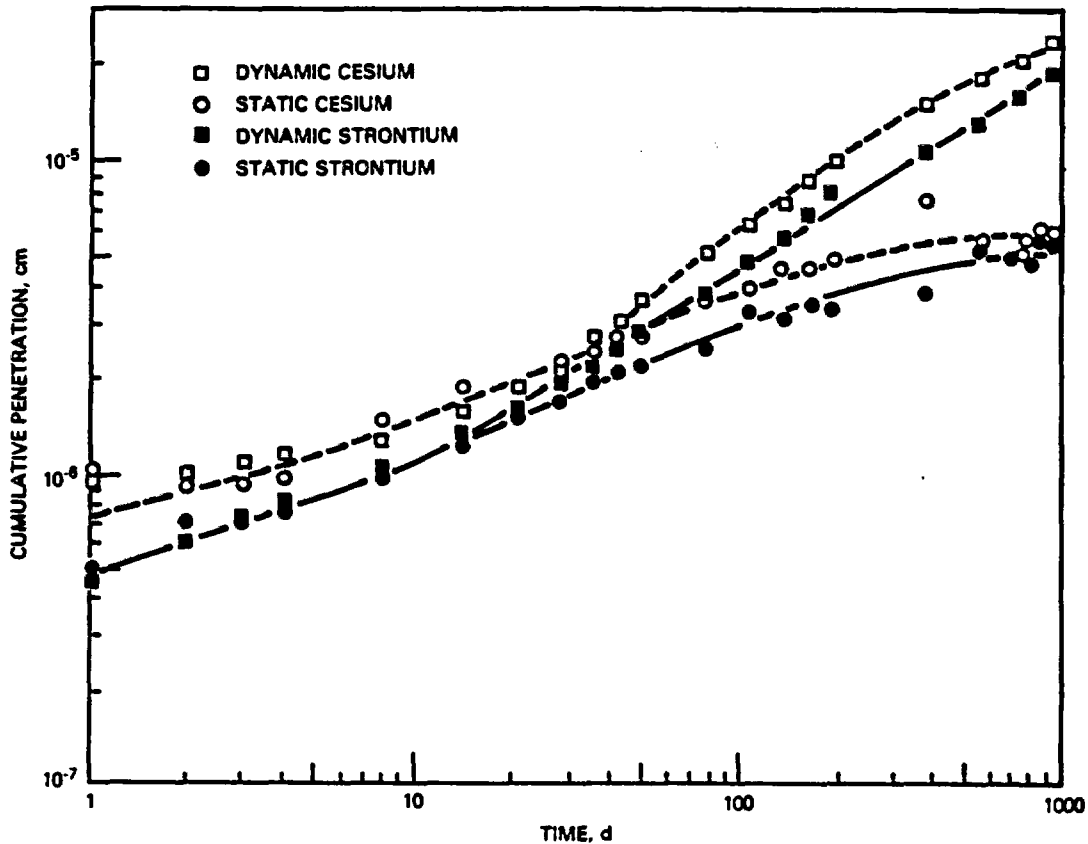


FIGURE 7. Comparison of Static and IAEA (Simulated Flow) Leach Test Results for a 72-68 Glass

RADIATION EFFECTS

Perhaps the most unique feature of waste glass is the high levels of contained radioactivity potentially possible. Depending on the type and amount of radioactivity incorporated in waste glass, the total beta-gamma dose to the glass may reach 10^{12} rads in the first one thousand years; the alpha events resulting from decay of the contained actinides, many of which have long half-lives, may exceed 10^{19} per cm^3 of glass in 250,000 years.

Will self-radiation for thousands of years change the properties of waste glass in any way, making the assumptions concerning the glass used in various long-term behavior analyses invalid? It must be proven that, once the thermal and hydrothermal devitrification effects are defined, the glass will no longer change, and that long-term radiation effects can be discounted. With some

reservations, described in the following sections, all evidence indicates that it is indeed legitimate to discount radiation effects. The evidence shows waste glass to be very radiation-resistant material.

Radiation can potentially cause:

- stored energy buildup;
- bulk or localized density changes;
- changes in rates of devitrification;
- amorphization of crystalline species (metamictization);
- changes in mechanical strength;
- changes in leach rate;
- helium buildup (from alpha decay).

Although the list of possible radiation effects is long, the tests performed to date have revealed no effects that would jeopardize the use of glass for the long-term immobilization of up to at least 1×10^5 Ci of fission products per liter of glass and 1×10^3 Ci of actinides per liter of glass.

The actinide content of waste glass is made up of a mixture of uranium, neptunium, plutonium, americium, and curium isotopes, plus their decay products. The relative amounts of actinides in a waste glass depends on the source of the radioactive waste incorporated in the waste glass. In all cases, however, the actinide alpha-decay effects will continue for long times. Table 9 lists the alpha decays during the first million years for one representative waste glass.

TABLE 9. Time Distribution of Alpha Decay in a Representative Waste Glass

<u>Time of Vitrification</u>	<u>Alpha Events, Percent of Total</u>
First 100 yr	3.4
100-1,000 yr	3.4
1,000-10,000 yr	6.8
10,000-100,000 yr	16.7
100,000-1,000,000 yr	69.7

Stored Energy

Stored energy is latent energy stored in a substance by radiation-induced displacement of atoms from their normal lattice position. The latent energy is released as heat when the temperature of the substance is raised sufficiently. The specific heat of waste glasses is usually about 0.2 cal/°C-g. The maximum stored energies in waste glasses are in the range of 30 to 60 cal/g; thus under adiabatic conditions, the maximum additional temperature rise that could occur due to rapid release of the stored energy is only 150° to 300°C. It may be concluded that the stored energy levels in waste glass are not a hazard. Stored energy data on 77-260 indicate a maximum value of about 30 cal/g (Weber et al. 1979).

Density Change

Density change is a commonly observed radiation effect in ceramic substances. The density changes observed in waste glasses generally are less than 1%.

The density change in waste glass reaches an equilibrium value after about 2×10^{18} α/g. Only minor density fluctuations occur with further increases in radiation dose.

As Figure 8 shows, density change in waste glass can be positive or negative; the glasses can either shrink or swell. The direction of the density change is apparently a function of composition. The density change for vitreous 77-260 was less than ~0.1%. However, devitrified samples show density changes of -0.45% and 1.0% depending on degree of devitrification (Weber et al. 1979).

Radiation Effects on Devitrification and Metamictization

Radiation seems to have little effect on thermal devitrification of waste glasses. Neither the species of devitrification crystals formed nor their rate of formation is believed to be significantly altered. Specimens of four different PNL glass compositions, including 77-260, have been prepared with full levels of radioactivity. Similar specimens, but with nonradioactive isotopes of the fission products and chemical standins (rare earths) for the actinides,

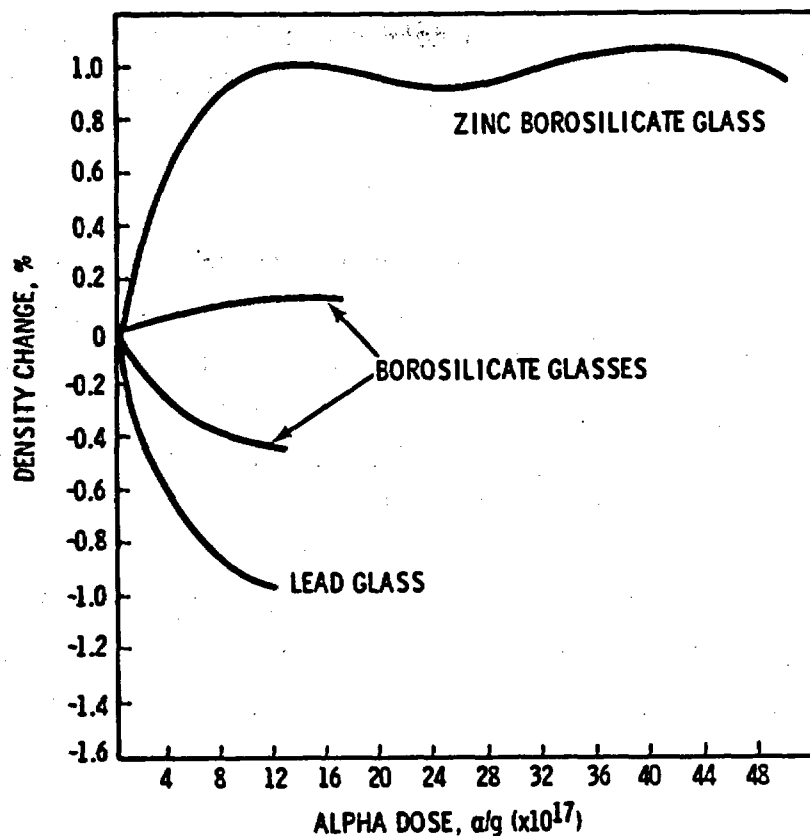


FIGURE 8. Radiation-Induced Density Change in Waste Glass

have also been prepared. The nonradioactive and radioactive specimens have been subjected to the same thermal devitrification conditions. Results confirm expectations; devitrification behavior is similar. Radiation would not be expected to affect thermal devitrification since radiation effects are annealed out at the temperatures where the devitrification rate is significant (above 500°C).

Radiation Effects on Leach Rates

Leach rates, measured on waste glasses containing up to 9×10^4 Ci/L of fission products, are not more than a factor of two higher than those made on nonradioactive simulated waste glasses of the same general chemical composition (Mendel and McElroy 1972; Mendel 1973). This difference is within the normal experimental deviation of leach test data. Similarly, the leach rate of a ²⁴⁴Cm-spiked waste glass was not significantly different from the leach rate of a comparable nonradioactive glass after a cumulative dose over 3×10^{17} disintegrations/cm³ (Mendel et al. 1977). Thus, radiation does not affect the leach

rate of waste glasses, and leach data obtained on nonradioactive simulated waste glass can be used to predict the leaching behavior of fully radioactive waste glass.

Helium Behavior

Helium atoms are generated wherever alpha-decay events occur in waste glass. Each alpha particle captures two electrons to become a helium atom. Helium is slightly soluble in glass; helium also diffuses through glass quite readily. The diffusion is retarded as the glass composition increases in complexity; thus, helium diffusion in waste glass is lower than in quartz glass or commercial soda-lime-silica glass (Turcotte 1976). Figure 9 shows that the diffusion of a portion of the helium produced by alpha decay is also further inhibited when compared to that of helium implanted in the glass by solubility at high temperatures. The inhibition is attributed to trapping of some of the alpha-produced helium at point defects. Expressions for both untrapped (D_u) and trapped (D_t) helium diffusion coefficients have been experimentally derived (Turcotte 1976):

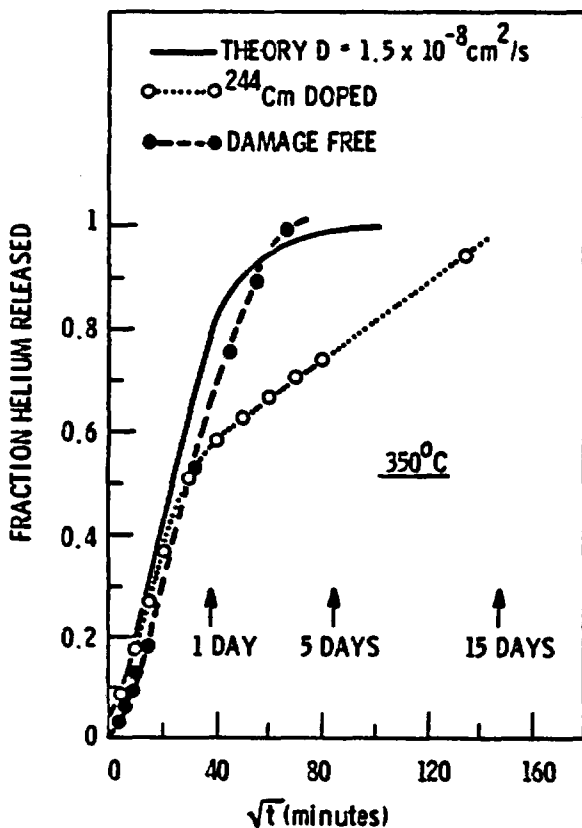


FIGURE 9. Isothermal Helium Release from Glass

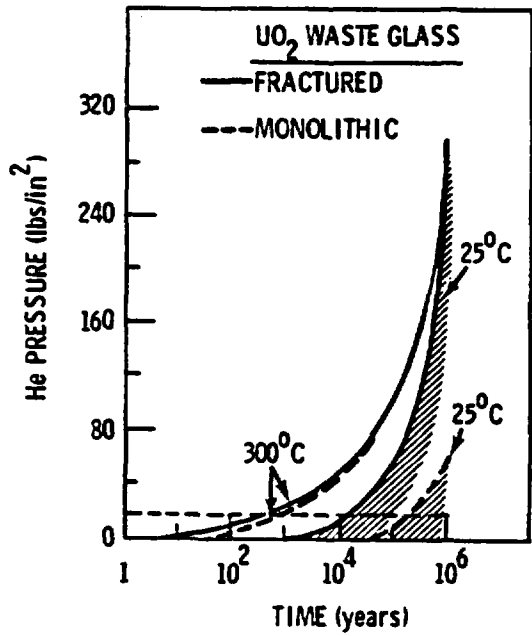
$$D_u = 2.1 \times 10^{-3} \exp (-15,000/RT) \text{ cm}^2/\text{s},$$

$$D_t = 1.7 \times 10^{-4} \exp (-15,000/RT) \text{ cm}^2/\text{s}.$$

Using these diffusion coefficients, canister pressurization was estimated at two temperatures, 25° and 300°C, as a function of time for waste glass containing LWR once-through and full recycle wastes. The estimated pressures are plotted in Figure 10a and 10b. The solid lines represent no trapped helium; the shaded portion below the lines represents the potential effect of trapped helium. A 10 vol% plenum in the canister and 30 wt% waste loading in the glass was assumed.

Transmutation

Radioactive decay results in the transmutation of the decaying isotope, often to atoms of significantly different valence and ionic radius. Some of the transmutations that occur in waste glass are shown in Table 10. Intralanthanide and actinide transmutations are not shown because the resultant changes are insignificant. The actual number of transmutations that will occur in a given waste glass depends on the fission product loading and the age of the waste when the glass is made. Even in glass with a high waste loading, the total number of nonoxygen atoms undergoing transmutations will not exceed 2%. Because of the nonstoichiometric nature of the glass, it is expected that the transmutations can be accommodated without effect. The exception may be severely devitrified glass because the effect of transmutation on the stability of crystals could be more severe.



a) ONCE THROUGH

b) FULL RECYCLE

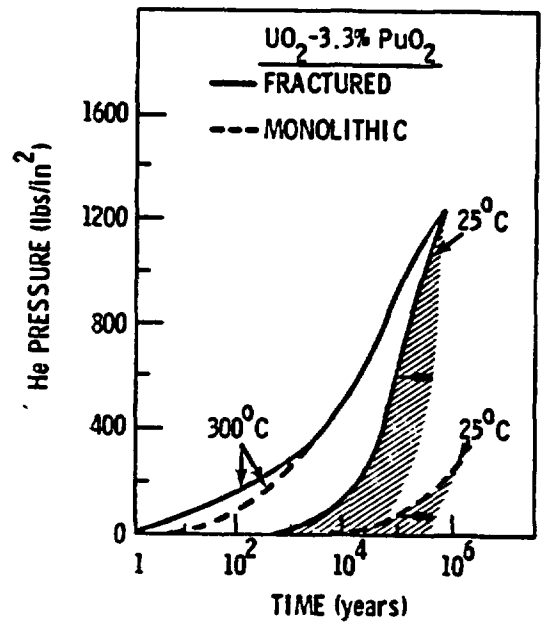


FIGURE 10. Potential Helium Pressure in Waste Glass Containers

TABLE 10. Radioactive Decay Transmutations That Occur in Waste Glass^(a)

<u>Initial Ion</u>	<u>Transmuted Ion</u>
Cs ⁺¹	Ba ⁺²
Tc ⁺⁷	Ru ⁺⁴
Sr ⁺²	Zr ⁺⁴
Zr ⁺⁴	Nb ⁺⁵
Ru ⁺⁴	Pd ⁺²
Pd ⁺⁰	Ag ⁺⁰

(a) Actinide and lanthanide transmutations are not shown because resulting effects are small.

HIGH-LEVEL WASTE CANISTER DESCRIPTION

The purpose of this section is to describe the primary glass-storage canister. The descriptions will include the canister design itself, canister processing, and properties of a filled canister, such as the radiation flux. In addition, background information related to the PNL canister studies will be provided to demonstrate the rationale for the reference selections.

The canister, of course, is a very important part of the waste management system. Its primary functions are to 1) provide high-integrity glass containment from processing to disposal, 2) protect the glass from physical damage; and 3) provide a means for handling the glass. The canister must be compatible with the environments it encounters during processing, handling, and storage operations. The following data were developed with these functions in mind.

BACKGROUND

Canister development at PNL has not been oriented to provide long-term containment of radionuclides during disposal since existing regulations (Code of Federal Regulations, Title 10, Part 50, 1978) have not required significant waste containment in the repository. Since currently proposed regulations (Code of Federal Regulations, Title 10, Part 60, 1980 and Code of Federal Regulations, Title 40, Part 191, 1979) emphasize radionuclide isolation from the repository media for approximately 1000 years, PNL researchers are now investigating concepts for a high-integrity canister with an extended life as well as various systems of overpack structures, liners, and absorbent mineral layers surrounding the canister within the repository.

Over 30 full-scale canisters have been filled by the in-can melting (ICM) process at PNL and approximately 60 canisters have been filled using the joule-heated glass melter (JHGM) process. In addition, two nearly full-scale canisters of radioactive waste glass were produced in the Waste Solidification Engineering Prototype Program at PNL in 1970, and two more were filled in the Nuclear Waste Vitrification Program in 1979. These canisters have provided data on canister performance under both filling and storage conditions that support the stress analysis and structural integrity evaluation.

Canister development work has also been carried out at Savannah River Laboratory (SRL) in support of the defense HLW solidification programs. Over 20 full-scale canisters of simulated waste have been produced in the ICM process and 5 canisters of simulated waste filled by the JHGM process. SRL has selected a nominally 3-m-high by 60-cm-dia stainless steel 304L canister to contain the defense-waste glass.

The French are using stainless steel canisters of approximately 1 m height and 50 cm dia to store radioactive waste glass in air-cooled storage vaults. This is being done on a production scale and approximately 500 canisters have been filled over the past 3 years.

PNL has been conducting studies on HLW canisters for about 5 years. Basic designs have been completed and demonstration, at least in principle, of all post-vitrification process steps has been completed. The primary references that describe the PNL canister development work are Simonen and Slate (1979) and Larson (1980). Most of the basic technical material included in this section were taken from these primary references.

TYPE OF GLASS VITRIFICATION PROCESS

The performance requirements of the canister depend on the type of vitrification process used for making the waste glass. Two processes, in-can melting and joule-heated glass melting, are principal candidates. In the ICM process, the canister serves as the crucible for melting the dried waste and glass formers. As a result, the canister is subjected to temperatures in the range of 1000° to 1100°C for a period of from 12 to 24 hours. Under these conditions, the canister undergoes some creep, internal corrosion from the glass, and external oxidation. In the JHGM process, the glass is made in a refractory-chambered melter and poured into the canister. Under these conditions, the canister may be at 400°C for 12 to 36 hours and may briefly experience local temperatures of 500° to 700°C at the rising glass levels. Creep, oxidation, and corrosion from glass are not significant problems for canisters in the JHGM process.

MATERIAL REQUIREMENTS

The canister is fabricated from standard single-walled pipe with formed heads welded to either end. Many alloys have been investigated. Stainless steel 304L and Inconel-601[®] are presently the reference candidates for canister materials, and serve to represent the 300 series stainless steels and the high nickel-alloys, respectively.

Specific performance requirements for the canister material arise from the high temperatures associated with the ICM process and the possibility of water-basin interim storage. These performance requirements can be summarized as follows:

- sufficient strength and creep resistance at the glass-forming or pouring temperature;
- resistance to corrosion by molten glass;
- resistance to outer surface oxidation and scale spallation;
- resistance to stress corrosion cracking (SCC) sensitization;
- resistance to SCC during water basin storage;
- amount of residual stress after cooling (the result of a smaller coefficient of thermal expansion for glass);
- ease of surface decontamination;
- ease of lid welding;
- resistance to damage from accidental impacts during handling and transportation;
- retention of geometry (roundness) sufficient to permit ease in overpacking;
- potential for demonstrable integrity during a retrieval period of approximately 150 years in a repository.

[®] Registered trademark of the Huntington Alloys Division of the International Nickel Company, Inc., Huntington, West Virginia.

These performance criteria are addressed in considerable detail in the primary references given earlier for the PNL canister development work. The conclusions from these studies are discussed below.

Process Temperature

The ICM process requires that the canister be held at $1050^{\circ} \pm 25^{\circ}\text{C}$ for approximately 12 hours. The canister is preheated to $\sim 250^{\circ}\text{C}$ in the JHGM process and may reach 700°C maximum at the level of the molten glass as it is being filled. Both SS 304L and Inconel 601 have the necessary strength to be free-standing during the ICM process.

Creep Properties

Creep is not a problem in the JHGM process because of the low canister temperatures. Some creep is evident at the higher temperature of the ICM process. In general, the imposed stress load is not high enough to cause more than 1% creep for the approximately 12-hour process period. Figures 11 and 12 show the isochronous stress-strain curves for 304L stainless steel and Inconel 601 at 1050°C . The curves are a plot of the value of total strain (elastic-plus-plastic-plus-creep) as a function of stress at a given constant end-of-test time. Inconel 601 exhibits less creep under the same temperature, stress, and time conditions than does SS 304L. The creep that does take place is uniform; therefore, the canister retains its original right cylinder shape.

Canister Oxidation

Oxidation and spallation of the exterior canister surface is a potential problem when SS 304L is used in the ICM process. Figure 13 compares the oxidation rates at 1000°C for several materials. At 1050°C , the reference-sized canister may lose ~ 1 kg of scale in the furnace, depending on its removal temperature. If it is removed above 700°C , only about 0.1 kg will fall in the furnace. The primary disadvantage of this loss is the accumulation of this scale in the bottom of the furnace and a possible difficulty of decontaminating the rough, oxidized surface of the canister. Inconel 601 experiences only mild oxidation at the ICM process temperature. Development work on SS 304L

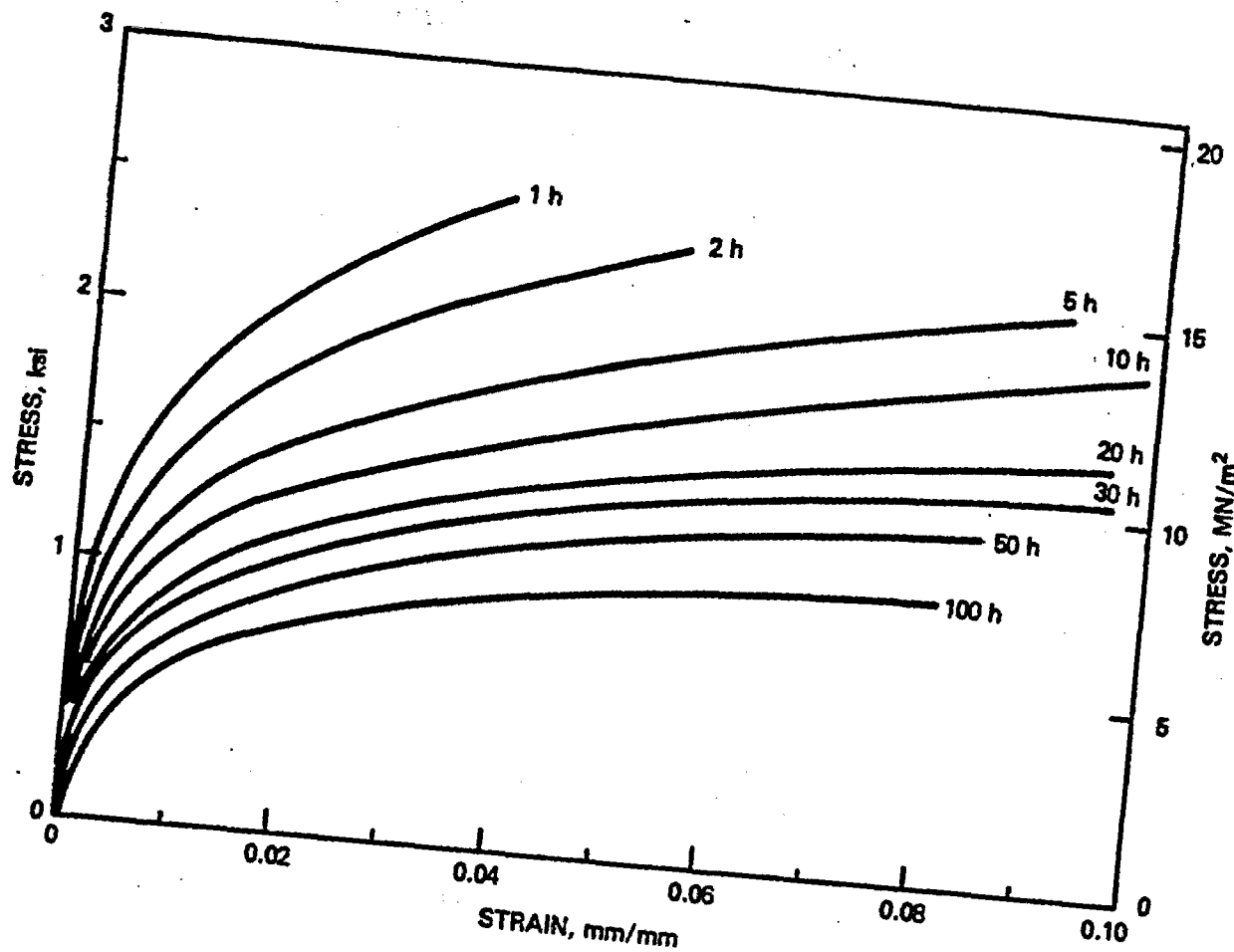


FIGURE 11. Isochronous Stress-Strain Curves for 304L Stainless Steel at 1050°C

canisters indicates that a surface coating or heat treatment may be used to reduce or eliminate the oxidation problem. In the JHGM process, oxidation is not a problem because of the lower canister temperature.

Corrosion from Molten Glass

The molten glass can corrode the interior of the canister. However, the processing period is so short relative to the time required to produce any significant corrosion that this corrosion mechanism is not a problem. Figure 14

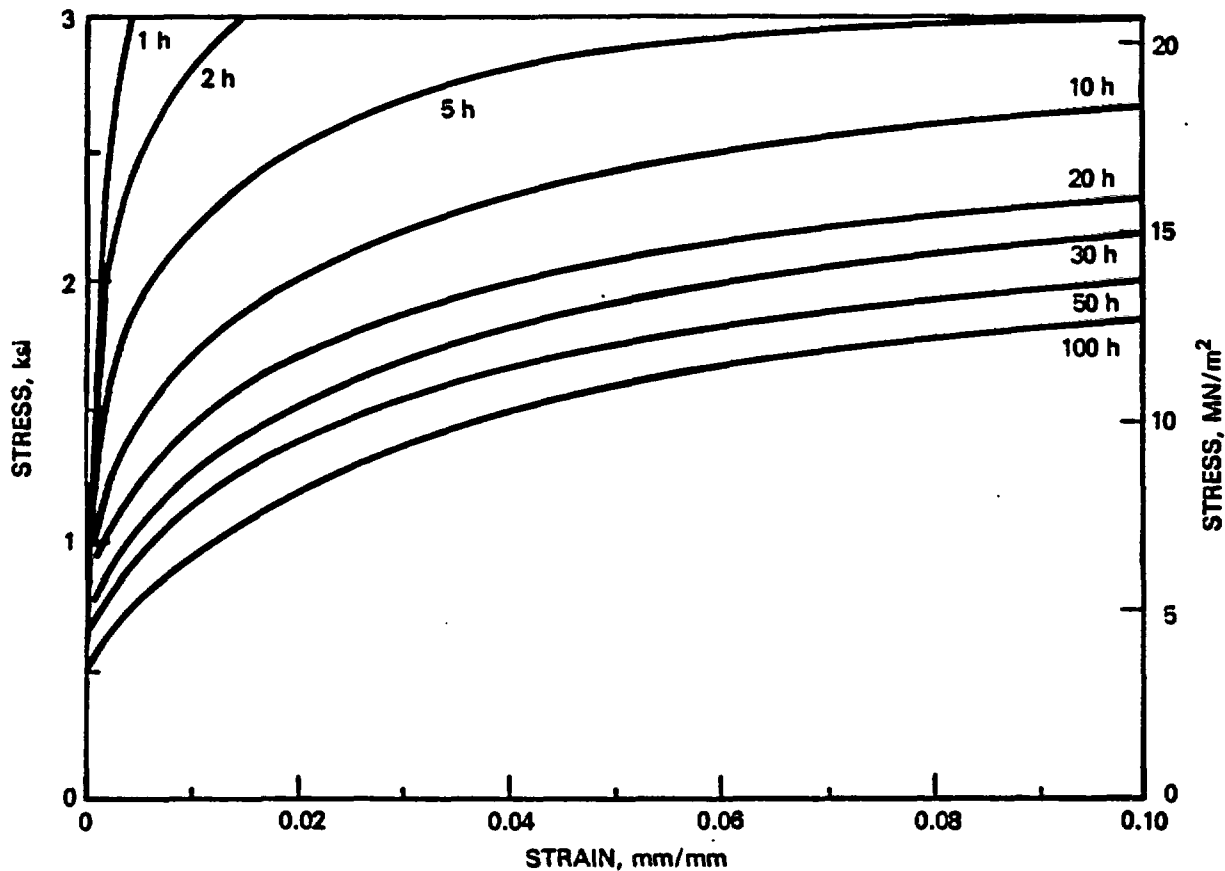


FIGURE 12. Isochronous Stress-Strain Curves for Inconel 601 at 1050°C

shows the corrosion of 304L in a typical commercial waste glass. Additional tests on Inconel 601 show that it can withstand this type of corrosion better than SS 304L.

Stress Corrosion Cracking

Stainless steel canisters are subject to SCC when stored in water basins. Figure 15 is a plot of the time-temperature sensitization for stainless steel as a function of the carbon content. While SS 304L has a relatively low carbon content, it is still subject to some sensitization during the cooldown period when the canister temperature is ~600°C. Since SCC can be prevented by careful control of water chemistry in the storage basin, it is best to assume that the canister has been sensitized, that it will have residual stresses, and that it should be protected by control of the water chemistry (Slate and Maness 1978).

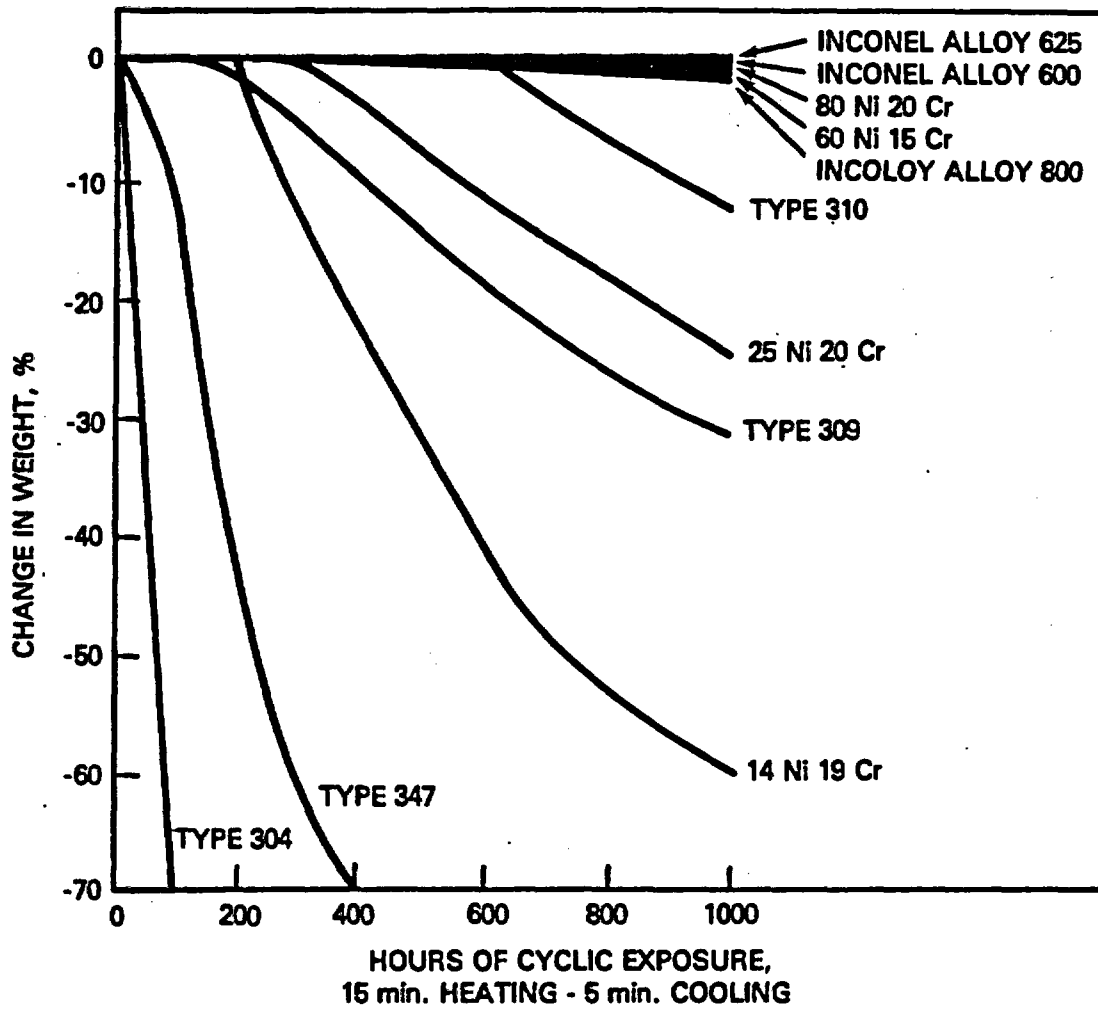


FIGURE 13. Comparison of Material Oxidation Rates at 1000°C (International Nickel Company, Inc. 1973)

Negligible canister sensitization to SCC is expected in the JHGM process. Investigation at PNL has shown that SCC does not occur in high-nickel alloys having greater than ~45% nickel (Inconel 601 consists of ~60% nickel.)

Residual Stress

Residual stress occurs in the canisters as a result of a larger coefficient of thermal expansion ($\sim 19 \times 10^{-6}/^{\circ}\text{C}$) for the canisters in comparison to that of the glass ($\sim 10 \times 10^{-6}/^{\circ}\text{C}$). As the canister cools, it is prevented from resuming its original diameter and length by the now-solidified glass.

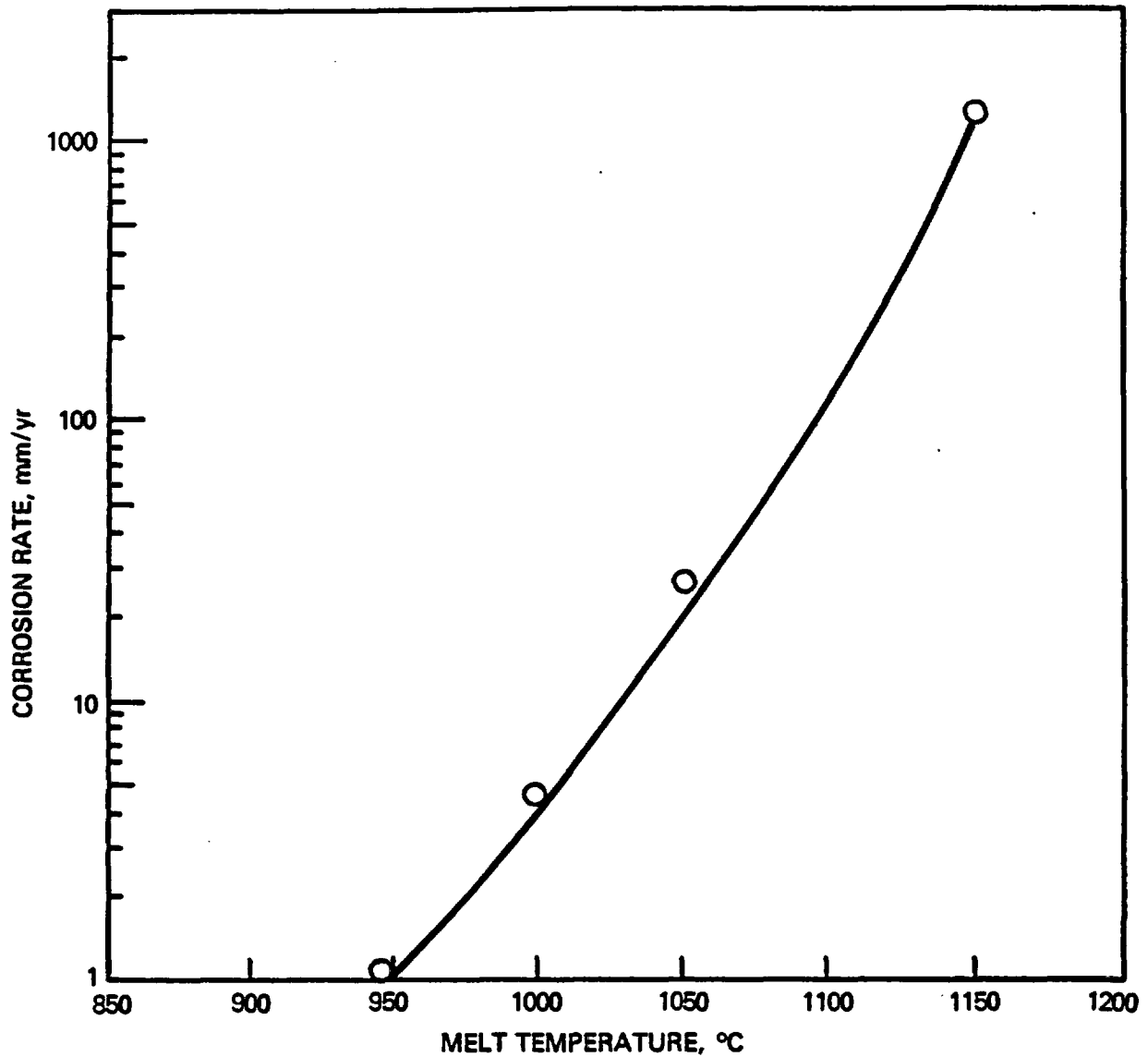


FIGURE 14. Corrosion Rate of AISI 304L in PW 4b Glass as a Function of Temperature

Residual-stress measurements made on a canister indicate 200 MPa (30 kpsi) hoop stress and 205 MPa (36 kpsi) axial stress. PNL has investigated stress-relief techniques and has found them to be ineffective or too complex. Since the canister materials exhibit a high degree of ductility, there is no reason to try and remove the residual stress in the canister. Impacts during handling or transportation will possibly lead to a material yield, but the ductility will prevent rupture except in extreme cases. The residual stress will

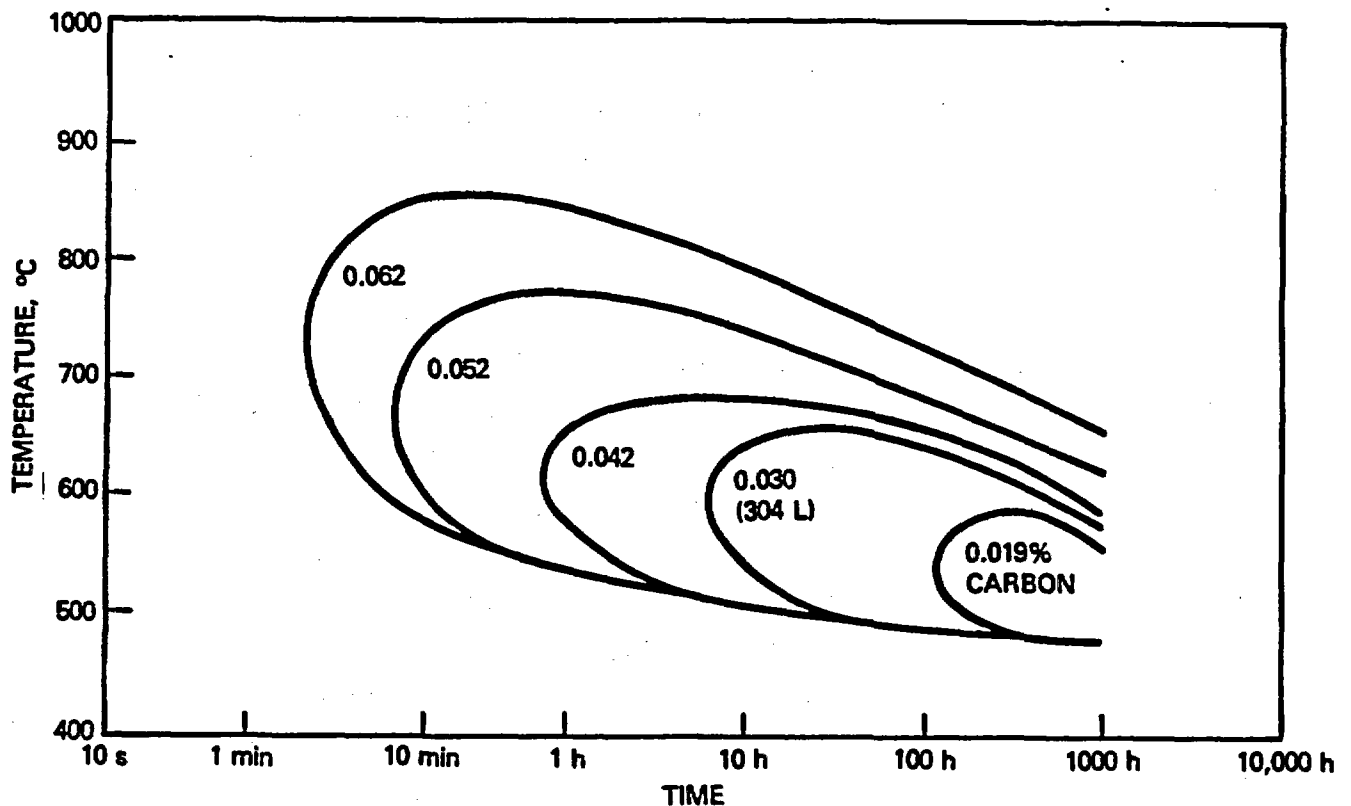


FIGURE 15. Time-Temperature-Sensitization curves for Stainless Steels with Various Carbon Contents

increase the rate of SCC in a sensitized canister, but development work has shown that control of water chemistry in the storage basin can prevent SCC in a sensitized canister that has residual stress.

Surface Decontamination

Both stainless steel and high-nickel alloys can be decontaminated with any of several methods when the glass is produced by the JHGM process. As described earlier, the use of stainless steel for the ICM process results in an oxidation of the surface that may increase the complexity of the decontamination process. The high-nickel alloys do not oxidize to the extent of forming a scale at the process temperature of the ICM process. A thorough study of canister decontamination techniques has been performed by Nesbitt, Slate and Fetrow (1980).

Lid Welding

PNL has investigated many techniques for lid welding and has selected the gas-tungsten-arc (GTA) fusion-weld process as a common, well-understood method of welding nuclear-related equipment. A remotely operated prototype has been demonstrated. The welder makes an autogeneous fillet that can range from 3.2 to 6.4 mm (1/8 to 1/4 in.) thick. Tight tolerances are maintained on the lid dimensions to maintain the appropriate gap between the welding tip and the lid. The welder is keyed from a hole in the center of the lid to simplify the fit-up requirements. The canister opening will have become oxidized in the ICM process, more so if the canister is stainless steel. This surface must be cleaned by mechanical or chemical milling, or by "sand-blasting," before lid placement and GTA welding takes place. Therefore, an Inconel 601 canister will require less preparation than an SS 304L canister in the ICM process. No significant difference has been observed for the JHGM process.

Impact Damage

An extensive program at PNL to investigate the behavior of canisters under impact conditions culminated with actual drop tests of full-sized canisters in 1975 and 1977. During the latter test, 13 canisters were subjected to both bottom impacts and top impacts. Drop heights ranged from 6.1 m to 31.7 m (20 ft to 104 ft). Canister conditions after impact were evaluated on the basis of visual inspection and, in several cases, by metallographic sectioning. No cracks were observed in bottom impacts of the 304L canisters that were built to accepted design and fabrication practices (for example, not all canisters were made according to the reference design). The reference twist-lock closure was not impacted during these tests. All canisters tested were either of SS 304L or carbon steel. Inconel 601 is expected to perform at least as well as the stainless steel.

Retention of Geometry

Canisters have been carefully measured before and after being filled with glass for both the ICM and JHGM processes. No bulges or out-of-roundness in

excess of the 1% limit was noted. In fact, the combination of a high canister temperature and a hydrostatic force of the molten glass in the ICM was observed to improve roundness.

Cost

Inconel 601 costs approximately three to four times more than SS 304L. Fabrication costs are higher for Inconel although inspection and transportation costs are comparable to SS 304L.

Reference Material

Stainless steel 304L is specified as the reference canister material for this study. Since the material costs less than Inconel and meets the performance criteria of the HLW glass production processes.

DESIGN DESCRIPTION

Size

The size of the canister is determined primarily by constraints on decay heat loading, canister weight, and compatibility with transportation systems. From a process standpoint, a 60-cm- or even a 70-cm-dia canister is attractive since either reduces the frequency of canister movement in the remotely operated process cell. However, the decay heat in commercial HLW is such that a 30-cm-dia canister 3 m long will produce ~3.7 kW for HLW aged 5 years from reactor discharge and 2.2 kW when the HLW is aged to 10 years. The current recommended thermal loading for a salt repository is 2.2 kW. Other repository media have lower recommended thermal loadings.

Considering the above design parameter, the reference canister is specified as having a 31.4-cm (12.25-in.) inner dia and a 3-m overall length (measured from the bottom to the top of the lid universal lifting connector). A view of the canister is shown in Figure 16. Internal fins are shown in the figure. These would be used in the ICM canisters to enhance heat transfer during glass melting in the furnace. These fins would not normally be used in a canister filled by the JHGM process.

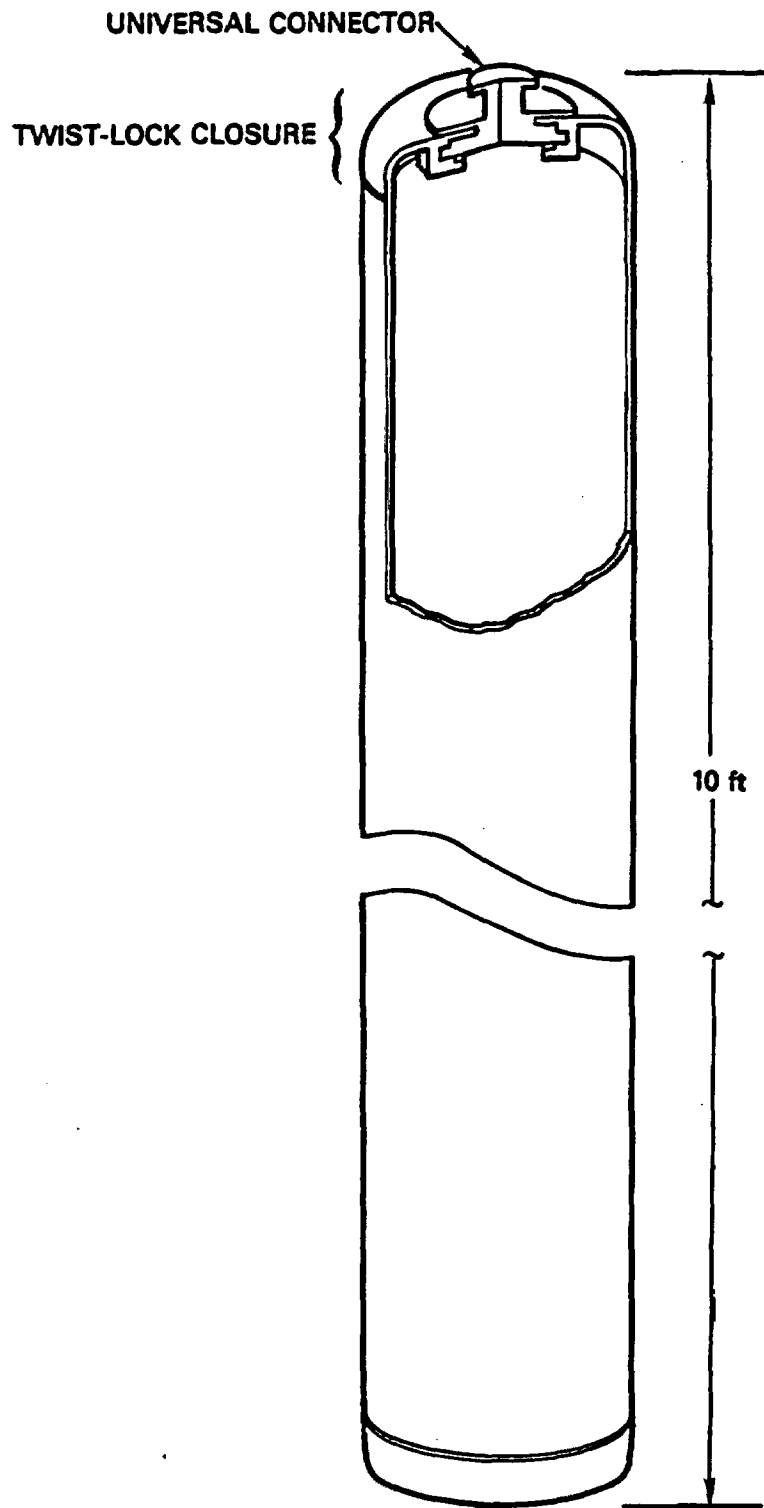


FIGURE 16. Schematic of the Reference HLW Canister

The canister-wall thickness is specified as 0.64 cm (1/4 in.) which is much thicker than is required to meet the process-imposed stresses plus the corrosion allowances for both the inside and outside surfaces. However, the dimension is a prudent specification for impact and transportation protection.

Closure

The top of the canister is formed from a flanged-only tank head. The bottom is a slightly-reversed-dished flanged tank head. Stress analysis indicates the turned corner and closure is less susceptible to impact damage than a simple flat-plate closure.

The actual lid closure at the top of the canister will be a twist-lock fitting developed at PNL. Figure 17 is a cutaway detail of the twist-lock

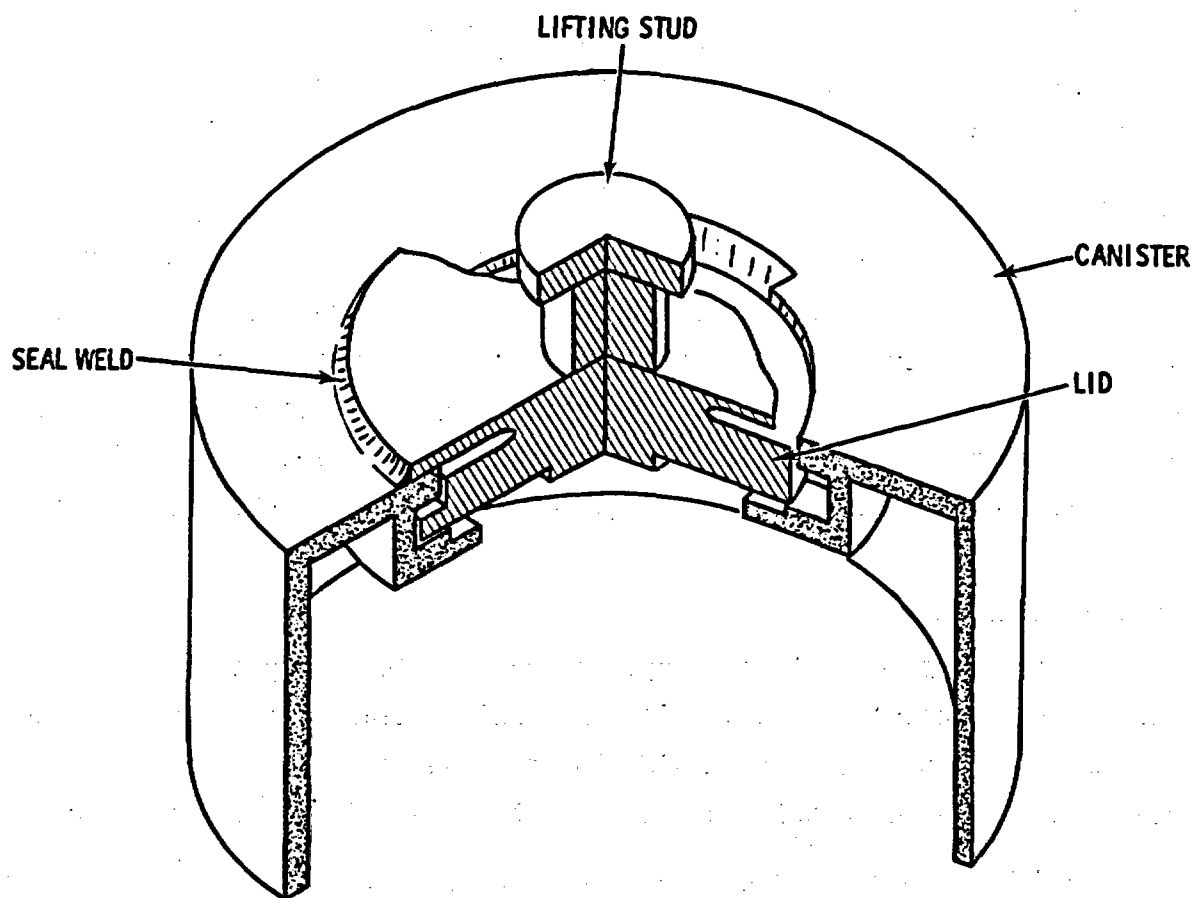


FIGURE 17. Schematic of the Twist-Lock Canister Closure

fitting. This type of closure has been developed to permit a simple, air-tight connection during filling that can be made with remote-handling equipment. The seal-weld surface is accessible for remote welding and can be checked for weld defects by ultrasonic scan. The weld leak check can be made with a bell-type helium detector that fits over the top of the canister. The twist-lock closure has been used in over 20 full-scale canister tests. It has been welded and leak tested using prototype remote equipment.

The level to which the canister can be filled with glass depends on the type of the glass-making process and the accuracy of the instrumentation that monitors the weight and fill level of the canister. As a reference value for this report, a fill level of 90% is assumed for a canister without fins produced by the JHGM process. This value is equivalent to 192 L of glass. Of course, in actual practice the canister fill level will assume some normal distribution around the desired fill level. A canister of glass produced with the ICM process will contain less glass because the internal fins occupy about 10% of the canister volume, and more void space must be reserved at the top for the glass batch to melt.

Design Parameters

The design parameters of the filled HLW canister are given in Table 11. These parameters are, of course, approximate. The average waste loading of the glass will be lower since the fuel history overestimates the average fuel burnup. In addition, the glass production process is easily adaptable. For example, the canister fill level can be changed or the glass waste loading can be changed to meet some other criteria of the overall waste disposal system.

THERMAL ANALYSIS

For the purpose of this study, several simple steady-state temperature profiles were calculated to predict the maximum glass temperature during interim water storage, interim air storage, and repository emplacement. The decay heat produced in the canister as a function of time is given in Table 12.

The CANIST code (developed at PNL) can perform transient thermal analyses for canisters that have radial fins and can provide detailed thermal profiles

TABLE 11. Design Parameters of the HLW Canister

<u>Parameter</u>	<u>Specifics</u>
Material	Stainless steel 304L
Dimensions	
● Outside diameter	32.4 cm (12-in. Pipe) ± 2 mm
● Length	3 m (10 ft) ± 2 mm
● Wall Thickness	0.64 cm (0.250-in. nominal pipe tolerance)
Fins	Not required
Closure	PNL "twist-lock"
Empty weight	160 kg ± 5%
Volume when 90% filled	192 L ± 5%
Weight of glass (3.1 g/c ³)	595 kg
MTU of HLW per canister	2.28 (@ 260.6 kg glass/MTU)
Decay heat	3.71 kW (at 5 yr after reactor discharge) 2.2 kW (at 10 yr after reactor discharge)
Activity	1.02 x 10 ⁶ Ci (at 5 yr after reactor discharge) 6.58 x 10 ⁵ Ci (at 10 yr after reactor discharge)

TABLE 12. Canister Decay Heat

<u>Decay Period, Yr</u>	<u>Canister Heat Generation Rate, W</u>
5	3690
10	2210
20	1600
50	798
10 ²	292
10 ³	20.1
10 ⁴	1.7
10 ⁵	0.264
10 ⁶	0.178

within the canister than can be used to predict glass devitrification and cracking as well as canister creep. The primary references report detailed thermal analyses of canisters during the glass-fill process, cooldown, and both interim and long-term storage. These analyses are not repeated here.

After the canister of HLW is produced, it will be stored onsite before being transported to a repository. The length of this interim storage period depends on many variables in the entire HLW disposal program. To ensure that the glass temperature at the centerline of the canister is within acceptable limits, the maximum glass temperature was calculated for a canister stored either in water or in air. If the canister is stored in a water basin, the maximum temperature is $\sim 153^{\circ}\text{C}$ for 5-year-aged HLW (time since the spent fuel was removed from the reactor). If the canisters are placed in air storage designed for convection cooling (radiative heat loss was assumed to be zero because of nearby canisters in an array), the maximum glass temperature will be $\sim 380^{\circ}\text{C}$ for 5-year-aged HLW. Both of these temperatures are below the point where devitrification of the glass will occur ($\sim 500^{\circ}\text{C}$ if maintained for periods greater than a week). These calculations were for a JHGM canister that has no internal fins. An ICM canister with internal fins would have a lower maximum glass temperature.

Also of interest are maximum temperatures in the repository. The thermal analysis models for repository emplacement must take into account the heat-sink behavior of the repository media and the type of canister overpack and back-fill. The thermal calculation must be a transient calculation since the repository temperature increases to a maximum several years after the canisters are put in place and then falls off slowly over a long period of time as the canister thermal output decays.

One of the primary objectives of this report is to supply a canister design and waste loading specification that can be used as input for detailed repository thermal history calculations by other contractors supporting the NWTs program. Therefore, the repository thermal analyses reported here are

simply for the purpose of verifying that the canister size and the decay-heat loading specified for the canister are compatible with existing repository design constraints.

The repository conditions developed by an ONWI-sponsored Interface Working Group (NWT-3 1980) for commercial high-level waste in a salt repository assumed a similar canister design and decay-heat content as that assumed in this report. The Interface Working Group also assumed an average repository heat loading of 25 W/m^2 (100 kW/acre). From this assumption, it is possible to calculate the average salt temperature in the repository as a function of time, reflecting the decay in thermal emission from the HLW canisters. Using the average salt temperature as the heat-sink temperature for the canister temperature profile calculation yields a time-dependent temperature plot of various points in the waste-form/overpack model.

A model of the canister emplacement in the repository borehole is shown in Figure 18. The canister is surrounded by a steel overpack. The space between the canister and the overpack is an empty airspace. The overpack/canister assembly is lowered into a borehole in the salt, which has a steel liner in the hole to facilitate retrieval should that become necessary. The annulus between the overpack and the liner is backfilled with crushed salt.

The temperature history for the glass centerline, the canister surface, and the nearby-salt temperature is shown in Figure 19. The maximum glass temperature is $\sim 320^\circ\text{C}$, which occurs shortly after emplacement. The canister wall temperature reaches a maximum of 265°C . The highest average temperature for the nearby salt is $\sim 160^\circ\text{C}$, which occurs 15 to 20 years after emplacement.

Researchers at the Advanced Energy Systems Division of the Westinghouse Electric Corporation have proposed a waste emplacement model that emphasizes maximum isolation of the waste form from ground-water attack or lithostatic forces for a period in excess of a thousand years. A cross section typical of a maximum isolation model is shown in Figure 20. The concept employs a thick steel overpack to withstand the lithostatic pressure within the repository. A titanium overpack acts as a corrosion barrier. A compressed mixture of bentonite and sand is used to seal the waste package against water intrusion. This

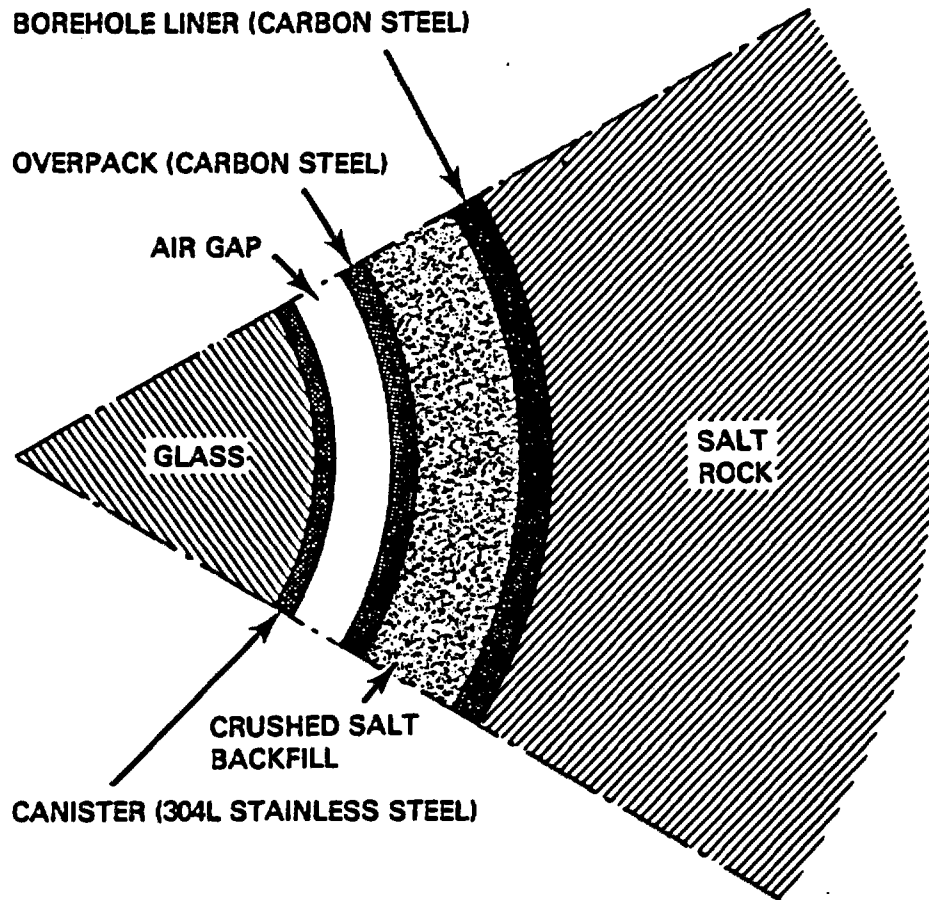


FIGURE 18. Canister Emplacement Model for a Salt Repository (NMTS-3 1980)

model may be unnecessarily complex for salt. It may be desirable to make the canister bear the lithostatic pressure and provide a titanium overpack for the corrosion protection. The compressed bentonite backfill is more appropriate for basalt or granite repositories where some ground-water intrusion is probable. Only a few liters of brine are predicted to reach the borehole in a salt repository. It can be argued that if sufficient water were to reach the emplacement site to warrant the bentonite backfill it would have already dissolved the surrounding salt. However, this complex model is useful since it tends to maximize the waste centerline temperature. The temperature profile for this model is also shown in Figure 20 for a time shortly after emplacement of 10-year-old HLW. The maximum glass centerline temperature is $\sim 430^{\circ}\text{C}$; the maximum canister wall temperature is $\sim 350^{\circ}\text{C}$. A temperature history for the

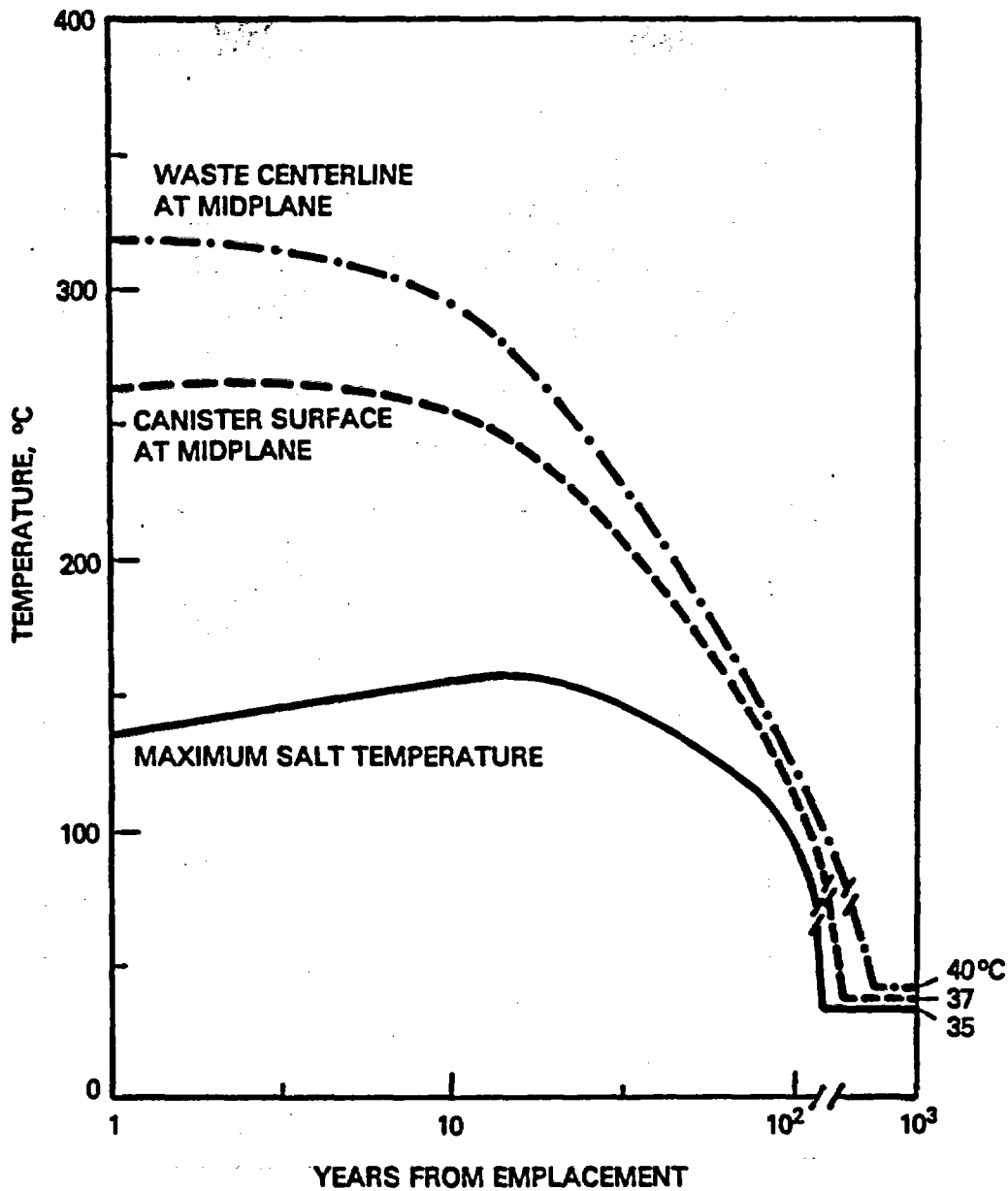


FIGURE 19. Thermal Response as a Function of Time for a Salt Repository with the Canister Emplacement Model of NWTs-3 (1980)

maximum isolation model in a salt repository is given for the first thousand years in Figure 21. The glass centerline temperature and the temperature of the titanium corrosion barrier are given. The average salt-bed temperature is taken from NWTs-3 (1980) for a repository having 100 kW/acre thermal loading from HLW canister placement.

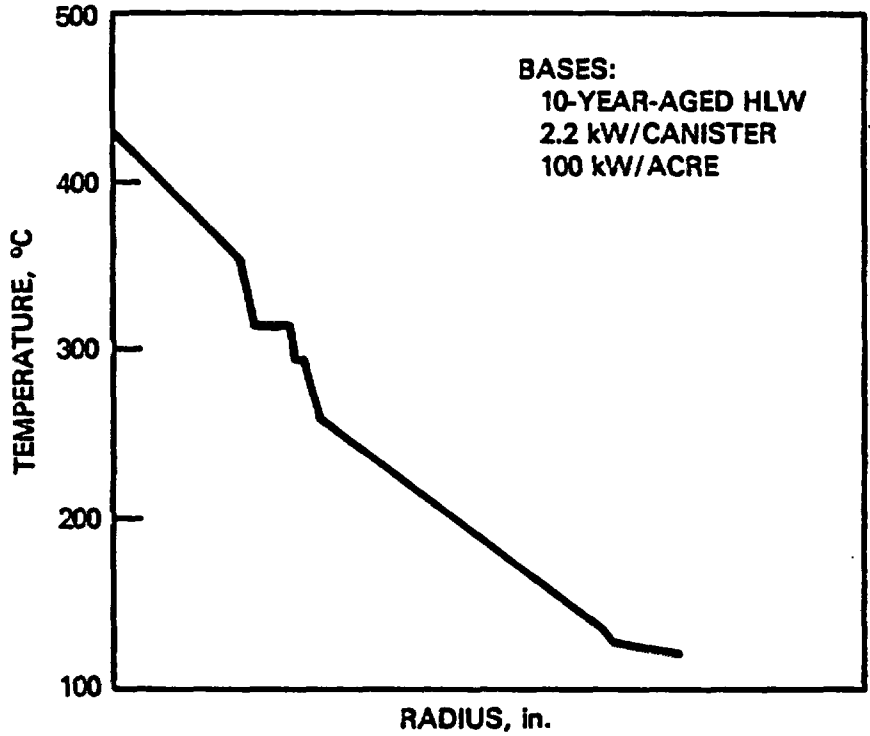
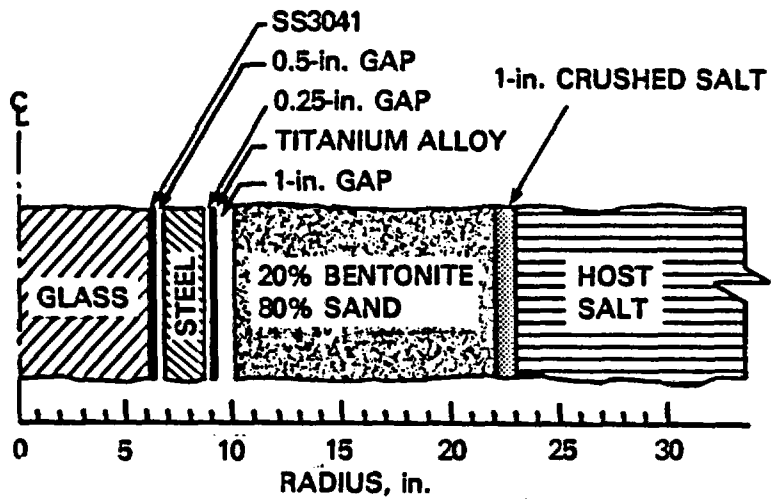


FIGURE 20. Maximum Temperature Profile for a Canister Emplacement in a Salt Repository with the Maximum Isolation Package Model

The maximum glass temperatures calculated for the two different emplacement models are acceptable. Interpretation of the effects of the maximum temperature for the steel and titanium overpacks and the salt or bentonite backfill are beyond the scope of this report.

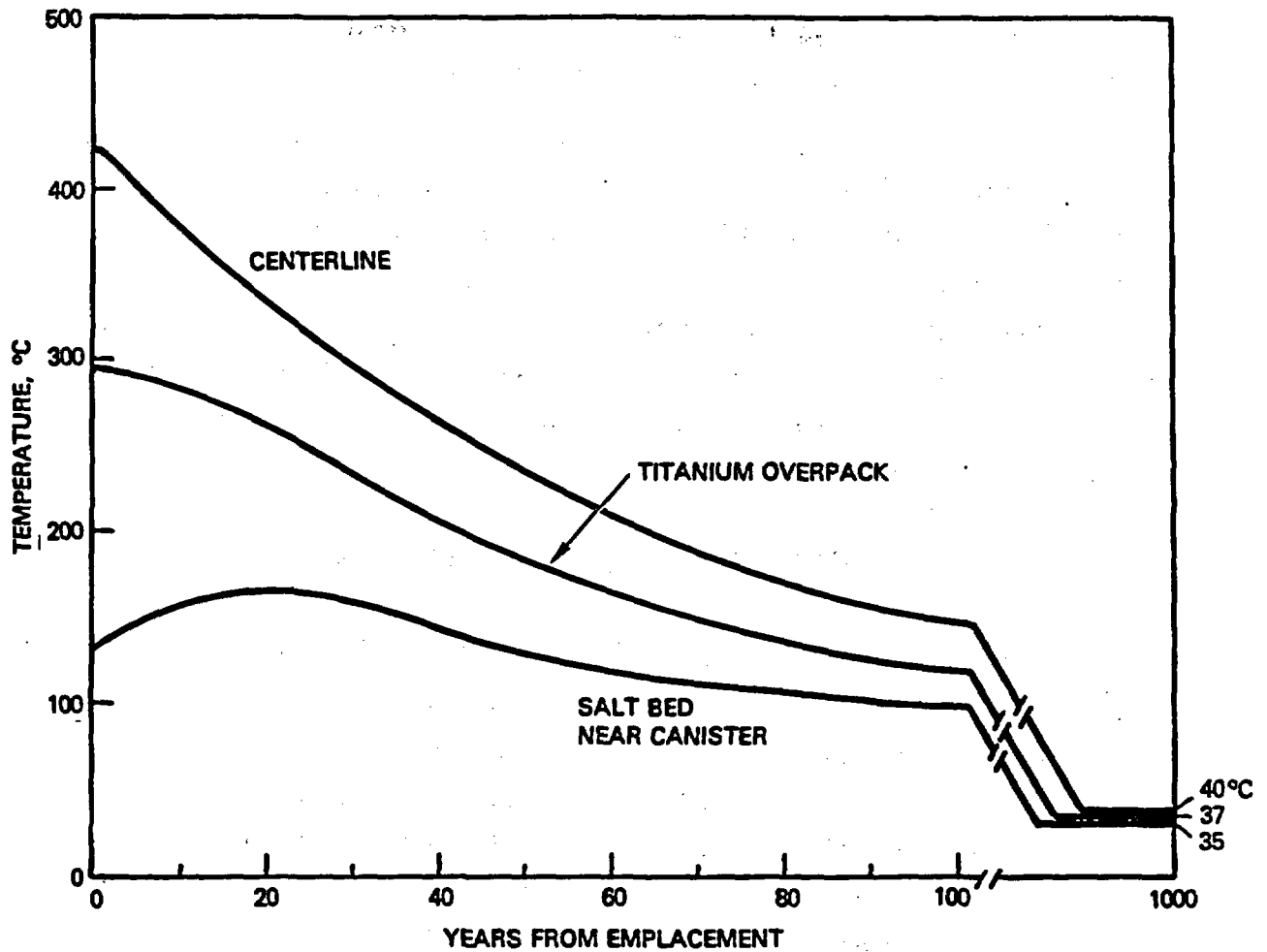


FIGURE 21. Thermal Response as a Function of Time for a Salt Repository with the Maximum Isolation Emplacement Package Model

RADIATION ANALYSIS

Radiation flux is an important consideration in the design of systems for canister storage and transportation of HLW canisters. The reference canister contains 2.28 MTU (metric tonne uranium waste equivalent). The complete description of the radionuclides is given in the ORIGEN II calculation in the appendix. The gamma radiation is the principal contributor to dose from the canisters. Beta radiation and neutrons can be neglected for the preliminary calculations. The ORIGEN II code calculates the source terms for the gamma radiation. The energy-dependent source terms are input to the QAD code (Cain

1977), and the gamma flux is calculated at the canister surface, taking into account the glass composition, canister wall, and canister geometry.

Predictions of the gamma flux and dose profiles at the canister surface for 5, 10, 50, and 100 years were calculated with the QAD code. The gamma source terms are given in Table 13, the gamma energy flux is given in Table 14, and the dose rate is given in Table 15. Also, Table 16 gives the direct gamma spectrum that can be used in combination with the energy flux of Table 14 to calculate the dose through various overpacks and repository backfill configurations. Figure 22 is a relative profile of the dose rate around a HLW canister containing 5-year-aged waste.

TABLE 13. Gamma Source Terms^(a) (MeV/W-s/MTU)

Group	E (MeV)	Decay Time, yr			
		5	10	50	100
1	0.085	1.3 + 6	8.6 + 5	3.0 + 5	9.4 + 4
2	0.125	1.7 + 6	1.0 + 6	3.0 + 5	9.0 + 4
3	0.225	3.0 + 6	1.9 + 6	7.0 + 5	2.1 + 5
4	0.375	2.7 + 6	1.5 + 6	5.0 + 5	1.5 + 5
5	0.575	7.5 + 7	4.9 + 7	1.8 + 7	5.6 + 6
6	0.85	2.4 + 7	6.1 + 6	2.6 + 5	5.8 + 4
7	1.25	7.5 + 6	3.6 + 6	2.1 + 5	3.0 + 4
8	1.75	3.9 + 5	1.6 + 5	1.5 + 4	3.1 + 3
9	2.25	2.7 + 5	4.3 + 3	1.4 + 0	0
10	2.75	1.0 + 4	3.3 + 2	0	0
11	3.5	1.7 + 3	5.4 + 1	0	0

Power = 38.4×10^6 W

2.28 MTU per canister

$S = (38.4 \times 10^6) \times 2.28 = 8.76 \times 10^7$ with above spectrum

(a) From ORIGEN.

TABLE 14. Energy Flux at Canister Surface Versus Decay Time (Flux in 10^{10} MeV/cm²-s)

Radial Surface (R = 15.875 cm)		Decay Time, yr			
Distance from Bottom of Canister		5	10	50	100
0		3.0	1.6	0.46	0.14
25		6.4	3.3	0.98	0.30
50		7.4	3.9	1.2	0.35
75		8.9	4.7	1.4	0.43
100		10.3	5.5	1.7	0.51
(Center at 132)	125	10.9	5.8	1.8	0.54
	150	10.5	5.6	1.9	0.52

Axial Surface (Z = 293.1 cm)		Decay Time, yr			
Distance from Axial Centerline, cm		5	10	50	100
0		1.1	0.61	0.19	0.054
15		0.94	0.50	0.15	0.047

TABLE 15. Dose Rate at Canister Surface Versus Decay Time (Dose Rate in 10^6 mrem/h)

Radial Surface (R = 15.875 cm)		Decay Time, yr			
Distance from Bottom of Canister		5	10	50	100
0		56	30	8.6	2.7
25		118	62	19	5.8
50		137	72	22	6.8
75		165	86	27	8.3
100		192	104	31	9.7
(Center at 132)	125	204	108	33	10
	150	196	105	32	9.7

Axial Surface (Z = 293.1 cm)		Decay Time, yr			
Distance from Axial Centerline, cm		5	10	50	100
0		21	12	3.5	1.1
15		18	9.4	2.9	0.90

TABLE 16. Direct Beam Gamma Spectrum Versus Decay Time (MeV/cm² s)
 (Detector at Z = 125 cm, R = 15.875 cm; Un-normalized Spectrum)

Group	E (MeV)	Decay Time, yr			
		5	10	50	100
1	0.085	7.1 + 1	4.6 + 1	1.6 + 1	5.1
2	0.125	3.0 + 5	1.8 + 5	5.2 + 4	1.6 + 4
3	0.225	8.4 + 7	5.4 + 7	2.0 + 7	5.9 + 6
4	0.375	3.6 + 8	2.0 + 8	6.7 + 7	2.0 + 7
5	0.575	1.9 + 10	1.2 + 10	4.6 + 9	1.4 + 9
6	0.850	9.2 + 9	2.3 + 9	9.9 + 7	2.2 + 7
7	1.250	3.9 + 9	1.9 + 9	1.1 + 8	1.6 + 7
8	1.750	2.7 + 8	1.1 + 8	1.0 + 7	2.2 + 6
9	2.250	2.2 + 8	3.5 + 6	1.1 + 3	0
10	2.750	9.5 + 6	3.0 + 5	0	0
11	3.500	1.7 + 6	5.5 + 4	0	0

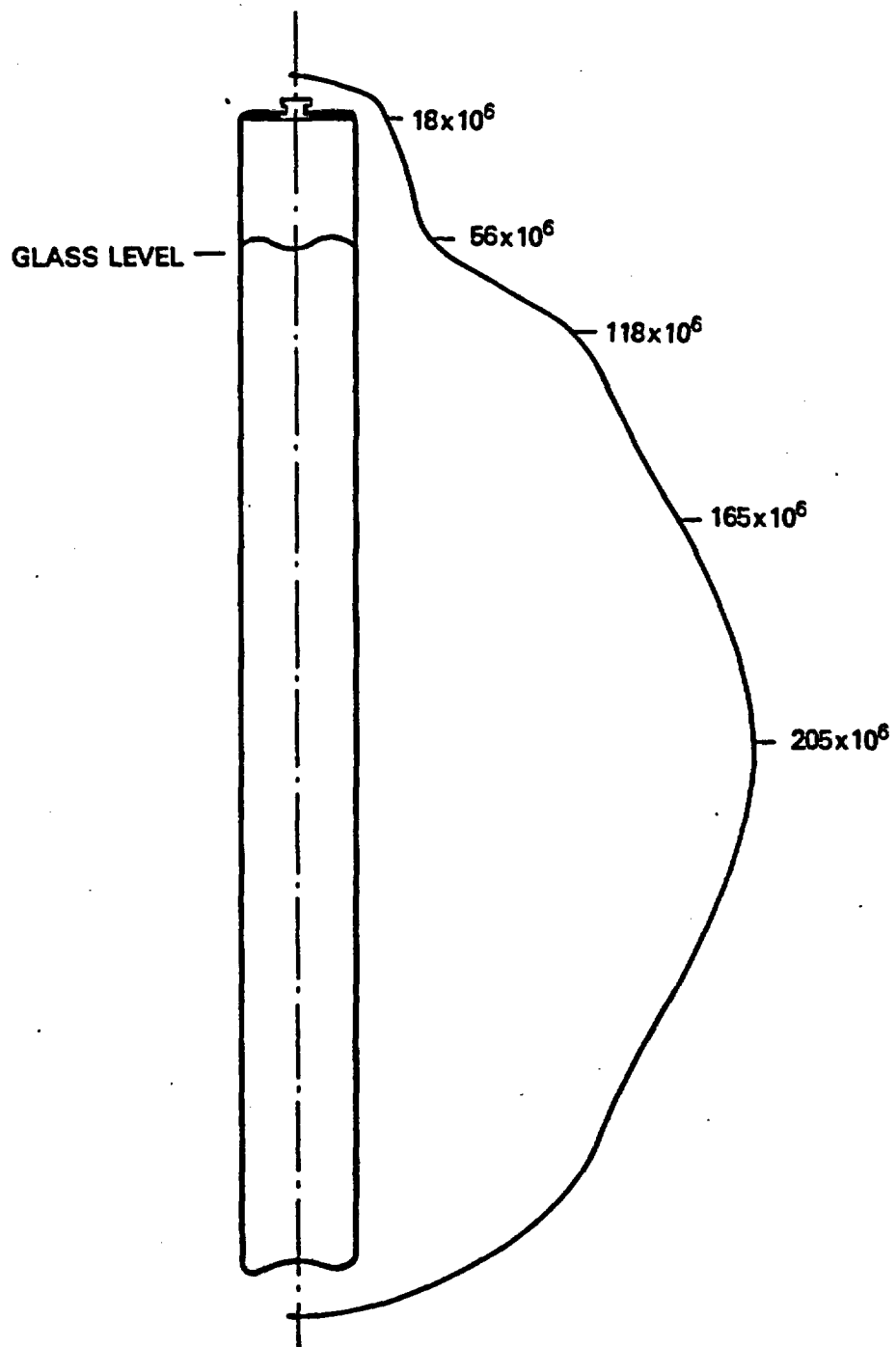


FIGURE 22. Profile of High-Level Waste Canister Dose Rate, mrem/h (at time of reprocessing, 5 years aged)

REFERENCES

- Bell, M. J. 1978. ORIGEN--The ORNL Isotope Generation and Depletion Code, ORNL-4628, Oak Ridge National Laboratory, Oak Ridge, Tennessee.
- Bunnell, L. R. 1979. Tests for Determining Impact Resistance and Strength of Glass Used for Nuclear Waste Disposal. PNL-2954, Pacific Northwest Laboratory, Richland, Washington.
- Cain, V. R. 1977. A Users Manual for QAD-CG, The Combinational Geometry Version of the QAD-P5A Point Kernel Shielding Code. CCC-307, Reactor Safety Information Center Computer Code Collection, Oak Ridge National Laboratory, Oak Ridge, Tennessee.
- Chick, L. A. et al. 1980. Annual Report on the Development and Characterization of Solidified Forms for Nuclear Wastes, 1979. PNL-3465, Pacific Northwest Laboratory, Richland, Washington.
- Code of Federal Regulations, Title 10, Part 60. 1980. "Technical Criteria for Regulating Geologic High-Level Radioactive Waste." Federal Register, Vol. 45, No. 94, Tuesday, May 13, 1980. Advanced Notice of Rule Making.
- Code of Federal Regulations, Title 40, Part 191. 1979. "Working Draft of Environmental Radiation Protection Standards for Management and Disposal of Spent Nuclear Fuel, High-Level and Transuranic Radioactive Waste."
- Code of Federal Regulations, Title 10, Part 50, Appendix F. 1978.
- Croff, A. G. 1980. A Users Manual for the ORIGEN-II Computer Code. ORNL-TM-7175, Oak Ridge National Laboratory, Oak Ridge, Tennessee.
- Doremus, R. H. 1973. "Phase Separation." Glass Science, pp. 44-73, John Wiley and Sons, New York, New York.
- E. I. duPont Nemours Co. 1978. Spent LWR Fuel Recycle Complex Conceptual Design, Case A-1, Separated Streams. DP-CFP-78-121, Savannah River Laboratory, Aiken, South Carolina.
- Elliot, R. M. 1945. "Glass Composition and Density Changes." Journal of the American Ceramic Society. 28:303-305.
- Exxon Nuclear Company. 1977. PSAR for Nuclear Fuel Recovery and Recycling Center. XN-FR-32, Rev. 1, Exxon Nuclear Company, Richland, Washington.
- Gray, W. J. 1976. Volatility of a Zinc Borosilicate Glass Containing Simulated High-Level Radioactive Waste. BNWL-2111, Pacific Northwest Laboratory, Richland, Washington.

- Goldman, M. I. et al. 1958. "Retention of Fission Products in Ceramic-Glaze-Type Fusions." In Proceedings of Second U.N. Int. Conf. Peaceful Uses At. Energy, 1958, Geneva. 18:27, United Nations, New York, New York.
- International Atomic Energy Agency (IAEA). 1977. Techniques for the Solidification of High-Level Wastes. Technical Reports Series No. 176, p. 16, International Atomic Energy Agency, Vienna, Austria.
- International Nickel Company, Inc. 1973. Huntington Alloys Bulletin on Inconel 601. International Nickel Company, New York, New York.
- Larson, D. E., Editor. 1980. Spray Calciner/In-Can Melter High-Level Waste Solidification Technical Manual. PNL-3495, Pacific Northwest Laboratory, Richland, Washington.
- Malow, G. and E. Schiewer. 1972. Fission Products in Glasses, Part I: Borosilicate Glasses Containing Fission Products. HMI-B217, Hahn-Meitner Institute, Berlin, Germany.
- Mendel, J. E. and J. L. McElroy. 1972. Waste Solidification Program, Volume 10, Evaluation of Solidified Waste Products. BNWL-1666, Pacific Northwest Laboratory, Richland, Washington.
- Mendel, J. E. 1973. "Measurements on Core-Drilled Samples." Quarterly Progress Report, Research and Development Activities, Waste Fixation Program, April through June 1973. BNWL-1761, pp. 16-18, Pacific Northwest Laboratory, Richland, Washington.
- Mendel, J. E. et al. 1977. Annual Report on the Characteristics of High-Level Waste Glasses. BNWL-2252, Pacific Northwest Laboratory, Richland, Washington.
- Mendel, J. E. 1978. The Storage and Disposal of Radioactive Waste as Glass in Canisters. PNL-2764, Pacific Northwest Laboratory, Richland, Washington.
- Merritt, W. F. and P. J. Parsons. 1964. "The Safe Burial of High-level Fission Product Solutions Incorporated into Glass." Health Physics. 10:655.
- Merritt, W. F. 1977. "High-level Waste Glass: Field Leach Test." Nuclear Technology. 32:88-91.
- Nesbitt, J. F., S. C. Slate, and L. K. Fetrow. 1980. Decontamination of High-Level Waste Canisters. PNL-3514, Pacific Northwest Laboratory, Richland, Washington.
- NWTS-3. 1980. Interim Reference Repository Conditions for Commercial and Defense High-Level Nuclear Waste and Spent Fuel Repositories in Salt. Office of Nuclear Waste Isolation, Battelle Memorial Institute, Columbus, Ohio.

- Perez, J. M. and J. H. Westsik. 1980. "Effects of Cracks on Glass Leaching." Presented at ORNL Conference on the Leachability of Radioactive Solids, Gatlinburg, Tennessee, December 9-12, 1980.
- Ross, W. A. "Process for Solidifying High-Level Nuclear Waste," U.S. Patent No. 4,094,809, June 13, 1978.
- Ross, W. A. et al. 1978. Annual Report on the Characterization of High-Level Waste Glasses. PNL-2625, Pacific Northwest Laboratory, Richland, Washington.
- Ross, W. A. et al. 1979. Annual Report on the Development and Characterization of Solidified Forms for High-Level Wastes, 1978. PNL-3060, Pacific Northwest Laboratory, Richland, Washington.
- Ross, W. A., R. P. Turcotte, J. E. Mendel, and J. M. Rusin. 1979. "A Comparison of Glass and Crystalline Waste Materials." Ceramics in Nuclear Waste Management, CONF-790420, May 1979.
- Shand, E. B. 1958. Glass Engineering Handbook. Second Edition, McGraw-Hill Book Company, New York, New York.
- Simonen, F. A. and S. C. Slate. 1979. Stress Analysis of High-Level Waste Canisters: Methods, Applications, and Design Data. PNL-3036, Pacific Northwest Laboratory, Richland, Washington.
- Slate, S. C. and R. F. Maness. 1978. "Corrosion Experience in Nuclear Waste Processing at Battelle-Northwest." In Materials Performance. 17(6):13-21.
- Slate, S. C., L. R. Bunnell, W. A. Ross, F. A. Simonen, and J. H. Westsik, Jr. 1978. "Stresses and Cracking in High-Level Waste Glass." In Proceedings of the Conference on High-Level Radioactive Solid Waste Forms. NUREG/CP-0005, U.S. Nuclear Regulatory Commission, December 1978.
- Smith, T. H. and W. A. Ross. 1975. Impact Testing of Vitreous Simulated High-Level Waste in Canisters. BNWL-1903, Pacific Northwest Laboratory, Richland, Washington.
- Turcotte, R. P. 1976. Radiation Effects in Solidified High-Level Wastes, Part 2--Helium Behavior. BNWL-2051, Pacific Northwest Laboratory, Richland, Washington.
- Turcotte, R. P. and J. W. Wald. 1978. Devitrification Behavior in a Zinc Borosilicate Waste Glass. PNL-2247, Pacific Northwest Laboratory, Richland, Washington.
- U.S. Department of Energy (DOE). 1979. Technology for Commercial Radioactive Waste Management. DOE/ET-0028.
- U.S. Department of Energy (DOE). 1980. Final Environmental Impact Statement Management of Commercially Generated Radioactive Waste. DOE/EIS-0046F.

Wald, J. W. and J. H. Westsik, Jr. 1979. Devitrification and Leaching Effects in HLW Glass--Comparison of Simulated and Fully Radioactive Waste Glasses. CONF-790420.

Weber, W. J. et al. 1979. Radiation Effects in Vitreous and Devitrified Simulated Waste Glass. CONF-790420.

ACKNOWLEDGMENTS

Much of the material reported here is based on detailed reports related to commercial high-level waste processing and immobilization. Background information on the glass description and canister design was summarized, respectively, from The Storage and Disposal of Radioactive Waste as Glass in Canisters (J. E. Mendel 1978), and the Spray Calciner/In-Can Melter High-Level Waste Solidification Technical Manual (D. E. Larson 1980). The authors wish to acknowledge J. L. Swanson, Pacific Northwest Laboratory, for his contribution related to the description of the high-level liquid-waste composition. ORIGEN-II calculations were carried out by the Nuclear Analysis Section of the Hanford Engineering Development Laboratory. L. R. Dodd and R. A. McCann of Pacific Northwest Laboratory prepared and performed, respectively, the radiation flux analysis of the canister and the thermal analysis for the canister.

The model for the overpack system used in the canister thermal analysis is based on a report by the Advanced Energy Systems Division of the Westinghouse Electric Corporation.

D. E. Gordon of Savannah River Plant provided valuable assistance and direction in formulating the objectives of the report.

Editing and word processing were performed, respectively, by G. B. Long and M. A. Eierdam of Pacific Northwest Laboratory.



APPENDIX A

ORIGEN-II CALCULATIONS

ORIGEN-II CALCULATIONS

The radioactivity and decay heat of the reference HLW composition are typical of what would be obtained from full burnup of PWR fuel. The fuel exposure and subsequent decay history are modeled with the ORIGEN-II computer code (Croff 1980). ORIGEN-II represents an improvement over the original ORIGEN code (Bell 1978). The fuel burnup calculations can be easily modeled as a series of exposure periods interrupted by decay periods (resulting from reactor refueling). The cross sections and the method of averaging these cross sections have been improved in the ORIGEN-II code. Radionuclide decay library information has been updated, and the format for displaying the decay histories has been improved.

The assumptions regarding the type of fuel, the reactor, and the exposure history are discussed beginning on page 13 ("Fuel Exposure History").

Reprocessing is specified at 5 years after fuel discharge from the reactor. However, note that some additional decay has occurred during the exposure period when the reactor is refueled. During reprocessing, all of the He, C, N, Ne, Ar, Kr, Xe and Rn are assumed to be separated from the fission products and the actinides. Likewise, 99% of the U, Pu, I and H are assumed to be separated. The decay histories of the separated elements are calculated and are included as part of the code output.

The selected code output supplies the following information about the fuel decay history:

- concentration, g
- radioactivity, Ci
- thermal power, W
- alpha radioactivity only, Ci
- neutron emissions
- photon emissions.

The information is given for three groups of radionuclides. The first group consists of all the elements in the total fuel assembly but which become the HLW at the 5-year decay point when the fuel is reprocessed. The second group of radionuclides use the 99% of uranium and plutonium recovered during

reprocessing. The third group are the gases released during reprocessing. An index of the ORIGEN-II output selected for this report is given in Table A.1.

A cutoff feature was exercised in the code output. For example, if the radioactivity of a radionuclide never exceeds 1×10^{-10} at any time in the decay history that radionuclide is not printed in the radionuclide table. This cutoff feature is applied to all calculated quantities. It is possible to have a radionuclide listed in the concentration table but not in the radioactivity or thermal power tables because of this feature.

A note of caution is required regarding the "Cumulative Table Totals" given of the end of each element summary table. The row title indicates "activation products plus actinides plus fission products," but this total is not valid until the last group, i.e., "fission products." It is in fact a cumulative table, but it is easily misinterpreted.

A full ORIGEN-II output for the case selected in this report is included on microfiche in an envelope at the end of the report. Copies may be requested from the lead author. In addition, abbreviated tables of concentration, radioactivity and thermal power for actinides (plus daughters) and fission products are given in Tables A.2 through A.7. A cutoff parameter of 10^{-3} was used to reduce the length of the tables.

TABLE A.1. Index to ORIGEN-II Output

Input

- Card image
- Neutron yield per neutron-induced fission (input)
- (Alpha, N) neutron yield in oxide fuels (input)
- Spontaneous fission neutron yield, neutron/fission (input)
- Individual element fractional recoveries (input)
- Group fractional recoveries (input)
- Element assignments to fractional recovery groups (input)
- Chemical toxicities, grams per M³ water (input--not used)

Tables of Fuel Decay Histories

- Reactivity and burnup data
- Activation products
 - Concentration, g (by radionuclide)
 - Concentration, g (by element)
 - Radioactivity, Ci (by radionuclide)
 - Radioactivity, Ci (by element)
 - Thermal power, W (by radionuclide)
 - Thermal power, W (by element)
- Actinides + Daughters
 - Concentration, g (by radionuclide)
 - Concentration, g (by element)
 - Radioactivity, Ci (by radionuclide)
 - Radioactivity, Ci (by element)
 - Thermal power, W (by radionuclide)
 - Thermal power, W (by element)
 - Alpha radioactivity, Ci (by radionuclide)
 - Alpha radioactivity, Ci (by element)
- Fission Products
 - Concentration, g (by radionuclide)
 - Concentration, g (by element)
 - Radioactivity, Ci (by radionuclide)
 - Radioactivity, Ci (by element)

TABLE A.1. (contd)

Tables of Fuel Decay Histories (contd)

- Thermal power, W (by radionuclide)
- Thermal power, W (by element)
- (Alpha, N) neutron source, neutrons/s
 - Spontaneous fission neutron source, neutrons/s
- Photon spectrum for activation products
 - 18 group photon release rates, photons/s
 - 18 group specific energy release rates, Mev/W-s
 - Principal photon sources in group (K), photons/s (individual tables for each of the 18 groups)
- Photon spectrum for actinides + daughters
 - 18 group photon release rates, photons/s
 - 18 group specific energy release rates, Mev/W-s
 - Principal photon sources in group (K), photons/s (individual tables for each of the 18 groups)
- Photon spectrum for fission products
 - 18 group photon release rates, photons/s
 - 18 group specific energy release rates, Mev/W-s
 - Principal photon sources in group (K), photons/s (individual tables for each of the 18 groups)

0.99 U and Pu Separated from the HLW Stream 5 Years After Discharge

- Reactivity and burnup data
- Activation products
 - Concentration, g
 - Radioactivity, Ci
 - Thermal power, W
- Actinides + daughters
 - Concentration, g (by radionuclide)
 - Concentration, g (by element)
 - Radioactivity, Ci (by radionuclide)
 - Radioactivity, Ci (by element)
 - Thermal power, W (by radionuclide)
 - Thermal power, W (by element)

TABLE A.1. (contd)

0.99 U and Pu Separated from the HLW Stream 5 Years After Discharge (contd)

Alpha radioactivity, Ci (by radionuclide)

Alpha radioactivity, Ci (by element)

● Fission products

Concentration, g

Radioactivity, Ci

Thermal power, W

● (Alpha, N) neutron source, neutrons/s

● Spontaneous fission neutron source, neutrons/s

● Photon spectrum for activation products

18 group photon release rates, photons/s

18 group specific energy release rates, Mev/W-s

● Photon spectrum for actinides + daughters

18 group photon release rates, photons/s

18 group specific energy release rates, Mev/W-s

Principal photon sources in group (K), photons/s (individual tables for each of the 18 groups)

● Photon spectrum for fission products

18 group photon release rates, photons/s

18 group specific energy release rates, Mev/W-s

Separate He, C, N, Ne, Ar, Kr, Xe, Rn, H, and I from the HLW Stream

● Reactivity and burnup data

● Activation products

Concentration, g (by radionuclide)

Concentration, g (by element)

Radioactivity, Ci (by radionuclide)

Radioactivity, Ci (by element)

Thermal power, W (by radionuclide)

Thermal power, W (by element)

● Actinides + Daughters

Concentration, g (by radionuclide)

Concentration, g (by element)

TABLE A.1. (contd)

Separate He, C, N, Ne, Ar, Kr, Xe, Rn, H, and I from the HLW Stream (contd)

- Radioactivity, Ci (by radionuclide)
- Radioactivity, Ci (by element)
- Thermal power, W (by radionuclide)
- Thermal power, W (by element)
- Alpha radioactivity, Ci (by radionuclide)
- Alpha radioactivity, Ci (by element)
- Fission products
 - Concentration, g (by radionuclide)
 - Concentration, g (by element)
 - Radioactivity, Ci (by radionuclide)
 - Radioactivity, Ci (by element)
 - Thermal power, W (by radionuclide)
 - Thermal power, W (by element)
- (Alpha, N) neutron source, neutrons/s
- Spontaneous fission neutron source, neutrons/s
- Photon spectrum for activation products
 - 18 group photon release rates, photons/s
 - 18 group specific energy release rates, Mev/W-s
 - Principal photon sources in group (K), photons/s (individual tables for each of the 18 groups)
- Photon spectrum for actinides + daughters
 - 18 group photon release rates, photons/s
 - 18 group specific energy release rates, Mev/watt-s
 - Principal photon sources in group (K), photons/s (individual tables for each of the 18 groups)
- Photon spectrum for fission products
 - 18 group photon release rates, photons/s
 - 18 group specific energy release rates, Mev/W-s
 - Principal photon sources in group (K), photons/s (individual tables for each of the 18 groups)

TABLE A.2. Concentration of Actinides (Plus Daughters)

OUTPUT UNIT = 6

WESTINGHOUSE 1164 MW(E) PWR, 3.1 PER CENT ENRICH., 32,700 MWD/MTU
 POWER= 3.84000+001MW, BURNUP= 3.26995+004MWD, FLUX= 3.41+014N/CM**2-SFC

SUMMARY TABLE: CONCENTRATIONS, GRAMS
 1 METRIC TON OF U AT 3.1 PER CENT ENRICHMENT

DISCHARGE	2.0YR	5.0YR	5YR(REPRO)	10.0YR	20.0YR	50.0YR	100.0YR	1.0MY	10.0MY	100.0MY	1.0BY	
HE 4	3.380-001	6.902-001	8.461-001	.000	1.127-001	3.045-001	7.188-001	1.196+000	5.088+000	7.859+000	1.184+001	3.230+001
BI209	1.401-011	2.623-011	4.409-011	4.409-011	7.747-011	1.705-010	1.137-009	8.245-009	1.014-005	1.125-002	3.689+000	1.488+002
U233	2.826-004	5.748-004	1.008-003	1.008-005	7.098-004	2.121-003	6.451-003	1.397-002	1.907-001	2.332+000	1.940+001	4.284+001
U235	7.492+003	7.493+003	7.493+003	7.493+001	7.494+001	7.495+001	7.499+001	7.507+001	7.644+001	9.605+001	2.267+002	2.370+002
U236	3.783+003	3.783+003	3.784+003	3.784+001	3.785+001	3.788+001	3.799+001	3.821+001	4.206+001	6.570+001	8.031+001	7.820+001
U238	9.452+005	9.452+005	9.452+005	9.452+003	9.452+003	9.452+003	9.452+003	9.452+003	9.452+003	9.452+003	9.453+003	9.455+003
NP237	4.256+002	4.370+002	4.382+002	4.382+002	4.407+002	4.458+002	4.607+002	4.841+002	6.989+002	7.636+002	7.421+002	5.544+002
PU239	4.853+003	4.951+003	4.951+003	4.951+001	4.959+001	4.975+001	5.012+001	5.060+001	5.714+001	8.829+001	1.075+001	1.572+006
PU240	2.044+003	2.045+003	2.047+003	2.047+001	2.046+001	2.045+001	3.917+001	4.244+001	3.913+001	1.507+001	1.081+003	2.543+008
PU241	1.352+003	1.227+003	1.062+003	1.062+001	8.357+000	4.161+000	1.219+000	1.114-001	1.552-003	7.450-004	4.834-007	.000
AM241	3.457+001	1.583+002	3.222+002	3.222+002	3.219+002	3.199+002	3.087+002	2.860+002	6.740+001	2.240+002	1.529+005	.000
AM243	9.985+001	9.999+001	9.997+001	9.997+001	9.992+001	9.983+001	9.954+001	9.909+001	9.105+001	3.910+001	8.340+003	4.901+007
CP244	2.824+001	2.617+001	2.333+001	2.333+001	1.926+001	1.314+001	4.167+000	6.148+001	6.969+015	6.314+015	6.486+015	7.172+015
SUMTOT	9.654+005	9.655+005	9.655+005	1.053+004	1.053+004	1.053+004	1.053+004	1.053+004	1.053+004	1.053+004	1.055+004	1.055+004
TOTAL	9.661+005	9.661+005	9.661+005	1.054+004	1.054+004	1.054+004	1.054+004	1.054+004	1.054+004	1.054+004	1.056+004	1.056+004

A.7

TABLE A.3. Activity of Actinides (Plus Daughters)

OUTPUT UNIT = 6

WESTINGHOUSE 1184 MWIEB FWR, 3.1 PER CENT ENRICH, 32,700 MW/D/MTU
 POWER = 3.84000+001MW, BURNUP = 3.26955+004MWD, FLUX = 3.41+014N/CM**2-5FC

DISCHARGE	SUMMARY TABLE: RADIOACTIVITY, CURIES											
	1 METRIC TON OF U AT 3.1 PER CENT ENRICHMENT											
	2.0YR	5.0YR	5YIREPROJ	10.0YR	20.0YR	50.0YR	100.0YR	1.0MY	10.0MY	100.0MY	1.0BY	
TL209	1.076-009	2.966-010	3.439-010	3.439-010	3.799-010	6.603-010	3.197-009	1.322-008	1.691-006	1.706-004	4.074-003	8.966-003
PB209	4.989-008	1.373-008	1.592-008	1.592-008	1.759-008	3.057-008	1.478-007	6.121-007	7.829-005	7.897-003	1.886-001	4.151-001
PB210	2.292-010	2.473-010	2.854-010	2.854-010	6.447-010	7.439-009	1.467-008	5.790-008	1.868-005	8.761-004	7.054-003	4.169-003
PR214	4.364-011	2.400-010	1.302-009	1.302-009	4.212-009	1.028-008	3.273-008	9.720-008	1.868-005	8.762-004	7.056-003	4.170-003
B121C	2.311-010	2.474-010	2.856-010	2.856-010	6.448-010	7.440-009	1.463-008	5.790-008	1.868-005	8.761-004	7.054-003	4.169-003
B1213	4.979-008	1.373-008	1.592-008	1.592-008	1.759-008	3.057-008	1.478-007	6.121-007	7.829-005	7.897-003	1.886-001	4.151-001
B1214	4.364-011	2.400-010	1.302-009	1.302-009	4.212-009	1.028-008	3.273-008	9.720-008	1.868-005	8.762-004	7.056-003	4.170-003
PO21C	1.235-010	2.431-010	2.709-010	2.709-010	6.448-010	7.440-009	1.463-008	5.790-008	1.868-005	8.761-004	7.054-003	4.169-003
PO213	4.872-008	1.344-008	1.558-008	1.558-008	1.721-008	2.991-008	1.446-007	5.989-007	7.660-005	7.727-003	1.845-001	4.061-001
PO214	1.027-008	2.399-010	1.302-009	1.302-009	4.211-009	1.028-008	3.272-008	9.718-008	1.868-005	8.761-004	7.054-003	4.169-003
PO214	4.365-011	2.400-010	1.302-009	1.302-009	4.213-009	1.028-008	3.273-008	9.722-008	1.868-005	8.764-004	7.057-003	4.171-003
AT217	4.979-008	1.373-008	1.592-008	1.592-008	1.759-008	3.057-008	1.478-007	6.121-007	7.829-005	7.897-003	1.886-001	4.151-001
FR222	4.365-011	2.400-010	1.302-009	1.302-009	4.213-009	1.028-008	3.273-008	9.722-008	1.868-005	8.764-004	7.057-003	4.171-003
FR221	4.979-008	1.373-008	1.592-008	1.592-008	1.759-008	3.057-008	1.478-007	6.121-007	7.829-005	7.897-003	1.886-001	4.151-001
RA225	4.961-008	1.373-008	1.592-008	1.592-008	1.759-008	3.057-008	1.478-007	6.121-007	7.829-005	7.897-003	1.886-001	4.151-001
RA226	4.361-011	2.400-010	1.302-009	1.302-009	4.213-009	1.028-008	3.273-008	9.722-008	1.868-005	8.764-004	7.057-003	4.171-003
AC225	4.979-008	1.373-008	1.592-008	1.592-008	1.759-008	3.057-008	1.478-007	6.121-007	7.829-005	7.897-003	1.886-001	4.151-001
TH229	1.294-008	1.373-008	1.592-008	1.592-008	1.759-008	3.057-008	1.478-007	6.121-007	7.829-005	7.897-003	1.886-001	4.151-001
TH230	9.769-008	3.985-007	1.334-006	1.334-006	1.362-006	1.465-006	2.112-006	4.143-006	1.069-004	1.128-003	7.046-003	4.171-003
PA233	2.906-001	3.082-001	3.090-001	3.090-001	3.108-001	3.144-001	3.249-001	3.414-001	4.929-001	5.385-001	5.233-001	3.910-001
U233	2.736-006	5.566-006	9.758-006	9.758-006	6.874-006	2.354-005	6.247-005	1.353-004	1.843-003	2.259-002	1.878-001	4.149-001
U234	9.740-003	2.386-002	4.533-002	4.533-004	8.041-004	1.475-003	3.264-003	5.647-003	1.329-002	1.310-002	1.087-002	3.779-003
U236	2.448-001	2.449-001	2.449-001	2.449-003	2.450-003	2.452-003	2.459-003	2.473-003	2.722-003	4.253-003	5.198-003	5.061-003
NP237	3.002-001	3.082-001	3.090-001	3.090-001	3.108-001	3.144-001	3.249-001	3.414-001	4.929-001	5.385-001	5.233-001	3.910-001
NP239	2.266-007	1.994-006	1.994-001	1.994-001	1.994-001	1.991-001	1.985-001	1.976-001	1.816-001	7.797-000	1.663-003	9.773-008
PU236	2.293-003	2.544-003	2.497-003	2.497-001	2.434-001	2.297-001	1.929-001	1.449-001	7.973-002	2.419-019	.000	.000
PU239	3.018-002	3.079-002	3.079-002	3.079-000	3.084-000	3.093-000	3.117-000	3.147-000	3.553-000	5.490-000	6.643-001	9.773-008
PU240	4.659-002	4.662-002	4.667-002	4.667-000	5.575-000	6.942-000	8.928-000	9.675-000	8.920-000	3.435-000	2.464-004	5.797-009
PU241	1.393-005	1.265-005	1.095-005	1.095-003	4.608-002	5.320-002	1.256-002	1.148-001	1.600-001	7.678-002	4.982-005	.000
PU242	1.944-000	1.944-000	1.944-000	1.944-002	1.945-002	1.947-002	1.953-002	1.962-002	1.997-002	1.995-002	1.707-002	3.404-003
AM241	1.187-002	5.436-002	1.106-003	1.106-003	1.105-003	1.098-003	1.067-003	4.820-002	2.321-002	7.691-002	5.249-005	.000
AM242M	7.836-000	7.765-000	7.659-000	7.659-000	7.486-000	7.153-000	6.238-000	4.966-000	8.198-002	1.232-019	.000	.001
AM242	1.007-005	7.726-000	7.621-000	7.621-000	7.449-000	7.117-000	6.207-000	4.942-000	8.157-002	1.225-019	.000	.000
AM243	1.991-001	1.994-001	1.994-001	1.994-001	1.997-001	1.991-001	1.985-001	1.976-001	1.816-001	7.797-000	1.663-003	9.773-008
CM242	5.444-004	2.467-003	2.975-001	2.975-001	6.177-000	5.886-000	5.133-000	4.067-000	6.746-002	1.016-019	.000	.000
CM243	2.371-001	2.258-001	2.100-001	2.100-001	1.859-001	1.458-001	7.028-000	2.083-000	6.495-010	.000	.000	.000
CM244	2.286-003	2.118-003	1.888-003	1.888-003	1.559-003	1.063-003	3.373-002	4.976-001	5.640-013	5.111-013	5.250-013	5.805-013
CM245	1.733-001	1.732-001	1.732-001	1.732-001	1.731-001	1.730-001	1.726-001	1.719-001	1.597-001	7.665-002	4.974-005	.000
SUMTOT	2.290-007	1.350-005	1.159-005	4.229-003	3.639-003	2.802-003	1.619-003	1.127-003	2.825-002	2.598-001	3.519-000	4.572-000
TOTAL	4.741-007	1.350-005	1.159-005	4.230-003	3.639-003	2.802-003	1.620-003	1.127-003	2.826-002	2.598-001	3.533-000	4.587-000

A.8

TABLE A.4. Decay Heat of Actinides (Plus Daughters)

OUTPUT UNIT = 6

WESTINGHOUSE 1184 MWIE PWR, 3.1 PER CENT ENRICH., 32,700 MW/MTU
POWER = 3.84000+001MW, BURNUP = 3.26995+004MMU, FLUX = 3.41+014N/CMP*2-5FC

SUMMARY TABLE: THERMAL POWER, WATTS

1 METRIC TON OF U AT 3.1 PER CENT ENRICHMENT

DISCHARGE	2.OYR	5.OYR	5YIREPROD	10.OYR	20.OYR	50.OYR	100.OYR	1.CMY	10.0KY	100.0KY	1.0MY	
T1209	1.787-011	4.928-012	5.713-012	5.713-012	6.317-012	1.097-011	5.304-011	2.197-010	2.810-008	2.834-006	6.768-005	1.490-004
PR209	5.737-011	1.579-011	1.831-011	1.431-011	2.023-011	3.514-011	1.700-010	7.039-010	9.003-008	9.082-006	2.169-004	4.773-004
B1213	2.093-010	5.773-011	6.692-011	6.692-011	7.395-011	1.205-010	6.214-010	2.573-009	3.291-007	3.320-005	7.928-004	1.745-003
B1214	5.592-013	3.076-012	1.668-011	1.668-011	5.398-011	1.318-010	4.194-010	1.246-009	2.394-007	1.123-005	9.042-005	5.344-005
P0210	3.958-012	7.792-012	8.683-012	8.683-012	2.067-011	7.820-011	4.689-010	1.856-009	5.987-007	2.808-005	2.261-004	1.337-004
P0213	2.465-009	6.799-010	7.882-010	7.882-010	4.709-010	1.514-009	7.320-009	7.031-008	3.876-006	3.910-004	9.337-003	2.055-002
P0214	4.766-010	1.114-011	6.043-011	6.043-011	1.954-010	4.773-010	1.514-009	4.512-009	8.671-007	4.068-005	3.275-004	1.936-004
P0218	1.582-012	8.698-012	4.718-011	4.718-011	1.527-010	3.726-010	1.186-009	3.523-009	6.770-007	3.176-005	2.557-004	1.511-004
AT217	2.125-009	5.863-010	6.793-010	6.793-010	7.506-010	1.305-009	6.309-009	2.612-008	3.341-006	3.373-004	8.048-003	1.771-002
RN222	1.446-012	7.954-012	4.315-011	.000	1.756-010	3.404-010	1.084-009	3.221-009	6.191-007	2.904-005	2.338-004	1.382-004
FR221	1.922-009	5.300-010	6.144-010	6.144-010	6.789-010	1.180-009	5.706-009	2.362-008	3.022-006	3.048-004	7.279-003	1.601-002
RA225	3.479-011	9.630-012	1.116-011	1.116-011	1.233-011	7.144-011	1.037-010	4.292-010	5.490-008	5.538-006	1.322-004	2.911-004
RA226	1.259-012	6.931-012	3.760-011	3.760-011	1.218-010	2.964-010	9.451-010	7.407-009	5.395-007	2.531-005	2.038-004	1.204-004
AC225	1.739-009	4.797-010	5.561-010	5.561-010	6.145-010	1.064-009	5.164-009	2.138-008	2.735-006	2.759-004	6.588-003	1.450-002
TH229	3.958-010	4.201-010	4.870-010	4.870-010	5.781-010	4.353-010	4.523-009	1.873-008	2.395-006	2.416-004	5.769-003	1.270-002
TH230	2.764-009	1.124-008	3.774-008	3.774-008	3.854-008	4.145-008	5.977-008	1.172-007	3.026-006	3.192-005	1.994-004	1.180-004
PA233	6.595-004	6.995-004	7.014-004	7.014-004	7.054-004	7.135-004	7.374-004	7.749-004	1.119-003	1.222-003	1.188-003	8.875-004
U233	7.954-008	1.618-007	2.837-007	2.837-007	1.998-007	5.977-007	1.816-006	3.933-006	5.357-005	6.563-004	5.461-003	1.206-002
U234	2.805-004	6.873-004	1.306-003	1.306-003	2.316-005	4.244-005	9.414-005	1.626-004	3.827-004	3.773-004	3.130-004	1.089-004
U236	6.633-003	6.633-003	6.634-003	6.634-003	6.637-005	6.642-005	6.661-004	6.699-005	7.374-005	1.152-004	1.408-004	1.371-004
NP237	9.174-003	9.420-003	9.444-003	9.444-003	9.499-003	9.608-003	9.924-003	1.043-002	1.506-002	1.646-002	1.599-002	1.195-002
NP239	5.463-004	4.820-002	4.819-002	4.819-002	4.817-002	4.817-002	4.799-002	4.776-002	4.389-002	1.885-002	4.021-006	2.362-010
PU238	7.592-001	8.432-001	8.275-001	8.275-001	8.073-001	7.613-001	6.392-001	4.802-001	2.642-003	8.017-021	.000	.000
PU239	9.301-000	9.488-000	9.488-000	9.488-002	9.504-002	9.533-002	9.604-002	9.697-002	1.095-001	1.692-001	2.060-002	3.012-009
PU240	1.451-001	1.457-001	1.453-001	1.453-001	1.736-001	2.167-001	2.787-001	3.012-001	2.777-001	1.073-001	7.671-006	1.805-010
PU241	4.318-000	3.922-000	3.395-000	3.395-002	2.669-002	1.644-002	3.895-003	7.558-004	4.959-006	2.380-006	1.545-009	.000
PU242	5.739-002	5.740-002	5.740-002	5.740-004	5.743-004	5.750-004	5.768-004	5.794-004	5.899-004	5.891-004	5.041-004	1.005-004
AM241	3.943-000	1.806-001	3.675-001	3.675-001	3.671-001	3.649-001	3.521-001	3.267-001	7.710-000	2.555-003	1.744-006	.000
AM243	6.401-001	6.410-001	6.409-001	6.409-001	6.406-001	6.400-001	6.387-001	6.352-001	5.837-001	2.507-001	5.347-005	3.142-009
CM242	6.325-001	2.866-000	3.456-002	3.456-002	7.172-003	6.838-003	5.944-003	4.748-003	7.838-005	1.181-022	.000	.000
CM243	8.698-001	8.285-001	7.702-001	7.702-001	6.820-001	5.348-001	2.578-001	7.642-002	2.383-011	.000	.000	.000
CM244	7.995-001	7.408-001	6.604-001	6.604-001	5.454-001	3.720-001	1.180-001	1.741-000	1.773-014	1.788-014	1.836-014	2.031-014
CM245	5.750-003	5.749-003	5.747-003	5.747-003	5.745-003	5.740-003	5.726-003	5.703-003	5.299-003	2.543-003	1.650-006	.000
SUMTOT	5.488-004	2.028-002	2.145-002	1.054-002	9.375-001	7.602-001	4.900-001	3.602-001	8.750-000	5.720-001	8.403-002	1.103-001
TOTAL	1.207-005	2.089-002	2.146-002	1.054-002	9.376-001	7.603-001	4.901-001	3.603-001	8.752-000	5.724-001	8.427-002	1.106-001

A.9

TABLE A.5. Concentration of Fission Products

OUTPUT UNIT = 6

WESTINGHOUSE 1184 MW(1) PWR, 3.1 PER CENT ENRICH., 32,700 MW/DHTU
POWER= 3.84000+001Mw, BURNUP= 3.26955+00MMWU, FLUX= 3.41+01M/CM^2-SFC

SUMMARY TABLE: CONCENTRATIONS, GRAMS

1 METRIC TON OF U AT 3.1 PER CENT ENRICHMENT
% CYR (VIREPRO)

DISCHARGE	2.0YR	5.0YR	10.0YR	20.0YR	50.0YR	100.0YR	1.0KY	10.0KY	100.0KY	1.0MY
SE 82	3.294+001	3.294+001	3.294+001	3.294+001	3.294+001	3.294+001	3.294+001	3.294+001	3.294+001	3.294+001
SR 83	3.989+001	3.990+001	3.990+001	.000	.000	.000	.000	.000	.000	.000
KR 84	1.109+002	1.109+002	1.109+002	.000	.000	.000	.000	.000	.000	.000
RB 85	9.525+001	9.608+001	1.017+002	1.017+002	1.017+002	1.017+002	1.017+002	1.017+002	1.017+002	1.017+002
KR 86	1.849+002	1.849+002	1.849+002	.000	.000	.000	.000	.000	.000	.000
RE 87	2.372+002	2.372+002	2.372+002	2.372+002	2.372+002	2.372+002	2.372+002	2.372+002	2.372+002	2.372+002
SA 88	3.402+002	3.402+002	3.402+002	3.402+002	3.402+002	3.402+002	3.402+002	3.402+002	3.402+002	3.402+002
Y 89	4.142+002	4.435+002	4.435+002	4.435+002	4.435+002	4.435+002	4.435+002	4.435+002	4.435+002	4.435+002
SR 90	5.177+002	4.936+002	4.596+002	4.596+002	4.060+002	7.216+002	1.575+002	4.790+001	2.382+000	.000
ZR 91	2.130+001	4.538+001	7.941+001	7.941+001	1.310+002	2.174+002	3.816+002	4.912+002	5.391+002	5.391+002
ZR 92	6.245+002	6.247+002	6.247+002	6.247+002	6.247+002	6.247+002	6.247+002	6.247+002	6.247+002	6.247+002
ZR 93	7.031+002	7.035+002	7.035+002	7.035+002	7.035+002	7.035+002	7.035+002	7.035+002	7.035+002	7.035+002
NB 94	6.001+005	1.660+004	4.199+004	4.199+004	1.057+003	2.929+003	1.094+003	2.640+002	3.132+001	3.175+000
ZF 94	7.268+002	7.268+002	7.268+002	7.268+002	7.268+002	7.268+002	7.268+002	7.268+002	7.268+002	7.268+002
HO 95	6.279+002	7.427+002	7.427+002	7.427+002	7.427+002	7.427+002	7.427+002	7.427+002	7.427+002	7.427+002
ZR 96	7.863+002	7.863+002	7.863+002	7.863+002	7.863+002	7.863+002	7.863+002	7.863+002	7.863+002	7.863+002
HO 96	3.445+001	3.445+001	3.445+001	3.445+001	3.445+001	3.445+001	3.445+001	3.445+001	3.445+001	3.445+001
HO 97	7.793+002	7.802+002	7.802+002	7.802+002	7.802+002	7.802+002	7.802+002	7.802+002	7.802+002	7.802+002
HO 98	8.150+002	8.150+002	8.150+002	8.150+002	8.150+002	8.150+002	8.150+002	8.150+002	8.150+002	8.150+002
TC 99	7.569+002	7.610+002	7.610+002	7.610+002	7.610+002	7.610+002	7.610+002	7.610+002	7.610+002	7.610+002
RU 99	3.625+003	8.578+003	1.601+002	1.601+002	2.639+002	5.315+002	1.274+001	2.512+001	2.476+000	2.437+001
HO100	9.195+002	9.195+002	9.195+002	9.195+002	9.195+002	9.195+002	9.195+002	9.195+002	9.195+002	9.195+002
RU100	9.531+001	9.532+001	9.532+001	9.532+001	9.532+001	9.532+001	9.532+001	9.532+001	9.532+001	9.532+001
RU101	7.649+002	7.650+002	7.650+002	7.650+002	7.650+002	7.650+002	7.650+002	7.650+002	7.650+002	7.650+002
RU102	7.669+002	7.669+002	7.669+002	7.669+002	7.669+002	7.669+002	7.669+002	7.669+002	7.669+002	7.669+002
RU103	4.113+002	4.635+002	4.635+002	4.635+002	4.635+002	4.635+002	4.635+002	4.635+002	4.635+002	4.635+002
RU104	5.472+002	5.472+002	5.472+002	5.472+002	5.472+002	5.472+002	5.472+002	5.472+002	5.472+002	5.472+002
PD104	2.225+002	2.225+002	2.225+002	2.225+002	2.225+002	2.225+002	2.225+002	2.225+002	2.225+002	2.225+002
PD105	3.788+002	3.803+002	3.803+002	3.803+002	3.803+002	3.803+002	3.803+002	3.803+002	3.803+002	3.803+002
RU106	1.663+002	4.204+001	5.342+000	5.342+000	1.716+001	1.770+000	1.944+013	2.273+028	.000	.000
PD106	2.062+002	3.305+002	3.671+002	3.671+002	3.723+002	3.725+002	3.725+002	3.725+002	3.725+002	3.725+002
PD107	2.255+002	2.255+002	2.255+002	2.255+002	2.255+002	2.255+002	2.255+002	2.255+002	2.255+002	2.255+002
PD108	1.556+002	1.556+002	1.556+002	1.556+002	1.556+002	1.556+002	1.556+002	1.556+002	1.556+002	1.556+002
AG109	7.858+001	7.877+001	7.877+001	7.877+001	7.877+001	7.877+001	7.877+001	7.877+001	7.877+001	7.877+001
PD110	5.098+001	5.098+001	5.098+001	5.098+001	5.098+001	5.098+001	5.098+001	5.098+001	5.098+001	5.098+001
CO110	3.523+001	3.504+001	3.516+001	3.516+001	3.517+001	3.517+001	3.517+001	3.517+001	3.517+001	3.517+001
CO111	2.796+001	2.850+001	2.850+001	2.850+001	2.850+001	2.850+001	2.850+001	2.850+001	2.850+001	2.850+001
TE126	7.516+001	7.671+001	7.677+001	7.677+001	7.686+001	7.705+001	7.762+001	7.858+001	7.959+001	8.060+001
1127	5.377+001	5.561+001	5.563+001	5.563+001	5.583+001	5.583+001	5.583+001	5.583+001	5.583+001	5.583+001
TE128	1.101+002	1.101+002	1.101+002	1.101+002	1.101+002	1.101+002	1.101+002	1.101+002	1.101+002	1.101+002
1129	1.765+002	1.783+002	1.783+002	1.783+002	1.783+002	1.783+002	1.783+002	1.783+002	1.783+002	1.783+002
TE130	3.523+002	3.523+002	3.523+002	3.523+002	3.523+002	3.523+002	3.523+002	3.523+002	3.523+002	3.523+002
XE131	4.171+002	4.258+002	4.258+002	.000	.000	.000	.000	.000	.000	.000
XE132	1.068+003	1.073+003	1.073+003	.000	.000	.000	.000	.000	.000	.000
CS133	1.100+003	1.113+003	1.113+003	1.113+003	1.113+003	1.113+003	1.113+003	1.113+003	1.113+003	1.113+003
XE134	1.452+003	1.452+003	1.452+003	.000	.000	.000	.000	.000	.000	.000
CS134	1.172+002	5.981+001	2.162+001	2.162+001	4.063+000	1.409+001	5.876+006	2.947+013	.000	.000
BA134	3.896+001	9.630+001	1.343+002	1.343+002	1.521+002	1.560+002	1.561+002	1.561+002	1.561+002	1.561+002
CS135	2.863+002	2.870+002	2.870+002	2.870+002	2.870+002	2.870+002	2.870+002	2.870+002	2.870+002	2.870+002
BA135	2.755+001	2.758+001	2.760+001	2.760+001	2.765+001	2.773+001	2.799+001	2.843+001	3.621+001	1.139+000
XE136	2.328+003	2.328+003	2.328+003	.000	.000	.000	.000	.000	.000	.000

A.10

TABLE A.5. (contd)

SUMMARY TABLE: CONCENTRATIONS, GRAMS
1 METRIC TON OF U AT 3.1 PER CENT ENRICHMENT

DISCHARGE	2.0YR	5.0YR	5YIR(FPRO)	10.0YR	20.0YR	50.0YR	100.0YR	1.0MY	10.0MY	100.0MY	1.0MY
CS137	1.179+003	1.126+003	1.050+003	1.050+003	9.354+002	7.424+002	3.717+002	1.169+002	1.088+002	.000	.000
BA137	4.017+001	9.341+001	1.688+002	1.688+002	2.834+002	4.764+002	8.477+002	1.102+003	1.219+003	1.219+003	1.219+003
BA138	1.257+003	1.257+003	1.257+003	1.257+003	1.257+003	1.257+003	1.257+003	1.257+003	1.257+003	1.257+003	1.257+003
LA139	1.199+003	1.200+003	1.200+003	1.200+003	1.200+003	1.200+003	1.200+003	1.200+003	1.200+003	1.200+003	1.200+003
CE140	1.186+003	1.214+003	1.214+003	1.214+003	1.214+003	1.214+003	1.214+003	1.214+003	1.214+003	1.214+003	1.214+003
PF141	1.041+003	1.100+003	1.100+003	1.100+003	1.100+003	1.100+003	1.100+003	1.100+003	1.100+003	1.100+003	1.100+003
CF142	1.109+003	1.109+003	1.109+003	1.109+003	1.109+003	1.109+003	1.109+003	1.109+003	1.109+003	1.109+003	1.109+003
ND143	7.382+002	7.626+002	7.626+002	7.626+002	7.626+002	7.626+002	7.626+002	7.626+002	7.626+002	7.626+002	7.626+002
CE144	3.447+002	5.805+001	4.013+000	4.013+000	4.671+002	6.331+002	1.574+017	7.203+037	.000	.000	.000
AD144	9.591+002	1.246+003	1.300+003	1.300+003	1.304+003	1.304+003	1.304+003	1.304+003	1.304+003	1.304+003	1.304+003
ND145	6.609+002	6.612+002	6.612+002	6.612+002	6.612+002	6.612+002	6.612+002	6.612+002	6.612+002	6.612+002	6.612+002
ND146	6.765+002	6.765+002	6.765+002	6.765+002	6.765+002	6.765+002	6.765+002	6.765+002	6.765+002	6.765+002	6.765+002
PF147	1.327+002	8.314+001	3.764+001	3.764+001	1.004+001	7.152+001	2.587+004	4.729+010	.000	.000	.000
SM147	6.299+001	1.209+002	1.664+002	1.664+002	1.940+002	7.033+002	2.040+002	7.040+002	2.040+002	2.040+002	2.040+002
ND148	3.659+002	3.659+002	3.659+002	3.659+002	3.659+002	3.659+002	3.659+002	3.659+002	3.659+002	3.659+002	3.659+002
SM148	1.624+002	1.653+002	1.653+002	1.653+002	1.653+002	1.653+002	1.653+002	1.653+002	1.653+002	1.653+002	1.653+002
ND150	1.762+002	1.762+002	1.762+002	1.762+002	1.762+002	1.762+002	1.762+002	1.762+002	1.762+002	1.762+002	1.762+002
SM150	3.101+002	3.101+002	3.101+002	3.101+002	3.101+002	3.101+002	3.101+002	3.101+002	3.101+002	3.101+002	3.101+002
SM152	1.324+002	1.324+002	1.324+002	1.324+002	1.324+002	1.324+002	1.324+002	1.324+002	1.324+002	1.324+002	1.324+002
EU153	1.079+002	1.091+002	1.091+002	1.091+002	1.091+002	1.091+002	1.091+002	1.091+002	1.091+002	1.091+002	1.091+002
SM154	3.798+001	3.843+001	3.843+001	3.843+001	3.843+001	3.843+001	3.843+001	3.843+001	3.843+001	3.843+001	3.843+001
GD154	2.697+000	8.568+000	1.578+001	1.578+001	2.452+001	7.426+001	4.147+001	4.213+001	4.213+001	4.213+001	4.213+001
GD156	6.259+001	6.659+001	6.659+001	6.659+001	6.659+001	6.659+001	6.659+001	6.659+001	6.659+001	6.659+001	6.659+001
SUMTOT	3.288+004	3.329+004	3.331+004	2.746+004	2.747+004	2.747+004	2.748+004	2.749+004	2.749+004	2.749+004	2.749+004
TOTAL	3.369+004	3.369+004	3.369+004	2.781+004	2.781+004	2.781+004	2.781+004	2.781+004	2.781+004	2.781+004	2.781+004

A.11

TABLE A.6. Activity of Fission Products

OUTPUT UNIT = 6

WESTINGHOUSE 1184 MW(E) PWR, 3.1 PER CENT ENRICH., 32,700 MW/MTU
 POWER = 3.84000E+09 MW, BURNUP = 3.26955E+04 MWU, FLUX = 3.41E+14 N/CM²-SEC

SUMMARY TABLE: RADIOACTIVITY, CURIES
 1 METRIC TON OF U AT 3.1 PER CENT ENRICHMENT

DISCHARGE	2.0YR	5.0YR	5YIREPROD	10.0YR	20.0YR	50.0YR	100.0YR	1.0KY	10.0KY	100.0KY	1.0MY	
SE 79	4.027-001	4.027-001	4.027-001	4.027-001	4.027-001	4.026-001	4.025-001	4.023-001	3.984-001	3.619-001	1.385-001	9.353-006
KR 85	9.062+003	7.965+003	6.560+003	.000	.000	.000	.000	.000	.000	.000	.000	.000
SR 90	7.064+004	6.738+004	6.272+004	6.272+004	5.568+004	4.389+004	2.149+004	6.537+003	3.251-006	.000	.000	.000
Y 90	7.465+004	6.738+004	6.273+004	6.273+004	5.569+004	4.390+004	2.149+004	6.538+003	3.252-006	.000	.000	.000
ZR 93	1.767+000	1.768+000	1.768+000	1.768+000	1.768+000	1.768+000	1.768+000	1.768+000	1.768+000	1.768+000	1.768+000	1.124+000
NB 93M	1.290-001	2.793-001	4.779-001	4.779-001	7.483-001	1.120+000	1.559+000	1.670+000	1.679+000	1.672+000	1.606+000	1.069+000
NB 95	1.568+006	1.303+003	9.116-003	9.116-003	2.330-011	.000	.000	.000	.000	.000	.000	.000
TC 99	1.284+001	1.291+001	1.291+001	1.291+001	1.291+001	1.291+001	1.291+001	1.290+001	1.287+001	1.249+001	9.322+000	4.984-001
RU106	5.567+005	1.407+005	1.788+004	1.788+004	5.744+002	5.923-001	6.506-010	7.608-025	.000	.000	.000	.000
HM106	6.377+005	1.407+005	1.788+004	1.788+004	5.744+002	5.926-001	6.506-010	7.608-025	.000	.000	.000	.000
PO107	1.160-001	1.160-001	1.160-001	1.160-001	1.160-001	1.160-001	1.160-001	1.160-001	1.159-001	1.148-001	1.043-001	1.043-001
SB125	1.430+004	8.759+003	4.135+003	4.135+003	1.167+003	9.688+001	5.319-002	1.958-002	.000	.000	.000	.000
TE125M	2.971+003	2.138+003	1.209+003	1.209+003	2.487+002	2.364+001	1.294-002	4.777-008	.000	.000	.000	.000
SA126	7.815-001	7.815-001	7.815-001	7.815-001	7.815-001	7.814-001	7.812-001	7.810-001	7.761-001	7.292-001	3.908-001	7.639-004
SB126	1.266+003	1.094-001	1.094-001	1.094-001	1.094-001	1.094-001	1.094-001	1.093-001	1.087-001	1.021-001	5.471-002	1.070-004
SB126M	5.590+002	7.815-001	7.815-001	7.815-001	7.815-001	7.814-001	7.812-001	7.810-001	7.761-001	7.292-001	3.908-001	7.639-004
CS134	1.516+005	7.742+004	2.824+004	2.824+004	5.259+003	1.824+002	7.607-003	3.815-010	.000	.000	.000	.000
CS135	3.298-001	3.306-001	3.306-001	3.306-001	3.306-001	3.306-001	3.306-001	3.306-001	3.305-001	3.296-001	3.208-001	2.446-001
CS137	1.026+005	9.795+004	9.139+004	9.139+004	8.142+004	6.467+004	3.231+004	1.018+004	9.472-006	.000	.000	.000
BA137M	9.729+004	9.266+004	8.646+004	8.646+004	7.707+004	6.117+004	3.057+004	9.627+003	8.961-006	.000	.000	.000
CE144	1.100+006	1.853+005	1.281+004	1.281+004	1.491+002	2.020-002	5.029-014	.000	.000	.000	.000	.000
PR144	1.112+006	1.853+005	1.281+004	1.281+004	1.491+002	2.020-002	5.029-014	.000	.000	.000	.000	.000
PR144M	1.322+004	2.223+003	1.537+002	1.537+002	1.789+000	2.424-004	6.034-016	.000	.000	.000	.000	.000
PM147	1.230+005	7.711+004	3.490+004	3.490+004	9.314+003	6.633+002	2.795-001	4.386-007	.000	.000	.000	.000
SM151	3.489+002	3.512+002	3.432+002	3.432+002	3.307+002	3.057+002	2.427+002	1.651+002	1.612-001	.000	.000	.000
EU154	1.065+004	9.064+003	7.117+003	7.117+003	4.756+002	2.124+003	1.897+002	3.365+000	.000	.000	.000	.000
EU155	6.578+003	4.974+003	3.270+003	3.270+003	1.626+003	4.019+002	6.064+000	5.597-003	.000	.000	.000	.000
SUMTOT	5.653+006	1.169+006	4.504+005	4.439+005	2.940+005	2.174+005	1.063+005	3.307+004	1.898+001	1.829+001	1.403+001	3.041+000
TOTAL	1.760+008	1.171+006	4.509+005	4.439+005	2.941+005	2.174+005	1.063+005	3.307+004	1.898+001	1.830+001	1.403+001	3.041+000

A.12

TABLE A.7. Decay Heat of Fission Products

OUTPUT UNIT = 6

WESTINGHOUSE 1184 MW(E) PWR, 3.1 PER CENT ENRICH., 37,700 MW(D)HTU
 POWER= 3.84000+001MW, BURNUP= 3.26945+004MWD, FLUX= 3.41+019A/CM**2-SEC

SUMMARY TABLE: THERMAL POWER, WATTS
 1 METRIC TON OF U AT 3.1 PER CENT ENRICHMENT

DISCHARGE	2.OYR	5.OYR	5Y(REPRO)	10.OYR	20.OYR	50.OYR	100.OYR	1.OKY	10.OKY	100.OKY	1.OYK	
SE 79	1.003-004	1.003-004	1.003-004	1.003-004	1.002-004	1.002-004	1.002-004	1.002-004	9.919-005	9.011-005	3.449-005	2.328-009
NR 85	1.357+001	1.193+001	9.827+000	.000	.000	.000	.000	.000	.000	.000	.000	.000
SR 90	8.199+001	7.818+001	7.279+001	7.279+001	6.462+001	5.394+001	2.494+001	7.587+000	3.773-009	.000	.000	.000
Y 90	4.138+002	3.734+002	3.477+002	3.477+002	3.087+002	2.433+002	1.191+002	3.624+001	1.802-008	.000	.000	.000
ZR 93	2.053-004	2.054-004	2.054-004	2.054-004	2.054-004	2.054-004	2.054-004	2.054-004	2.054-004	2.045-004	1.963-004	1.306-004
NB 93M	2.286-005	4.949-005	8.468-005	8.468-005	1.326-004	1.985-004	2.761-004	2.963-004	2.963-004	2.845-004	1.892-004	.000
ND 95	7.519+003	6.250+000	4.373-005	4.373-005	1.118-013	5.415-033	.000	.000	.000	.000	.000	.000
TC 99	6.438-003	6.473-003	6.473-003	6.473-003	6.473-003	6.472-003	6.472-003	6.471-003	6.457-003	6.266-003	4.675-003	2.499-004
RU106	3.310+001	8.366+000	1.063+000	1.063+000	3.415-002	3.522-005	3.868-014	4.523-029	.000	.000	.000	.000
RM106	6.117+003	1.350+003	1.715+002	1.715+002	5.509+000	5.684-003	6.240-012	7.297-027	.000	.000	.000	.000
PD107	6.877-006	6.877-006	6.877-006	6.877-006	6.877-006	6.877-006	6.877-006	6.877-006	6.876-006	6.870-006	6.804-006	6.181-006
AG110M	7.434+001	9.799+000	4.690-001	4.690-001	2.959-003	1.178-007	7.427-021	.000	.000	.000	.000	.000
SB125	4.472+001	2.738+001	1.293+001	1.293+001	3.699+000	3.029-001	1.663-004	6.120-010	.000	.000	.000	.000
SN126	9.747-004	9.747-004	9.746-004	9.746-004	9.746-004	9.745-004	9.743-004	9.740-004	9.689-004	9.094-004	4.874-004	9.528-007
SB126	2.340+001	2.022-003	2.021-003	2.021-003	2.021-003	2.021-003	2.021-003	2.020-003	2.008-003	1.886-003	1.011-003	1.976-006
SB126M	7.118+000	9.951-003	9.950-003	9.950-003	9.950-003	9.949-003	9.947-003	9.944-003	9.887-003	9.284-003	4.976-003	9.727-006
CS134	1.543+003	7.880+002	2.874+002	2.874+002	5.353+001	1.856+000	7.747-005	3.983-012	.000	.000	.000	.000
CS135	1.101-004	1.103-004	1.103-004	1.103-004	1.103-004	1.103-004	1.103-004	1.103-004	1.103-004	1.100-004	1.071-004	8.162-005
CS137	1.135+002	1.083+002	1.011+002	1.011+002	9.006+001	7.148+001	3.574+001	1.126+001	1.048+008	.000	.000	.000
EA137M	3.820+002	3.638+002	3.395+002	3.395+002	3.024+002	2.400+002	1.200+002	3.760+001	3.518-008	.000	.000	.000
CE144	7.297+002	1.229+002	8.494+000	8.494+000	9.889+002	1.340-005	3.334-017	1.525-036	.000	.000	.000	.000
PR144	8.174+003	1.362+003	9.413+001	9.413+001	1.096+000	1.485-004	3.696-016	.000	.000	.000	.000	.000
PM147	4.413+001	2.766+001	1.252+001	1.252+001	3.341+000	2.379+001	8.591-005	1.573-010	.000	.000	.000	.000
EU154	9.525+001	8.107+001	6.366+001	6.366+001	4.255+001	1.900+001	1.693+000	3.010-002	.000	.000	.000	.000
EU155	4.784+000	3.618+000	2.379+000	2.379+000	1.183+000	7.923-001	4.417-003	4.071-006	.000	.000	.000	.000
SUMTOT	2.541+004	4.727+003	1.525+003	1.516+003	8.768+002	6.275+002	3.015+002	9.293+001	2.003-002	1.905-002	1.178-002	6.702-004
TOTAL	2.094+006	4.729+003	1.527+003	1.517+003	8.772+002	6.276+002	3.016+002	9.295+001	2.007-002	1.905-002	1.178-002	6.704-004

A.13

DISTRIBUTION

No. of
Copies

No. of
Copies

OFFSITE

A. A. Churm
DOE Chicago Patent Group
9800 South Cass Avenue
Argonne, IL 60439

2 R. Y. Lowrey
DOE Albuquerque Operations
Office
P.O. Box 5400
Albuquerque, NM 87185

A. L. Taboas
DOE Albuquerque Operations
Office
P.O. Box 5400
Albuquerque, NM 87185

S. A. Mann
DOE Chicago Operations and
Region Office
Argonne, IL 60439

J. O. Neff
Department of Energy
Columbus Program Office
505 King Avenue
Columbus, OH 43201

W. E. Mott
DOE Division of Environmental
Control Technology
Washington, DC 20545

J. P. Hamric
DOE Idaho Operations Office
550 2nd St.
Idaho Falls, ID 83401

J. W. Peel
DOE Idaho Operations Office
550 2nd St.
Idaho Falls, ID 83401

J. B. Whitsett
DOE Idaho Operations Office
550 2nd St.
Idaho Falls, ID 83401

C. R. Cooley
DOE Nuclear Waste Management
Programs
NE-331, GTN
Washington, DC 20545

G. H. Daly
DOE Nuclear Waste Management
Programs
NE-322, GTN
Washington, DC 20545

J. E. Dieckhoner
DOE Nuclear Waste Management
Programs
NE-321, GTN
Washington, DC 20545

C. H. George
DOE Nuclear Waste Management
Programs
NE-330, GTN
Washington, DC 20545

C. A. Heath
DOE Nuclear Waste Management
Programs
NE-330, GTN
Washington, DC 20545

No. of
Copies

M. L. Lawrence
DOE Nuclear Waste Management
Programs
NE-340, GTN
Washington, DC 20545

D. J. McGoff
DOE Nuclear Waste Management
Programs
NE-320, GTN
Washington, DC 20545

S. Meyers/R. Romatowski
DOE Nuclear Waste Management
Programs
NE-30, GTN
Washington, DC 20545

G. Oertel
DOE Nuclear Waste Management
Programs
NE-320, GTN
Washington, DC 20545

A. F. Perge
DOE Nuclear Waste Management
Programs
NE-30, GTN
Washington, DC 20545

R. W. Ramsey, Jr.
DOE Nuclear Waste Management
Programs
NE-301, GTN
Washington, DC 20545

R. Romatowski
DOE Nuclear Waste Management
Programs
NE-30, GTN
Washington, DC 20545

V. Trice
DOE Nuclear Waste Management
Program
NE-30, GTN
Washington, DC 20545

No. of
Copies

D. L. Vieth
DOE Nuclear Waste Management
Programs
NE-332, GTN
Washington, DC 20545

2 S. W. Ahrends
DOE Oak Ridge Operations Office
P.O. Box E
Oak Ridge, TN 37830

D. E. Large
DOE Oak Ridge Operations Office
P.O. Box E
Oak Ridge, TN 37830

S. G. Harbinson
DOE San Francisco Operations
Office
1333 Broadway
Oakland, CA 94612

W. B. Wilson
DOE Savannah River Operations
Office
P.O. Box A
Aiken, SC 29801

R. P. Whitfield
DOE Savannah River Operations
Office
P.O. Box A
Aiken, SC 29801

J. B. Martin
Division of Waste Management
Nuclear Regulatory Commission
Washington, DC 20555

D. B. Rohrer
Division of Waste Management
Nuclear Regulatory Commission
Washington, DC 20555

No. of
Copies

No. of
Copies

R. D. Smith
Division of Waste Management
Nuclear Regulatory Commission
Washington, DC 20555

R. E. Cunningham
Office of Nuclear Safety
Materials and Safeguards
Nuclear Regulatory Commission
Room 562, 7915 Eastern Avenue
Silver Springs, MD 20910

27 DOE Technical Information Center

J. A. Buckham
Allied-General Nuclear Services
P.O. Box 847
Barnwell, SC 29812

A. Williams
Allied-General Nuclear Services
P.O. Box 847
Barnwell, SC 29812

J. H. Kittel
Argonne National Laboratory
Office of Waste Management
Programs
9700 South Cass Avenue
Argonne, IL 60439

M. J. Steindler/L. E. Trevorrow
Argonne National Laboratory
9700 South Cass Avenue
Argonne, IL 60439

W. Carbiener
Battelle Memorial Institute
Office of Nuclear Waste
Isolation
505 King Avenue
Columbus, OH 43201

Beverly Rawles
Battelle Memorial Institute
Office of Nuclear Waste
Isolation
505 King Avenue
Columbus, OH 43201

Research Library
Battelle Memorial Institute
505 King Avenue
Columbus, OH 43201

R. Maher, Program Manager
Waste Management Programs
Savannah River Plant
E. I. Du Pont de Nemours & Co.
Aiken, SC 29801

M. D. Boersma
E. I. Du Pont de Nemours & Co.
Savannah River Laboratory
Aiken, SC 29801

R. G. Garvin
E. I. Du Pont de Nemours & Co.
Savannah River Laboratory
Aiken, SC 29801

D. L. McIntosh
E. I. Du Pont de Nemours & Co.
Savannah River Laboratory
Aiken, SC 29801

A. L. Ayers
EG & G Idaho
P.O. Box 1625
Idaho Falls, ID 83415

R. Williams
Electric Power Research
Institute
3412 Hillview Avenue
Palo Alto, CA 94304

No. of
Copies

J. L. Larocca, Chairman
Engineering Research and
Development Authority
Empire State Plaza
Albany, NY 12223

2 Environmental Protection Agency
Technological Assessment
Division (AW-559)
Office of Radiation Programs
U.S. Environmental Protection
Agency
Washington, DC 20460

J. R. Berreth
Exxon Nuclear Idaho
P.O. Box 2800
Idaho Falls, ID 83401

G. L. Ritter
Exxon Nuclear Idaho
P.O. Box 2800
Idaho Falls, ID 83401

File Copy
Exxon Nuclear Idaho
P.O. Box 2800
Idaho Falls, ID 83401

3 J. Campbell
Lawrence Livermore Laboratory
P.O. Box 808
Livermore, CA 94550

R. Roy
202 Materials Research
Laboratory
Pennsylvania State University
University Park, PA 16802

J. P. Duckworth
Plant Manager
Nuclear Fuels Services, Inc.
P.O. Box 124
West Valley, NY 14171

No. of
Copies

R. E. Blanco
Oak Ridge National Laboratory
P.O. Box Y
Oak Ridge, TN 37830

J. O. Blomeke
Oak Ridge National Laboratory
P.O. Box Y
Oak Ridge, TN 37830

3 A. L. Lotts
Oak Ridge National Laboratory
P.O. Box X
Oak Ridge, TN 37830

2 A. B. Martin
Rockwell International
Energy Systems Group
8900 DeSoto Avenue
Canoga Park, CA 91304

Paul Hagen
Chemical Operations
Rockwell International
Rocky Flats Plant
P.O. Box 464
Golden, CO 80401

E. Vejvoda, Director
Chemical Operations
Rockwell International
Rocky Flats Plant
P.O. Box 464
Golden, CO 80401

R. G. Kepler
Organic and Electronic
Dept. 5810
Sandia Laboratories
Albuquerque, NM 87185

W. Weart
Sandia Laboratories
Albuquerque, NM 87185

No. of
Copies

No. of
Copies

P. B. Macedo
Keane Hall
Vitreous State Laboratory
The Catholic University of
America
Washington, DC 20017

R. G. Post
College of Engineering
University of Arizona
Tucson, AZ 85721

L. L. Hench
Dept. of Materials Science
and Engineering
University of Florida
Gainesville, FL 32611

Dr. Hayne Palmour III
2140 Burlington Engineering
Laboratories
North Carolina State University
Raleigh, NC 27607

ONSITE

4 DOE Richland Operations Office

P. A. Craig (2)
R. E. Gerton
H. E. Ransom

4 Rockwell Hanford Operations

I. E. Reep
D. D. Wodrich (3)

68 Pacific Northwest Laboratory

S. M. Barnes
W. J. Bjorklund

H. T. Blair
W. F. Bonner
D. W. Brite
R. A. Brouns
J. L. Buel
R. L. Bunnett
J. R. Carrell
J. G. Carter
L. A. Chick
T. D. Chikalla
R. D. Dierks
G. J. Exarhos
M. S. Hanson
L. K. Holton
J. H. Jarrett
D. E. Knowlton
C. A. Knox
W. L. Kuhn
L. T. Lakey
D. E. Larson
R. O. Lokken
G. B. Long (3)
J. L. McElroy
G. B. Mellinger
J. E. Mendel
R. D. Nelson
J. F. Nesbitt
R. E. Nightingale
R. D. Peters
A. M. Platt
W. A. Ross (5)
J. M. Rusin
D. H. Siemens
S. C. Slate (15)
C. L. Timmerman
R. L. Treat
R. P. Turcotte
H. H. Van Tuijl
J. W. Wald
Technical Information (5)
Publishing Coordination (2)(KC)

The canister-wall thickness is specified as 0.64 cm (1/4 in.) which is much thicker than is required to meet the process-imposed stresses plus the corrosion allowances for both the inside and outside surfaces. However, the dimension is a prudent specification for impact and transportation protection.

Closure

The top of the canister is formed from a flanged-only tank head. The bottom is a slightly-reversed-dished flanged tank head. Stress analysis indicates the turned corner and closure is less susceptible to impact damage than a simple flat-plate closure.

The actual lid closure at the top of the canister will be a twist-lock fitting developed at PNL. Figure 17 is a cutaway detail of the twist-lock

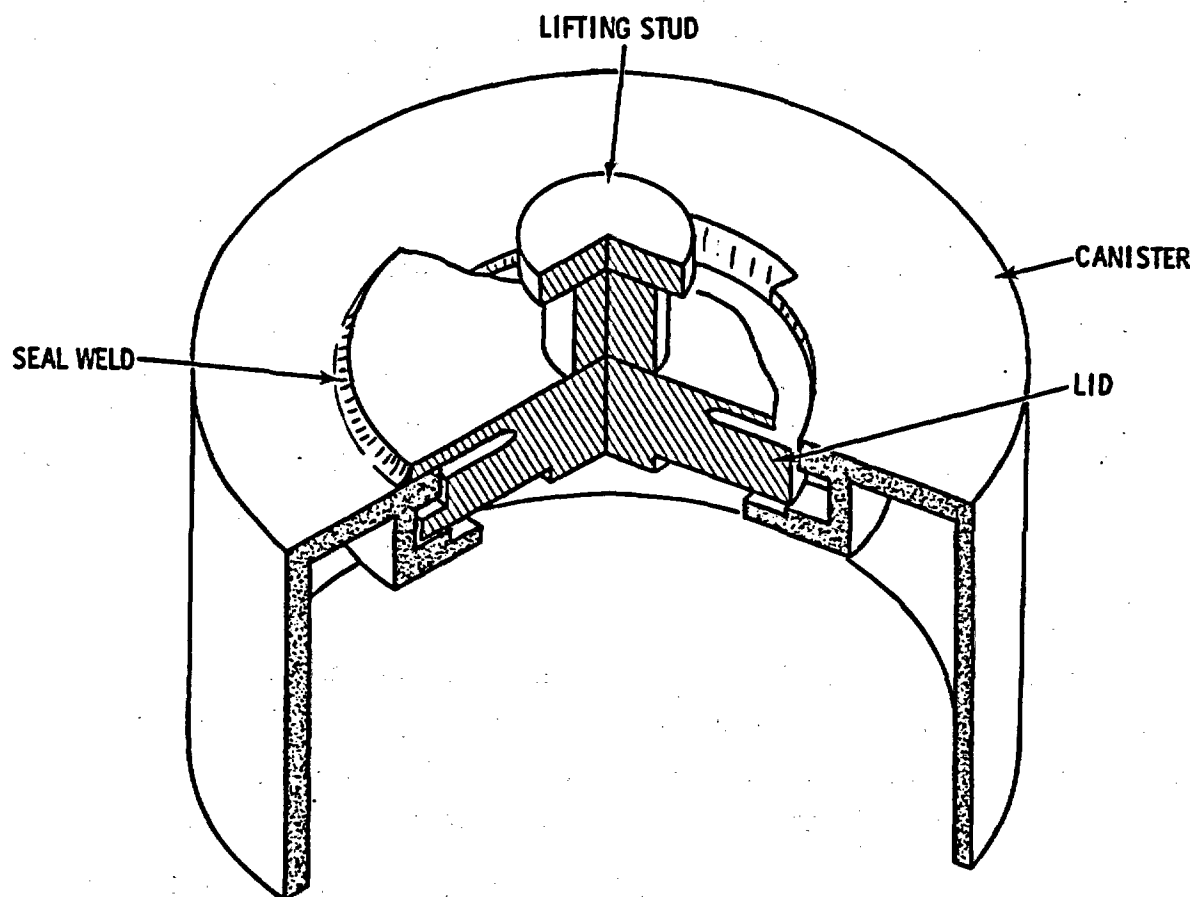


FIGURE 17. Schematic of the Twist-Lock Canister Closure

fitting. This type of closure has been developed to permit a simple, air-tight connection during filling that can be made with remote-handling equipment. The seal-weld surface is accessible for remote welding and can be checked for weld defects by ultrasonic scan. The weld leak check can be made with a bell-type helium detector that fits over the top of the canister. The twist-lock closure has been used in over 20 full-scale canister tests. It has been welded and leak tested using prototype remote equipment.

The level to which the canister can be filled with glass depends on the type of the glass-making process and the accuracy of the instrumentation that monitors the weight and fill level of the canister. As a reference value for this report, a fill level of 90% is assumed for a canister without fins produced by the JHGM process. This value is equivalent to 192 L of glass. Of course, in actual practice the canister fill level will assume some normal distribution around the desired fill level. A canister of glass produced with the ICM process will contain less glass because the internal fins occupy about 10% of the canister volume, and more void space must be reserved at the top for the glass batch to melt.

Design Parameters

The design parameters of the filled HLW canister are given in Table 11. These parameters are, of course, approximate. The average waste loading of the glass will be lower since the fuel history overestimates the average fuel burnup. In addition, the glass production process is easily adaptable. For example, the canister fill level can be changed or the glass waste loading can be changed to meet some other criteria of the overall waste disposal system.

THERMAL ANALYSIS

For the purpose of this study, several simple steady-state temperature profiles were calculated to predict the maximum glass temperature during interim water storage, interim air storage, and repository emplacement. The decay heat produced in the canister as a function of time is given in Table 12.

The CANIST code (developed at PNL) can perform transient thermal analyses for canisters that have radial fins and can provide detailed thermal profiles

TABLE 11. Design Parameters of the HLW Canister

<u>Parameter</u>	<u>Specifics</u>
Material	Stainless steel 304L
Dimensions	
● Outside diameter	32.4 cm (12-in. Pipe) ± 2 mm
● Length	3 m (10 ft) ± 2 mm
● Wall Thickness	0.64 cm (0.250-in. nominal pipe tolerance)
Fins	Not required
Closure	PNL "twist-lock"
Empty weight	160 kg ± 5%
Volume when 90% filled	192 L ± 5%
Weight of glass (3.1 g/c ³)	595 kg
MTU of HLW per canister	2.28 (@ 260.6 kg glass/MTU)
Decay heat	3.71 kW (at 5 yr after reactor discharge) 2.2 kW (at 10 yr after reactor discharge)
Activity	1.02 x 10 ⁶ Ci (at 5 yr after reactor discharge) 6.58 x 10 ⁵ Ci (at 10 yr after reactor discharge)

TABLE 12. Canister Decay Heat

<u>Decay Period, Yr</u>	<u>Canister Heat Generation Rate, W</u>
5	3690
10	2210
20	1600
50	798
10 ²	292
10 ³	20.1
10 ⁴	1.7
10 ⁵	0.264
10 ⁶	0.178

within the canister than can be used to predict glass devitrification and cracking as well as canister creep. The primary references report detailed thermal analyses of canisters during the glass-fill process, cooldown, and both interim and long-term storage. These analyses are not repeated here.

After the canister of HLW is produced, it will be stored onsite before being transported to a repository. The length of this interim storage period depends on many variables in the entire HLW disposal program. To ensure that the glass temperature at the centerline of the canister is within acceptable limits, the maximum glass temperature was calculated for a canister stored either in water or in air. If the canister is stored in a water basin, the maximum temperature is $\sim 153^{\circ}\text{C}$ for 5-year-aged HLW (time since the spent fuel was removed from the reactor). If the canisters are placed in air storage designed for convection cooling (radiative heat loss was assumed to be zero because of nearby canisters in an array), the maximum glass temperature will be $\sim 380^{\circ}\text{C}$ for 5-year-aged HLW. Both of these temperatures are below the point where devitrification of the glass will occur ($\sim 500^{\circ}\text{C}$ if maintained for periods greater than a week). These calculations were for a JHGM canister that has no internal fins. An ICM canister with internal fins would have a lower maximum glass temperature.

Also of interest are maximum temperatures in the repository. The thermal analysis models for repository emplacement must take into account the heat-sink behavior of the repository media and the type of canister overpack and back-fill. The thermal calculation must be a transient calculation since the repository temperature increases to a maximum several years after the canisters are put in place and then falls off slowly over a long period of time as the canister thermal output decays.

One of the primary objectives of this report is to supply a canister design and waste loading specification that can be used as input for detailed repository thermal history calculations by other contractors supporting the NWS program. Therefore, the repository thermal analyses reported here are

simply for the purpose of verifying that the canister size and the decay-heat loading specified for the canister are compatible with existing repository design constraints.

The repository conditions developed by an ONWI-sponsored Interface Working Group (NMTS-3 1980) for commercial high-level waste in a salt repository assumed a similar canister design and decay-heat content as that assumed in this report. The Interface Working Group also assumed an average repository heat loading of 25 W/m^2 (100 kW/acre). From this assumption, it is possible to calculate the average salt temperature in the repository as a function of time, reflecting the decay in thermal emission from the HLW canisters. Using the average salt temperature as the heat-sink temperature for the canister temperature profile calculation yields a time-dependent temperature plot of various points in the waste-form/overpack model.

A model of the canister emplacement in the repository borehole is shown in Figure 18. The canister is surrounded by a steel overpack. The space between the canister and the overpack is an empty airspace. The overpack/canister assembly is lowered into a borehole in the salt, which has a steel liner in the hole to facilitate retrieval should that become necessary. The annulus between the overpack and the liner is backfilled with crushed salt.

The temperature history for the glass centerline, the canister surface, and the nearby-salt temperature is shown in Figure 19. The maximum glass temperature is $\sim 320^\circ\text{C}$, which occurs shortly after emplacement. The canister wall temperature reaches a maximum of 265°C . The highest average temperature for the nearby salt is $\sim 160^\circ\text{C}$, which occurs 15 to 20 years after emplacement.

Researchers at the Advanced Energy Systems Division of the Westinghouse Electric Corporation have proposed a waste emplacement model that emphasizes maximum isolation of the waste form from ground-water attack or lithostatic forces for a period in excess of a thousand years. A cross section typical of a maximum isolation model is shown in Figure 20. The concept employs a thick steel overpack to withstand the lithostatic pressure within the repository. A titanium overpack acts as a corrosion barrier. A compressed mixture of bentonite and sand is used to seal the waste package against water intrusion. This

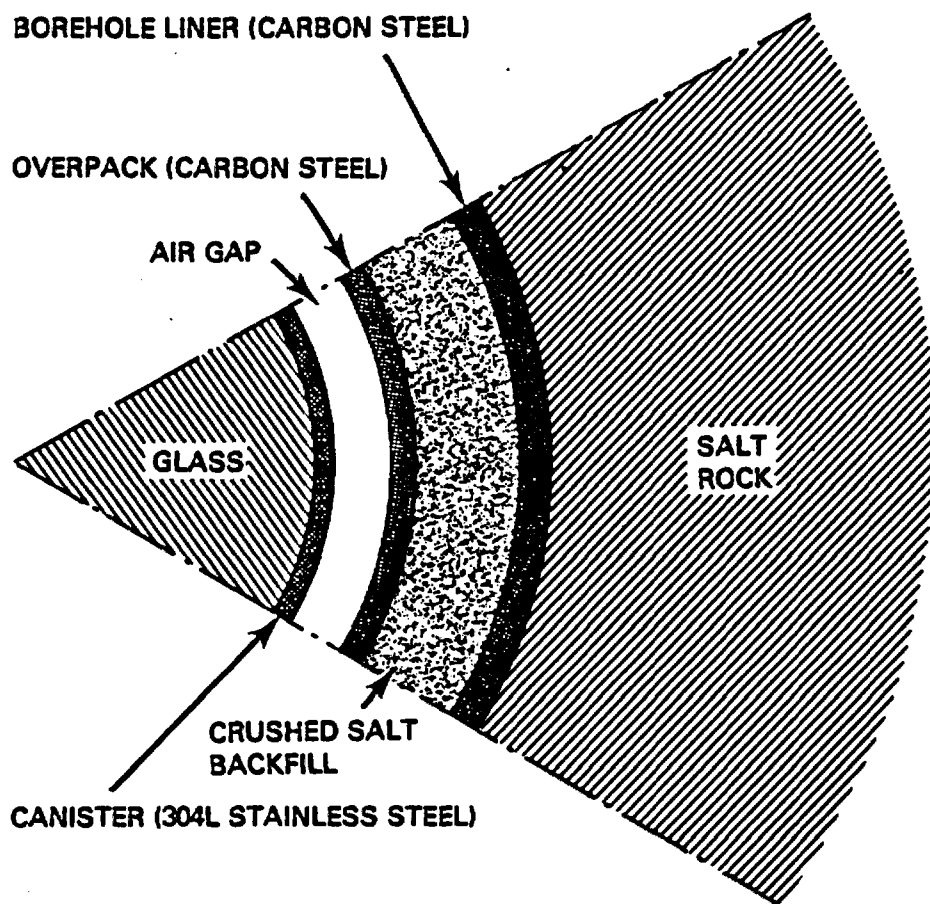


FIGURE 18. Canister Emplacement Model for a Salt Repository (MWS-3 1980)

model may be unnecessarily complex for salt. It may be desirable to make the canister bear the lithostatic pressure and provide a titanium overpack for the corrosion protection. The compressed bentonite backfill is more appropriate for basalt or granite repositories where some ground-water intrusion is probable. Only a few liters of brine are predicted to reach the borehole in a salt repository. It can be argued that if sufficient water were to reach the emplacement site to warrant the bentonite backfill it would have already dissolved the surrounding salt. However, this complex model is useful since it tends to maximize the waste centerline temperature. The temperature profile for this model is also shown in Figure 20 for a time shortly after emplacement of 10-year-old HLW. The maximum glass centerline temperature is $\sim 430^{\circ}\text{C}$; the maximum canister wall temperature is $\sim 350^{\circ}\text{C}$. A temperature history for the

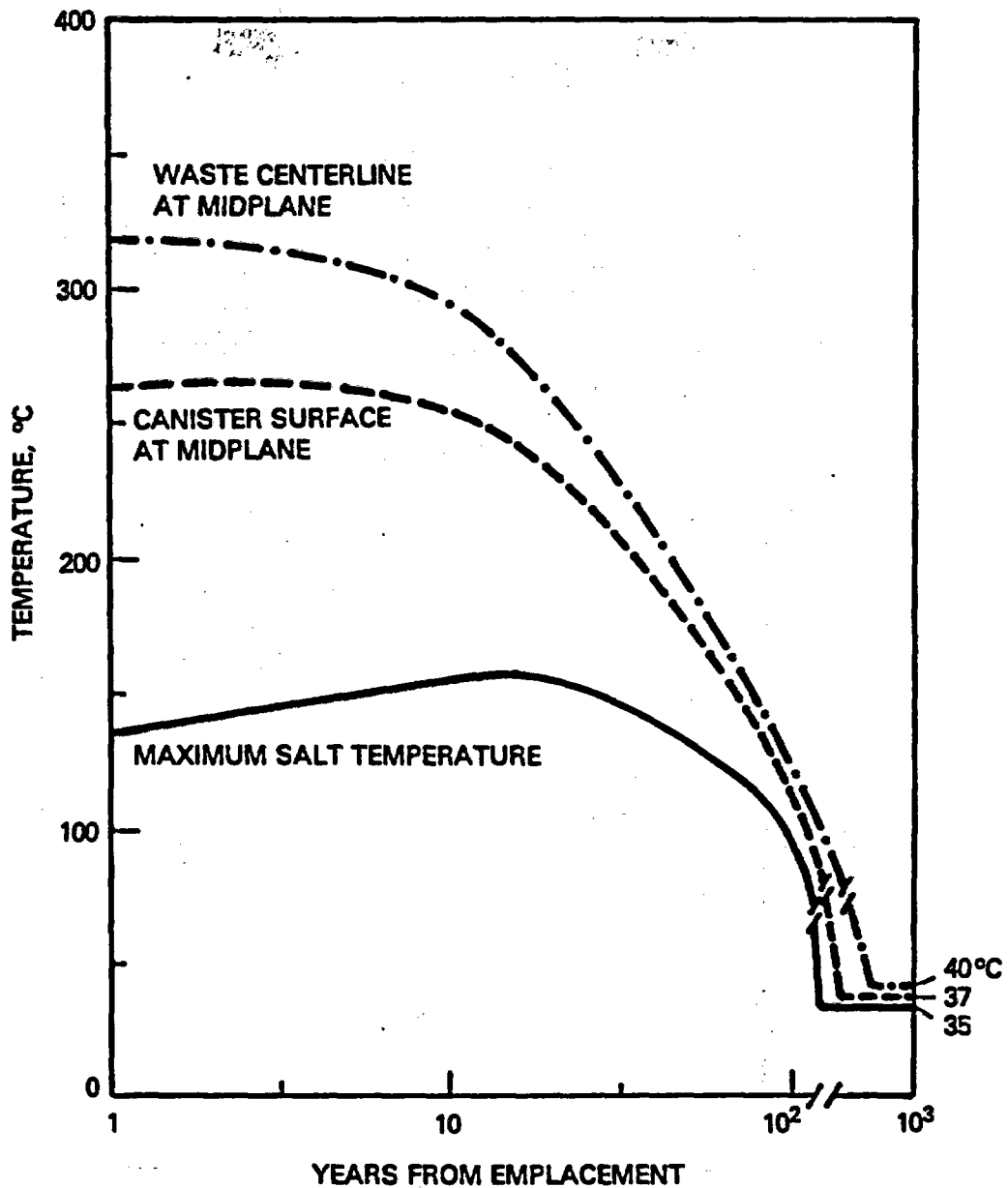


FIGURE 19. Thermal Response as a Function of Time for a Salt Repository with the Canister Emplacement Model of NWTs-3 (1980)

maximum isolation model in a salt repository is given for the first thousand years in Figure 21. The glass centerline temperature and the temperature of the titanium corrosion barrier are given. The average salt-bed temperature is taken from NWTs-3 (1980) for a repository having 100 kW/acre thermal loading from HLW canister placement.

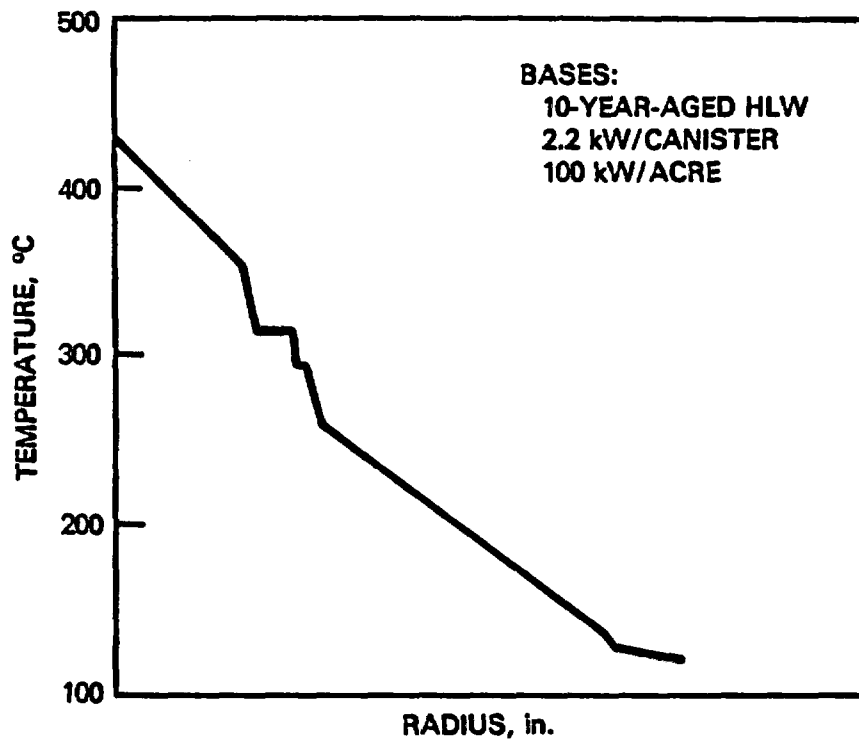
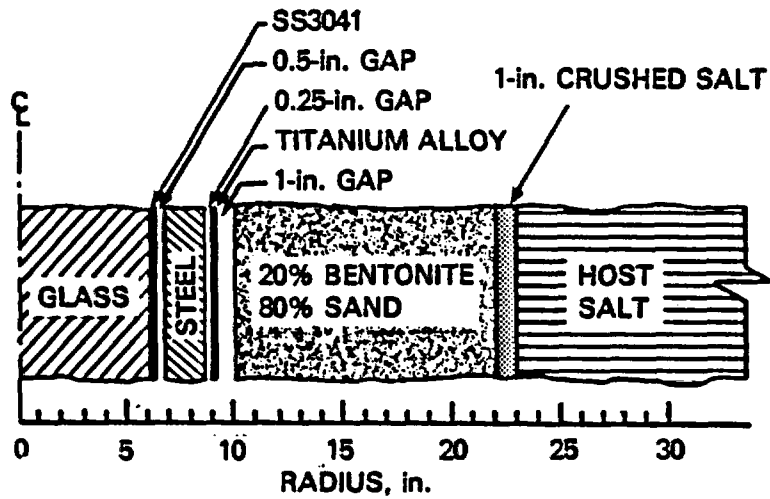


FIGURE 20. Maximum Temperature Profile for a Canister Emplacement in a Salt Repository with the Maximum Isolation Package Model

The maximum glass temperatures calculated for the two different emplacement models are acceptable. Interpretation of the effects of the maximum temperature for the steel and titanium overpacks and the salt or bentonite backfill are beyond the scope of this report.

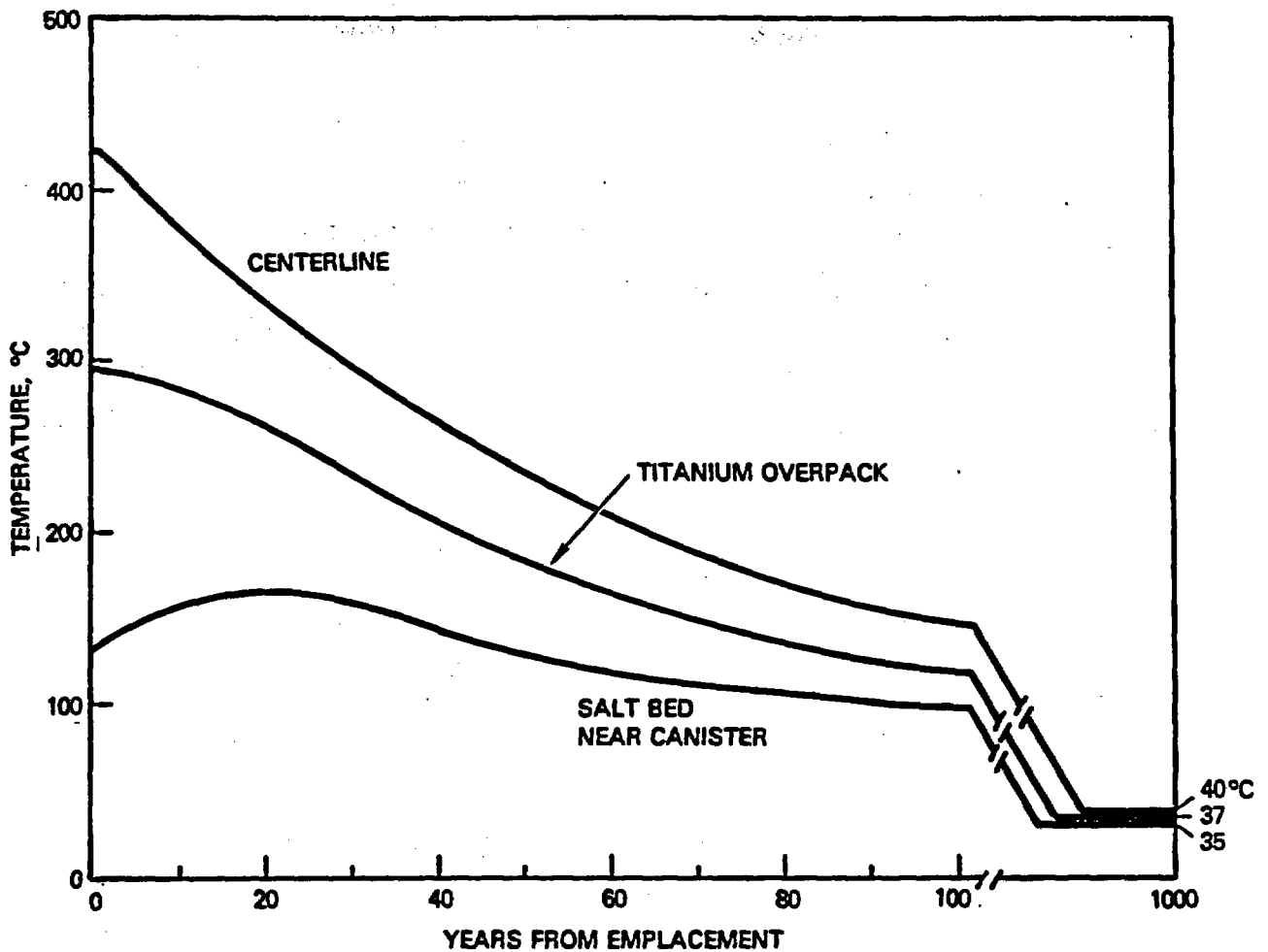


FIGURE 21. Thermal Response as a Function of Time for a Salt Repository with the Maximum Isolation Emplacement Package Model

RADIATION ANALYSIS

Radiation flux is an important consideration in the design of systems for canister storage and transportation of HLW canisters. The reference canister contains 2.28 MTU (metric tonne uranium waste equivalent). The complete description of the radionuclides is given in the ORIGEN II calculation in the appendix. The gamma radiation is the principal contributor to dose from the canisters. Beta radiation and neutrons can be neglected for the preliminary calculations. The ORIGEN II code calculates the source terms for the gamma radiation. The energy-dependent source terms are input to the QAD code (Cain

1977), and the gamma flux is calculated at the canister surface, taking into account the glass composition, canister wall, and canister geometry.

Predictions of the gamma flux and dose profiles at the canister surface for 5, 10, 50, and 100 years were calculated with the QAD code. The gamma source terms are given in Table 13, the gamma energy flux is given in Table 14, and the dose rate is given in Table 15. Also, Table 16 gives the direct gamma spectrum that can be used in combination with the energy flux of Table 14 to calculate the dose through various overpacks and repository backfill configurations. Figure 22 is a relative profile of the dose rate around a HLW canister containing 5-year-aged waste.

TABLE 13. Gamma Source Terms^(a) (MeV/W-s/MTU)

Group	E (MeV)	Decay Time, yr			
		5	10	50	100
1	0.085	1.3 + 6	8.6 + 5	3.0 + 5	9.4 + 4
2	0.125	1.7 + 6	1.0 + 6	3.0 + 5	9.0 + 4
3	0.225	3.0 + 6	1.9 + 6	7.0 + 5	2.1 + 5
4	0.375	2.7 + 6	1.5 + 6	5.0 + 5	1.5 + 5
5	0.575	7.5 + 7	4.9 + 7	1.8 + 7	5.6 + 6
6	0.85	2.4 + 7	6.1 + 6	2.6 + 5	5.8 + 4
7	1.25	7.5 + 6	3.6 + 6	2.1 + 5	3.0 + 4
8	1.75	3.9 + 5	1.6 + 5	1.5 + 4	3.1 + 3
9	2.25	2.7 + 5	4.3 + 3	1.4 + 0	0
10	2.75	1.0 + 4	3.3 + 2	0	0
11	3.5	1.7 + 3	5.4 + 1	0	0

Power = 38.4×10^6 W

2.28 MTU per canister

$S = (38.4 \times 10^6) \times 2.28 = 8.76 \times 10^7$ with above spectrum

(a) From ORIGEN.

TABLE 14. Energy Flux at Canister Surface Versus Decay Time (Flux in 10^{10} MeV/cm²-s)

Radial Surface (R = 15.875 cm)		Decay Time, yr			
Distance from Bottom of Canister		5	10	50	100
0		3.0	1.6	0.46	0.14
25		6.4	3.3	0.98	0.30
50		7.4	3.9	1.2	0.35
75		8.9	4.7	1.4	0.43
100		10.3	5.5	1.7	0.51
(Center at 132)	125	10.9	5.8	1.8	0.54
	150	10.5	5.6	1.9	0.52

Axial Surface (Z = 293.1 cm)		Decay Time, yr			
Distance from Axial Centerline, cm		5	10	50	100
0		1.1	0.61	0.19	0.054
15		0.94	0.50	0.15	0.047

TABLE 15. Dose Rate at Canister Surface Versus Decay Time (Dose Rate in 10^6 mrem/h)

Radial Surface (R = 15.875 cm)		Decay Time, yr			
Distance from Bottom of Canister		5	10	50	100
0		56	30	8.6	2.7
25		118	62	19	5.8
50		137	72	22	6.8
75		165	86	27	8.3
100		192	104	31	9.7
(Center at 132)	125	204	108	33	10
	150	196	105	32	9.7

Axial Surface (Z = 293.1 cm)		Decay Time, yr			
Distance from Axial Centerline, cm		5	10	50	100
0		21	12	3.5	1.1
15		18	9.4	2.9	0.90

TABLE 16. Direct Beam Gamma Spectrum Versus Decay Time (MeV/cm² s)
 (Detector at Z = 125 cm, R = 15.875 cm; Un-normalized
 Spectrum)

Group	E (MeV)	Decay Time, yr			
		5	10	50	100
1	0.085	7.1 + 1	4.6 + 1	1.6 + 1	5.1
2	0.125	3.0 + 5	1.8 + 5	5.2 + 4	1.6 + 4
3	0.225	8.4 + 7	5.4 + 7	2.0 + 7	5.9 + 6
4	0.375	3.6 + 8	2.0 + 8	6.7 + 7	2.0 + 7
5	0.575	1.9 + 10	1.2 + 10	4.6 + 9	1.4 + 9
6	0.850	9.2 + 9	2.3 + 9	9.9 + 7	2.2 + 7
7	1.250	3.9 + 9	1.9 + 9	1.1 + 8	1.6 + 7
8	1.750	2.7 + 8	1.1 + 8	1.0 + 7	2.2 + 6
9	2.250	2.2 + 8	3.5 + 6	1.1 + 3	0
10	2.750	9.5 + 6	3.0 + 5	0	0
11	3.500	1.7 + 6	5.5 + 4	0	0

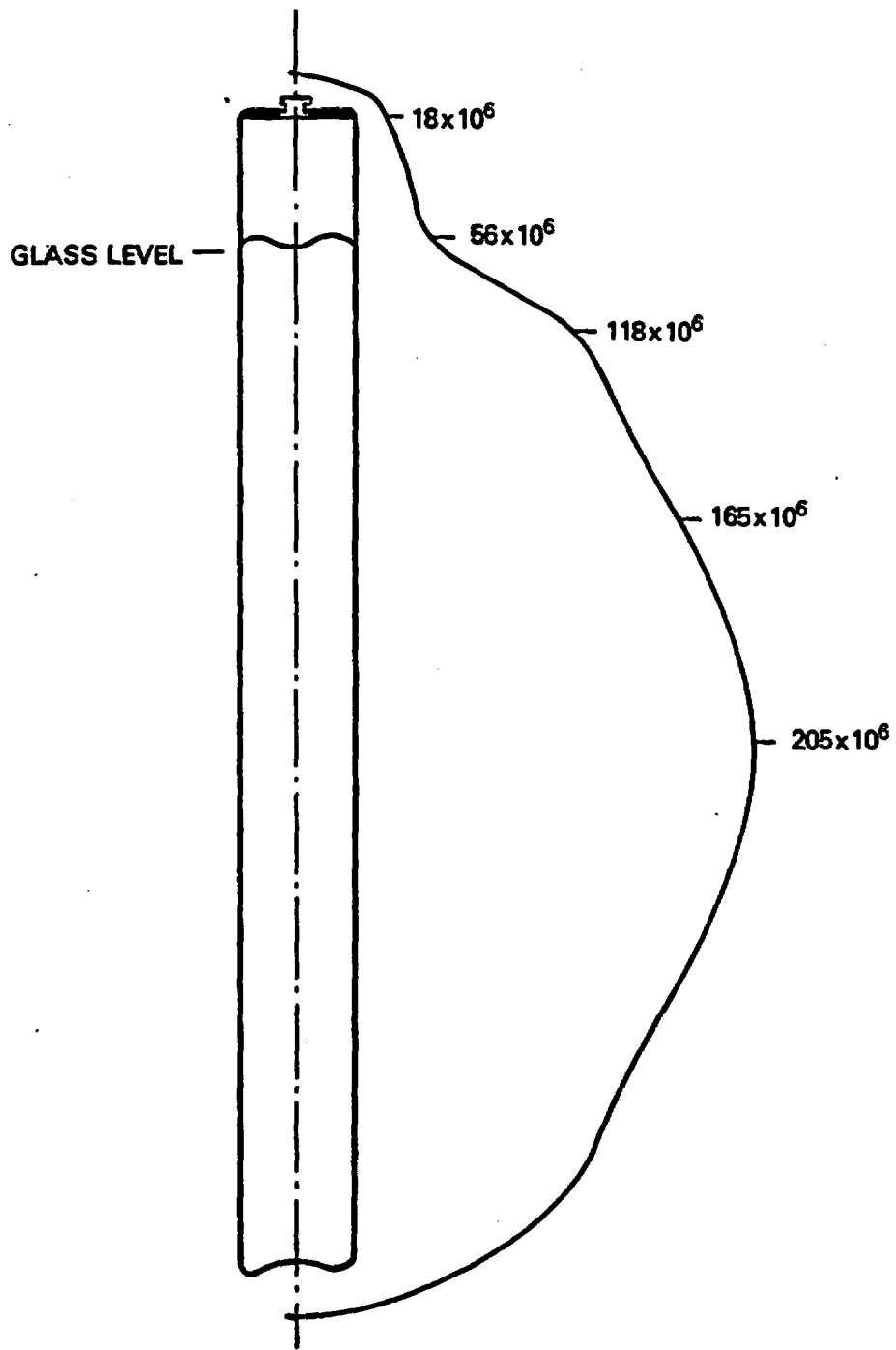


FIGURE 22. Profile of High-Level Waste Canister Dose Rate, mrem/h (at time of reprocessing, 5 years aged)

REFERENCES

- Bell, M. J. 1978. ORIGEN--The ORNL Isotope Generation and Depletion Code, ORNL-4628, Oak Ridge National Laboratory, Oak Ridge, Tennessee.
- Bunnell, L. R. 1979. Tests for Determining Impact Resistance and Strength of Glass Used for Nuclear Waste Disposal. PNL-2954, Pacific Northwest Laboratory, Richland, Washington.
- Cain, V. R. 1977. A Users Manual for QAD-CG, The Combinational Geometry Version of the QAD-P5A Point Kernel Shielding Code. CCC-307, Reactor Safety Information Center Computer Code Collection, Oak Ridge National Laboratory, Oak Ridge, Tennessee.
- Chick, L. A. et al. 1980. Annual Report on the Development and Characterization of Solidified Forms for Nuclear Wastes, 1979. PNL-3465, Pacific Northwest Laboratory, Richland, Washington.
- Code of Federal Regulations, Title 10, Part 60. 1980. "Technical Criteria for Regulating Geologic High-Level Radioactive Waste." Federal Register, Vol. 45, No. 94, Tuesday, May 13, 1980. Advanced Notice of Rule Making.
- Code of Federal Regulations, Title 40, Part 191. 1979. "Working Draft of Environmental Radiation Protection Standards for Management and Disposal of Spent Nuclear Fuel, High-Level and Transuranic Radioactive Waste."
- Code of Federal Regulations, Title 10, Part 50, Appendix F. 1978.
- Croff, A. G. 1980. A Users Manual for the ORIGEN-II Computer Code. ORNL-TM-7175, Oak Ridge National Laboratory, Oak Ridge, Tennessee.
- Doremus, R. H. 1973. "Phase Separation." Glass Science, pp. 44-73, John Wiley and Sons, New York, New York.
- E. I. duPont Nemours Co. 1978. Spent LWR Fuel Recycle Complex Conceptual Design, Case A-1, Separated Streams. DP-CFP-78-121, Savannah River Laboratory, Aiken, South Carolina.
- Elliot, R. M. 1945. "Glass Composition and Density Changes." Journal of the American Ceramic Society. 28:303-305.
- Exxon Nuclear Company. 1977. PSAR for Nuclear Fuel Recovery and Recycling Center. XN-FR-32, Rev. 1, Exxon Nuclear Company, Richland, Washington.
- Gray, W. J. 1976. Volatility of a Zinc Borosilicate Glass Containing Simulated High-Level Radioactive Waste. BNWL-2111, Pacific Northwest Laboratory, Richland, Washington.

- Goldman, M. I. et al. 1958. "Retention of Fission Products in Ceramic-Glaze-Type Fusions." In Proceedings of Second U.N. Int. Conf. Peaceful Uses At. Energy, 1958, Geneva. 18:27, United Nations, New York, New York.
- International Atomic Energy Agency (IAEA). 1977. Techniques for the Solidification of High-Level Wastes. Technical Reports Series No. 176, p. 16, International Atomic Energy Agency, Vienna, Austria.
- International Nickel Company, Inc. 1973. Huntington Alloys Bulletin on Inconel 601. International Nickel Company, New York, New York.
- Larson, D. E., Editor. 1980. Spray Calciner/In-Can Melter High-Level Waste Solidification Technical Manual. PNL-3495, Pacific Northwest Laboratory, Richland, Washington.
- Malow, G. and E. Schiewer. 1972. Fission Products in Glasses, Part I: Borosilicate Glasses Containing Fission Products. HMI-8217, Hahn-Meitner Institute, Berlin, Germany.
- Mendel, J. E. and J. L. McElroy. 1972. Waste Solidification Program, Volume 10, Evaluation of Solidified Waste Products. BNWL-1666, Pacific Northwest Laboratory, Richland, Washington.
- Mendel, J. E. 1973. "Measurements on Core-Drilled Samples." Quarterly Progress Report, Research and Development Activities, Waste Fixation Program, April through June 1973. BNWL-1761, pp. 16-18, Pacific Northwest Laboratory, Richland, Washington.
- Mendel, J. E. et al. 1977. Annual Report on the Characteristics of High-Level Waste Glasses. BNWL-2252, Pacific Northwest Laboratory, Richland, Washington.
- Mendel, J. E. 1978. The Storage and Disposal of Radioactive Waste as Glass in Canisters. PNL-2764, Pacific Northwest Laboratory, Richland, Washington.
- Merritt, W. F. and P. J. Parsons. 1964. "The Safe Burial of High-level Fission Product Solutions Incorporated into Glass." Health Physics. 10:655.
- Merritt, W. F. 1977. "High-level Waste Glass: Field Leach Test." Nuclear Technology. 32:88-91.
- Nesbitt, J. F., S. C. Slate, and L. K. Fetrow. 1980. Decontamination of High-Level Waste Canisters. PNL-3514, Pacific Northwest Laboratory, Richland, Washington.
- NWTS-3. 1980. Interim Reference Repository Conditions for Commercial and Defense High-Level Nuclear Waste and Spent Fuel Repositories in Salt. Office of Nuclear Waste Isolation, Battelle Memorial Institute, Columbus, Ohio.

- Perez, J. M. and J. H. Westsik. 1980. "Effects of Cracks on Glass Leaching." Presented at ORNL Conference on the Leachability of Radioactive Solids, Gatlinburg, Tennessee, December 9-12, 1980.
- Ross, W. A. "Process for Solidifying High-Level Nuclear Waste," U.S. Patent No. 4,094,809, June 13, 1978.
- Ross, W. A. et al. 1978. Annual Report on the Characterization of High-Level Waste Glasses. PNL-2625, Pacific Northwest Laboratory, Richland, Washington.
- Ross, W. A. et al. 1979. Annual Report on the Development and Characterization of Solidified Forms for High-Level Wastes, 1978. PNL-3060, Pacific Northwest Laboratory, Richland, Washington.
- Ross, W. A., R. P. Turcotte, J. E. Mendel, and J. M. Rusin. 1979. "A Comparison of Glass and Crystalline Waste Materials." Ceramics in Nuclear Waste Management, CONF-790420, May 1979.
- Shand, E. B. 1958. Glass Engineering Handbook. Second Edition, McGraw-Hill Book Company, New York, New York.
- Simonen, F. A. and S. C. Slate. 1979. Stress Analysis of High-Level Waste Canisters: Methods, Applications, and Design Data. PNL-3036, Pacific Northwest Laboratory, Richland, Washington.
- Slate, S. C. and R. F. Maness. 1978. "Corrosion Experience in Nuclear Waste Processing at Battelle-Northwest." In Materials Performance. 17(6):13-21.
- Slate, S. C., L. R. Bunnell, W. A. Ross, F. A. Simonen, and J. H. Westsik, Jr. 1978. "Stresses and Cracking in High-Level Waste Glass." In Proceedings of the Conference on High-Level Radioactive Solid Waste Forms. NUREG/CP-0005, U.S. Nuclear Regulatory Commission, December 1978.
- Smith, T. H. and W. A. Ross. 1975. Impact Testing of Vitreous Simulated High-Level Waste in Canisters. BNWL-1903, Pacific Northwest Laboratory, Richland, Washington.
- Turcotte, R. P. 1976. Radiation Effects in Solidified High-Level Wastes, Part 2--Helium Behavior. BNWL-2051, Pacific Northwest Laboratory, Richland, Washington.
- Turcotte, R. P. and J. W. Wald. 1978. Devitrification Behavior in a Zinc Borosilicate Waste Glass. PNL-2247, Pacific Northwest Laboratory, Richland, Washington.
- U.S. Department of Energy (DOE). 1979. Technology for Commercial Radioactive Waste Management. DOE/ET-0028.
- U.S. Department of Energy (DOE). 1980. Final Environmental Impact Statement Management of Commercially Generated Radioactive Waste. DOE/EIS-0046F.

Wald, J. W. and J. H. Westsik, Jr. 1979. Devitrification and Leaching Effects in HLW Glass--Comparison of Simulated and Fully Radioactive Waste Glasses. CONF-790420.

Weber, W. J. et al. 1979. Radiation Effects in Vitreous and Devitrified Simulated Waste Glass. CONF-790420.

ACKNOWLEDGMENTS

Much of the material reported here is based on detailed reports related to commercial high-level waste processing and immobilization. Background information on the glass description and canister design was summarized, respectively, from The Storage and Disposal of Radioactive Waste as Glass in Canisters (J. E. Mendel 1978), and the Spray Calciner/In-Can Melter High-Level Waste Solidification Technical Manual (D. E. Larson 1980). The authors wish to acknowledge J. L. Swanson, Pacific Northwest Laboratory, for his contribution related to the description of the high-level liquid-waste composition. ORIGEN-II calculations were carried out by the Nuclear Analysis Section of the Hanford Engineering Development Laboratory. L. R. Dodd and R. A. McCann of Pacific Northwest Laboratory prepared and performed, respectively, the radiation flux analysis of the canister and the thermal analysis for the canister.

The model for the overpack system used in the canister thermal analysis is based on a report by the Advanced Energy Systems Division of the Westinghouse Electric Corporation.

D. E. Gordon of Savannah River Plant provided valuable assistance and direction in formulating the objectives of the report.

Editing and word processing were performed, respectively, by G. B. Long and M. A. Eierdam of Pacific Northwest Laboratory.

APPENDIX A
ORIGEN-II CALCULATIONS

ORIGEN-II CALCULATIONS

The radioactivity and decay heat of the reference HLW composition are typical of what would be obtained from full burnup of PWR fuel. The fuel exposure and subsequent decay history are modeled with the ORIGEN-II computer code (Croff 1980). ORIGEN-II represents an improvement over the original ORIGEN code (Bell 1978). The fuel burnup calculations can be easily modeled as a series of exposure periods interrupted by decay periods (resulting from reactor refueling). The cross sections and the method of averaging these cross sections have been improved in the ORIGEN-II code. Radionuclide decay library information has been updated, and the format for displaying the decay histories has been improved.

The assumptions regarding the type of fuel, the reactor, and the exposure history are discussed beginning on page 13 ("Fuel Exposure History").

Reprocessing is specified at 5 years after fuel discharge from the reactor. However, note that some additional decay has occurred during the exposure period when the reactor is refueled. During reprocessing, all of the He, C, N, Ne, Ar, Kr, Xe and Rn are assumed to be separated from the fission products and the actinides. Likewise, 99% of the U, Pu, I and H are assumed to be separated. The decay histories of the separated elements are calculated and are included as part of the code output.

The selected code output supplies the following information about the fuel decay history:

- concentration, g
- radioactivity, Ci
- thermal power, W
- alpha radioactivity only, Ci
- neutron emissions
- photon emissions.

The information is given for three groups of radionuclides. The first group consists of all the elements in the total fuel assembly but which become the HLW at the 5-year decay point when the fuel is reprocessed. The second group of radionuclides use the 99% of uranium and plutonium recovered during

reprocessing. The third group are the gases released during reprocessing. An index of the ORIGEN-II output selected for this report is given in Table A.1.

A cutoff feature was exercised in the code output. For example, if the radioactivity of a radionuclide never exceeds 1×10^{-10} at any time in the decay history that radionuclide is not printed in the radionuclide table. This cutoff feature is applied to all calculated quantities. It is possible to have a radionuclide listed in the concentration table but not in the radioactivity or thermal power tables because of this feature.

A note of caution is required regarding the "Cumulative Table Totals" given of the end of each element summary table. The row title indicates "activation products plus actinides plus fission products," but this total is not valid until the last group, i.e., "fission products." It is in fact a cumulative table, but it is easily misinterpreted.

A full ORIGEN-II output for the case selected in this report is included on microfiche in an envelope at the end of the report. Copies may be requested from the lead author. In addition, abbreviated tables of concentration, radioactivity and thermal power for actinides (plus daughters) and fission products are given in Tables A.2 through A.7. A cutoff parameter of 10^{-3} was used to reduce the length of the tables.

TABLE A.1. Index to ORIGEN-II Output

Input

- Card image
- Neutron yield per neutron-induced fission (input)
- (Alpha, N) neutron yield in oxide fuels (input)
- Spontaneous fission neutron yield, neutron/fission (input)
- Individual element fractional recoveries (input)
- Group fractional recoveries (input)
- Element assignments to fractional recovery groups (input)
- Chemical toxicities, grams per M³ water (input—not used)

Tables of Fuel Decay Histories

- Reactivity and burnup data
- Activation products
 - Concentration, g (by radionuclide)
 - Concentration, g (by element)
 - Radioactivity, Ci (by radionuclide)
 - Radioactivity, Ci (by element)
 - Thermal power, W (by radionuclide)
 - Thermal power, W (by element)
- Actinides + Daughters
 - Concentration, g (by radionuclide)
 - Concentration, g (by element)
 - Radioactivity, Ci (by radionuclide)
 - Radioactivity, Ci (by element)
 - Thermal power, W (by radionuclide)
 - Thermal power, W (by element)
 - Alpha radioactivity, Ci (by radionuclide)
 - Alpha radioactivity, Ci (by element)
- Fission Products
 - Concentration, g (by radionuclide)
 - Concentration, g (by element)
 - Radioactivity, Ci (by radionuclide)
 - Radioactivity, Ci (by element)

TABLE A.1. (contd)

Tables of Fuel Decay Histories (contd)

Thermal power, W (by radionuclide)

Thermal power, W (by element)

- (Alpha, N) neutron source, neutrons/s

Spontaneous fission neutron source, neutrons/s

- Photon spectrum for activation products

18 group photon release rates, photons/s

18 group specific energy release rates, Mev/W-s

Principal photon sources in group (K), photons/s (individual tables for each of the 18 groups)

- Photon spectrum for actinides + daughters

18 group photon release rates, photons/s

18 group specific energy release rates, Mev/W-s

Principal photon sources in group (K), photons/s (individual tables for each of the 18 groups)

- Photon spectrum for fission products

18 group photon release rates, photons/s

18 group specific energy release rates, Mev/W-s

Principal photon sources in group (K), photons/s (individual tables for each of the 18 groups)

0.99 U and Pu Separated from the HLW Stream 5 Years After Discharge

- Reactivity and burnup data

- Activation products

Concentration, g

Radioactivity, Ci

Thermal power, W

- Actinides + daughters

Concentration, g (by radionuclide)

Concentration, g (by element)

Radioactivity, Ci (by radionuclide)

Radioactivity, Ci (by element)

Thermal power, W (by radionuclide)

Thermal power, W (by element)

TABLE A.1. (contd)

0.99 U and Pu Separated from the HLW Stream 5 Years After Discharge (contd)

Alpha radioactivity, Ci (by radionuclide)

Alpha radioactivity, Ci (by element)

● Fission products

Concentration, g

Radioactivity, Ci

Thermal power, W

● (Alpha, N) neutron source, neutrons/s

● Spontaneous fission neutron source, neutrons/s

● Photon spectrum for activation products

18 group photon release rates, photons/s

18 group specific energy release rates, Mev/W-s

● Photon spectrum for actinides + daughters

18 group photon release rates, photons/s

18 group specific energy release rates, Mev/W-s

Principal photon sources in group (K), photons/s (individual tables for each of the 18 groups)

● Photon spectrum for fission products

18 group photon release rates, photons/s

18 group specific energy release rates, Mev/W-s

Separate He, C, N, Ne, Ar, Kr, Xe, Rn, H, and I from the HLW Stream

● Reactivity and burnup data

● Activation products

Concentration, g (by radionuclide)

Concentration, g (by element)

Radioactivity, Ci (by radionuclide)

Radioactivity, Ci (by element)

Thermal power, W (by radionuclide)

Thermal power, W (by element)

● Actinides + Daughters

Concentration, g (by radionuclide)

Concentration, g (by element)

TABLE A.1. (contd)

Separate He, C, N, Ne, Ar, Kr, Xe, Rn, H, and I from the HLW Stream (contd)

- Radioactivity, Ci (by radionuclide)
- Radioactivity, Ci (by element)
- Thermal power, W (by radionuclide)
- Thermal power, W (by element)
- Alpha radioactivity, Ci (by radionuclide)
- Alpha radioactivity, Ci (by element)
- Fission products
 - Concentration, g (by radionuclide)
 - Concentration, g (by element)
 - Radioactivity, Ci (by radionuclide)
 - Radioactivity, Ci (by element)
 - Thermal power, W (by radionuclide)
 - Thermal power, W (by element)
- (Alpha, N) neutron source, neutrons/s
- Spontaneous fission neutron source, neutrons/s
- Photon spectrum for activation products
 - 18 group photon release rates, photons/s
 - 18 group specific energy release rates, Mev/W-s
 - Principal photon sources in group (K), photons/s (individual tables for each of the 18 groups)
- Photon spectrum for actinides + daughters
 - 18 group photon release rates, photons/s
 - 18 group specific energy release rates, Mev/watt-s
 - Principal photon sources in group (K), photons/s (individual tables for each of the 18 groups)
- Photon spectrum for fission products
 - 18 group photon release rates, photons/s
 - 18 group specific energy release rates, Mev/W-s
 - Principal photon sources in group (K), photons/s (individual tables for each of the 18 groups)

TABLE A.2. Concentration of Actinides (Plus Daughters)

OUTPUT UNIT = 6

WESTINGHOUSE 1104 MW(E) PWR, 3.1 PER CENT ENRICH., 32,700 MWD/MTU
 POWER= 3.84000+001MW, BURNUP= 3.26995+004MWD, FLUX= 3.41+014N/CM**2-SFC

SUMMARY TABLE: CONCENTRATIONS, GRAMS

	1 METRIC TON OF U AT 3.1 PFR CENT ENRICHMENT											
DISCHARGE	2.OYR	5.OYR	5Y(REPRO)	10.CYR	20.OYR	50.OYR	100.OYR	1.OKY	10.OKY	100.OKY	1.OHY	
HE 4	3.380-001	6.902-001	8.461-001	.000	1.127-001	3.045-001	7.188-001	1.196+000	5.088+000	7.859+000	1.184+001	3.230+001
B1209	1.401-011	2.623-011	4.409-011	4.409-011	7.747-011	1.705-010	1.133-009	8.245-009	1.014-005	1.125-002	3.689+000	1.488+002
U233	2.826-004	5.748-004	1.008-003	1.008-005	7.098-004	2.121-003	6.451-003	1.397-002	1.903-001	2.332+000	1.940+001	4.284+001
U235	7.492+003	7.493+003	7.493+003	7.493+001	7.494+001	7.495+001	7.499+001	7.507+001	7.644+001	9.605+001	2.267+002	2.370+002
U236	3.783+003	3.783+003	3.784+003	3.784+001	3.785+001	3.788+001	3.799+001	3.821+001	4.206+001	6.570+001	8.031+001	7.820+001
U238	9.452+005	9.452+005	9.452+005	9.452+003	9.452+003	9.452+003	9.452+003	9.452+003	9.452+003	9.452+003	9.453+003	9.455+003
NP237	4.256+002	4.370+002	4.382+002	4.382+002	4.407+002	4.458+002	4.607+002	4.841+002	6.989+002	7.636+002	7.421+002	5.544+002
PU239	4.853+003	4.951+003	4.951+003	4.951+001	4.959+001	4.975+001	5.012+001	5.060+001	5.714+001	8.829+001	1.075+001	1.572+006
PU240	2.044+003	2.045+003	2.047+003	2.047+001	2.446+001	3.045+001	3.917+001	4.244+001	3.913+001	1.507+001	1.081+003	2.543+008
PU241	1.352+003	1.227+003	1.062+003	1.062+001	8.352+000	4.161+000	1.219+000	1.114+001	1.552+003	7.450+004	4.834+007	.000
AM241	3.457+001	1.583+002	3.222+002	3.222+002	3.219+002	3.199+002	3.087+002	2.860+002	6.760+001	2.240+002	1.529+005	.000
AM243	9.985+001	9.999+001	9.997+001	9.997+001	9.992+001	9.983+001	9.954+001	9.909+001	9.105+001	3.910+001	8.340+003	4.901+007
CM244	2.824+001	2.617+001	2.333+001	2.333+001	1.926+001	1.314+001	4.167+000	6.148+001	6.969+015	6.314+015	6.486+015	7.172+015
SUMTOT	9.654+005	9.655+005	9.655+005	1.053+004	1.053+004	1.053+004	1.053+004	1.053+004	1.053+004	1.053+004	1.055+004	1.055+004
TOTAL	9.661+005	9.661+005	9.661+005	1.054+004	1.054+004	1.054+004	1.054+004	1.054+004	1.054+004	1.054+004	1.056+004	1.056+004

A.7

TABLE A.3. Activity of Actinides (Plus Daughters)

OUTPUT UNIT = 6

WESTINGHOUSE 1184 MWIC FWR, 3.1 PER CENT ENRICH, 32,700 MW/MTU
 POWER = 3.84000+001MW, BURNDUP = 3.26955+004MWD, FLUX = 3.41+014M/CW+02-SFC

SUMMARY TABLE: RADIOACTIVITY, CURIES
 1 METRIC TON OF U AT 3.1 PER CENT ENRICHMENT

DISCHARGE	7.0YR	5.0YR	5YREPROJ	10.0YR	20.0YR	50.0YR	100.0YR	1.0KY	10.0KY	100.0KY	1.0MY	
TL204	1.076-009	2.966-010	3.439-010	3.439-010	3.799-010	6.603-010	3.197-009	1.322-009	1.691-006	1.706-004	4.074-003	8.966-003
PB209	4.989-008	1.373-008	1.592-008	1.592-008	1.759-008	3.057-008	1.478-007	6.121-007	7.829-005	7.897-003	1.886-001	4.151-001
PB210	2.292-010	2.473-010	2.854-010	2.854-010	6.447-010	7.439-009	1.463-008	5.799-008	1.868-005	8.761-004	7.054-003	4.169-003
PF214	4.364-011	2.400-010	1.302-009	1.302-009	4.212-009	1.028-008	3.273-008	9.720-008	1.868-005	8.762-004	7.056-003	4.170-003
6121C	2.311-010	2.474-010	2.856-010	2.856-010	6.448-010	7.440-009	1.463-008	5.799-008	1.868-005	8.761-004	7.054-003	4.169-003
61213	4.979-008	1.373-008	1.592-008	1.592-008	1.759-008	3.057-008	1.478-007	6.121-007	7.829-005	7.897-003	1.886-001	4.151-001
61214	4.364-011	2.400-010	1.302-009	1.302-009	4.212-009	1.028-008	3.273-008	9.720-008	1.868-005	8.762-004	7.056-003	4.170-003
P021C	1.235-010	2.431-010	2.709-010	2.709-010	6.448-010	7.440-009	1.463-008	5.799-008	1.868-005	8.761-004	7.054-003	4.169-003
P0213	4.872-008	1.344-008	1.558-008	1.558-008	1.721-008	2.991-008	1.446-007	5.989-007	7.660-005	7.727-003	1.845-001	4.061-001
P0214	1.027-008	2.399-010	1.302-009	1.302-009	4.211-009	1.028-008	3.272-008	9.718-008	1.868-005	8.761-004	7.054-003	4.169-003
P0218	4.365-011	2.400-010	1.302-009	1.302-009	4.213-009	1.028-008	3.273-008	9.722-008	1.868-005	8.764-004	7.057-003	4.171-003
A1217	4.979-008	1.373-008	1.592-008	1.592-008	1.759-008	3.057-008	1.478-007	6.121-007	7.829-005	7.897-003	1.886-001	4.151-001
RA222	4.365-011	2.400-010	1.302-009	.000	4.213-009	1.028-008	3.273-008	9.722-008	1.868-005	8.764-004	7.057-003	4.171-003
FR221	4.979-008	1.373-008	1.592-008	1.592-008	1.759-008	3.057-008	1.478-007	6.121-007	7.829-005	7.897-003	1.886-001	4.151-001
RA225	4.961-008	1.373-008	1.592-008	1.592-008	1.759-008	3.057-008	1.478-007	6.121-007	7.829-005	7.897-003	1.886-001	4.151-001
RA226	4.361-011	2.400-010	1.302-009	1.302-009	4.213-009	1.028-008	3.272-008	9.722-008	1.868-005	8.764-004	7.057-003	4.171-003
AC225	4.979-008	1.373-008	1.592-008	1.592-008	1.759-008	3.057-008	1.478-007	6.121-007	7.829-005	7.897-003	1.886-001	4.151-001
TH229	1.294-008	1.373-008	1.592-008	1.592-008	1.759-008	3.057-008	1.478-007	6.121-007	7.829-005	7.897-003	1.886-001	4.151-001
TH230	9.769-008	3.985-007	1.334-006	1.334-006	1.362-006	1.465-006	2.112-006	4.143-006	1.069-004	1.128-003	7.046-003	4.171-003
PA233	2.906-001	3.082-001	3.090-001	3.090-001	3.108-001	3.144-001	3.249-001	3.414-001	4.929-001	5.385-001	5.233-001	3.910-001
U233	2.736-006	5.566-006	9.758-006	9.758-006	6.874-006	2.354-005	6.247-005	1.353-004	1.843-003	2.259-002	1.878-001	4.149-001
U234	9.740-003	2.386-002	4.533-002	4.533-002	8.641-002	1.475-001	3.269-003	5.647-003	1.329-002	1.310-002	1.087-002	3.779-003
U236	2.448-001	2.449-001	2.449-001	2.449-001	2.450-001	2.452-001	2.459-001	2.473-001	2.722-001	4.253-001	5.198-001	5.061-001
NP237	3.002-001	3.082-001	3.090-001	3.090-001	3.108-001	3.144-001	3.249-001	3.414-001	4.929-001	5.385-001	5.233-001	3.910-001
NP239	2.266-007	1.994-006	1.994-006	1.994-006	1.993-006	1.991-006	1.985-006	1.976-006	1.816-006	7.797-000	1.663-003	9.773-008
PU236	2.293-003	2.544-003	2.497-003	2.497-003	2.436-003	2.297-003	1.929-003	1.449-003	7.973-002	2.419-019	.000	.000
PU239	3.038-002	3.079-002	3.079-002	3.079-002	3.084-002	3.093-002	3.117-002	3.147-002	3.553-002	5.490-002	6.663-001	9.773-008
PU240	4.659-002	4.662-002	4.667-002	4.667-002	5.575-002	6.942-002	8.928-002	9.675-002	8.920-002	3.435-000	2.464-004	5.797-009
PU241	1.393-005	1.265-005	1.095-005	1.095-005	4.608-005	5.320-005	1.256-005	1.148-005	1.600-001	7.678-002	4.982-005	.000
PU242	1.944-000	1.944-000	1.944-000	1.944-000	1.945-000	1.947-000	1.953-000	1.962-000	1.997-000	1.995-002	1.707-002	3.404-003
AM241	1.187-002	5.436-002	1.106-003	1.106-003	1.165-003	1.098-003	1.068-003	4.820-002	2.321-002	7.691-002	5.249-005	.000
AM242M	7.836-000	7.765-000	7.659-000	7.659-000	7.486-000	7.153-000	6.238-000	4.966-000	8.198-002	1.232-019	.000	.001
AM242	1.007-005	7.726-000	7.621-000	7.621-000	7.449-000	7.117-000	6.207-000	4.942-000	8.157-002	1.225-019	.000	.000
AM243	1.991-001	1.994-001	1.994-001	1.994-001	1.993-001	1.991-001	1.985-001	1.976-001	1.816-001	7.797-000	1.663-003	9.773-008
CM242	5.444-004	2.467-003	2.975-001	2.975-001	6.173-000	5.886-000	5.133-000	4.087-000	6.746-002	1.016-019	.000	.000
CM243	2.371-001	2.258-001	2.100-001	2.100-001	1.859-001	1.458-001	7.028-000	2.083-000	6.495-010	.000	.000	.000
CM244	2.286-003	2.118-003	1.888-003	1.888-003	1.559-003	1.063-003	3.373-002	4.976-001	5.640-013	5.111-013	5.250-013	5.805-013
CH245	1.733-001	1.732-001	1.732-001	1.732-001	1.731-001	1.730-001	1.726-001	1.719-001	1.597-001	7.665-002	4.974-005	.000
SUMTOT	2.290-007	1.350-005	1.159-005	4.230-003	3.639-003	2.802-003	1.620-003	1.127-003	2.826-002	2.598-001	3.533-000	4.587-000
TOTAL	4.741-007	1.350-005	1.159-005	4.230-003	3.639-003	2.802-003	1.620-003	1.127-003	2.826-002	2.598-001	3.533-000	4.587-000

A.8

TABLE A.4. Decay Heat of Actinides (Plus Daughters)

OUTPUT UNIT = 6

WESTINGHOUSE 1184 MW(e) PWR, 3.1 PER CENT ENRICH., 32,700 MW/MTU
 POWER = 3.84000+001MW, BURNUP = 3.26995+00MMWD, FLUX = 3.41+014N/CM**2-5FC

SUMMARY TABLE: THERMAL POWER, WATTS

DISCHARGE	I METRIC TON OF U AT 3.1 PFR CENT ENRICHMENT											
	2.OYR	5.OYR	5YIREPROD	10.OYR	20.OYR	50.OYR	100.OYR	1.CMY	10.0MY	100.0MY	1.0MY	
TL209	1.787-011	4.928-012	5.713-012	5.713-012	6.317-012	1.097-011	5.304-011	2.197-010	2.810-008	2.834-006	6.768-005	1.490-004
PE209	5.737-011	1.579-011	1.831-011	1.731-011	2.023-011	3.514-011	1.700-010	7.039-010	9.003-008	9.082-006	2.169-004	4.773-004
B1213	2.093-010	5.773-011	6.692-011	6.692-011	7.395-011	1.285-010	6.215-010	2.573-009	3.291-007	3.320-005	7.928-004	1.745-003
B1214	5.592-013	3.076-012	1.668-011	1.668-011	5.398-011	1.318-010	4.194-010	1.246-009	2.394-007	1.123-005	9.042-005	5.344-005
PO210	3.958-012	7.792-012	8.683-012	8.683-012	2.067-011	7.820-011	4.689-010	1.056-009	5.987-007	2.808-005	2.261-004	1.337-004
PO213	2.465-009	6.799-010	7.882-010	7.882-010	4.709-010	1.514-009	7.320-009	7.031-008	3.876-006	3.910-004	9.337-003	2.055-002
PO214	4.766-010	1.114-011	6.043-011	6.043-011	1.955-010	4.773-010	1.510-009	4.512-009	8.671-007	4.068-005	3.275-004	1.934-004
PO218	1.582-012	8.698-012	4.718-011	4.718-011	1.527-010	3.726-010	1.186-009	3.523-009	6.770-007	3.176-005	2.557-004	1.511-004
AT217	2.125-009	5.860-010	6.793-010	6.793-010	7.506-010	1.305-009	6.309-009	2.612-008	3.341-006	3.370-004	8.048-003	1.771-002
RN222	1.446-012	7.954-012	4.315-011	.000	1.756-010	3.408-010	1.088-009	3.221-009	6.191-007	2.904-005	2.338-004	1.382-004
FR221	1.922-009	5.300-010	6.144-010	6.144-010	6.789-010	1.180-009	5.706-009	2.362-008	3.022-006	3.048-004	7.279-003	1.607-002
RA225	3.479-011	9.630-012	1.116-011	1.116-011	1.233-011	7.144-011	1.037-010	4.292-010	5.490-008	5.538-006	1.322-004	2.911-004
RA226	1.259-012	6.931-012	3.760-011	3.760-011	1.216-010	7.969-010	9.451-010	7.807-009	5.395-007	2.531-005	2.038-004	1.204-004
AC225	1.739-009	4.797-010	5.561-010	5.561-010	6.145-010	1.180-009	5.706-009	2.362-008	3.022-006	3.048-004	7.279-003	1.607-002
TM229	3.958-010	4.201-010	4.870-010	4.870-010	5.381-010	9.353-010	4.523-009	1.873-008	2.395-006	2.416-004	5.769-003	1.270-002
TM230	2.764-009	1.128-008	3.774-008	3.774-008	3.854-008	4.145-008	5.977-008	1.172-007	3.026-006	3.192-005	1.994-004	1.180-004
Pa233	6.595-004	6.995-004	7.014-004	7.014-004	7.054-004	7.135-004	7.374-004	7.749-004	1.119-003	1.222-003	1.188-003	8.875-004
U233	7.954-008	1.618-007	2.837-007	2.837-007	1.998-007	5.977-007	1.416-006	3.933-006	5.357-005	6.563-004	5.461-003	1.206-002
U234	2.805-004	6.873-004	1.306-003	1.306-003	2.316-005	4.244-005	9.414-005	1.626-004	3.827-004	3.773-004	3.130-004	1.089-004
U236	6.633-003	6.633-003	6.634-003	6.634-003	6.637-003	6.647-003	6.661-003	6.699-003	7.374-003	1.152-004	1.408-004	1.371-004
NP237	9.174-003	9.420-003	9.444-003	9.444-003	9.499-003	9.608-003	9.929-003	1.043-002	1.508-002	1.646-002	1.599-002	1.195-002
NP239	5.463-004	4.820-002	4.819-002	4.819-002	4.817-002	4.817-002	4.799-002	4.776-002	4.389-002	1.885-002	4.021-006	2.362-010
PU238	7.598-001	8.432-001	8.275-001	8.275-001	8.073-001	7.613-001	6.392-001	4.802-001	2.642-003	8.017-021	.000	.000
PU239	9.301-000	9.488-000	9.488-000	9.488-000	9.504-002	9.533-002	9.605-002	9.697-002	1.095-001	1.692-001	2.060-002	3.012-009
PU240	1.451-001	1.457-001	1.453-001	1.453-001	1.736-001	2.167-001	2.780-001	3.012-001	2.777-001	1.070-001	7.671-006	1.805-010
PU241	4.318-000	3.922-000	3.395-000	3.395-000	2.664-002	1.644-002	3.895-003	7.558-004	4.959-006	2.380-006	1.545-009	.000
PU242	5.739-002	5.740-002	5.740-002	5.740-002	5.743-004	5.750-004	5.768-004	5.794-004	5.899-004	5.891-004	5.041-004	1.005-004
AM241	3.943-000	1.806-001	3.675-001	3.675-001	3.671-001	3.649-001	3.521-001	3.262-001	7.710-000	2.555-003	1.744-006	.000
AM243	6.401-001	6.410-001	6.409-001	6.409-001	6.406-001	6.400-001	6.387-001	6.352-001	5.837-001	2.507-001	5.347-005	3.142-009
CM242	6.325-001	2.866-000	3.456-002	3.456-002	7.172-003	6.830-003	5.964-003	4.748-003	7.838-005	1.181-022	.000	.000
CM243	8.698-001	8.285-001	7.702-001	7.702-001	6.820-001	5.344-001	2.578-001	7.642-002	2.383-011	.000	.000	.000
CM244	7.995-001	7.408-001	6.604-001	6.604-001	5.454-001	3.720-001	1.180-001	1.741-000	1.973-014	1.788-014	1.836-014	2.031-014
CM245	5.750-003	5.749-003	5.747-003	5.747-003	5.745-003	5.740-003	5.726-003	5.703-003	5.299-003	2.543-003	1.650-006	.000
SUMTOT	5.488-004	2.088-002	2.145-002	1.054-002	9.375-001	7.602-001	4.900-001	3.602-001	8.750-000	5.720-001	8.403-002	1.103-001
TOTAL	1.207-005	2.089-002	2.146-002	1.054-002	9.376-001	7.603-001	4.901-001	3.603-001	8.752-000	5.724-001	8.427-002	1.106-001

A.9

TABLE A.5. (contd)

SUMMARY TABLE: CONCENTRATIONS, GRAMS
1 METRIC TON OF U AT 3.1 PER CENT ENRICHMENT

DISCHARGE	2.0YR	5.0YR	SVIRPROJ	10.0YR	20.0YR	50.0YR	100.0YR	1.0MY	10.0MY	100.0MY	1.0MY
CS137	1.179+003	1.126+003	1.050+003	1.050+003	9.354+002	7.424+002	3.717+002	1.169+002	1.000+002	.000	.000
BA137	4.017+001	9.341+001	1.688+002	1.688+002	2.834+002	4.764+002	8.477+002	1.102+003	1.219+003	1.219+003	1.219+003
BA138	1.257+003	1.257+003	1.257+003	1.257+003	1.257+003	1.257+003	1.257+003	1.257+003	1.257+003	1.257+003	1.257+003
LA139	1.199+003	1.200+003	1.200+003	1.200+003	1.200+003	1.200+003	1.200+003	1.200+003	1.200+003	1.200+003	1.200+003
CE140	1.186+003	1.214+003	1.214+003	1.214+003	1.214+003	1.214+003	1.214+003	1.214+003	1.214+003	1.214+003	1.214+003
PR141	1.041+003	1.100+003	1.100+003	1.100+003	1.100+003	1.100+003	1.100+003	1.100+003	1.100+003	1.100+003	1.100+003
CE142	1.109+003	1.109+003	1.109+003	1.109+003	1.109+003	1.109+003	1.109+003	1.109+003	1.109+003	1.109+003	1.109+003
ND143	7.382+002	7.626+002	7.626+002	7.626+002	7.626+002	7.626+002	7.626+002	7.626+002	7.626+002	7.626+002	7.626+002
CE144	3.447+002	5.805+001	4.013+000	4.013+000	4.671+002	4.331+002	1.574+017	7.203+037	.000	.000	.000
AD144	9.591+002	1.246+003	1.300+003	1.300+003	1.304+003	1.304+003	1.304+003	1.304+003	1.304+003	1.304+003	1.304+003
ND145	6.609+002	6.612+002	6.612+002	6.612+002	6.612+002	6.612+002	6.612+002	6.612+002	6.612+002	6.612+002	6.612+002
NC146	6.765+002	6.765+002	6.765+002	6.765+002	6.765+002	6.765+002	6.765+002	6.765+002	6.765+002	6.765+002	6.765+002
PM147	1.327+002	8.314+001	3.764+001	3.764+001	1.004+001	7.152+001	2.587+004	4.729+019	.000	.000	.000
SM147	6.299+001	1.209+002	1.664+002	1.664+002	1.940+002	7.033+002	2.040+002	7.040+002	2.040+002	2.040+002	2.040+002
ND148	3.659+002	3.659+002	3.659+002	3.659+002	3.659+002	3.659+002	3.659+002	3.659+002	3.659+002	3.659+002	3.659+002
SM148	1.624+002	1.653+002	1.653+002	1.653+002	1.653+002	1.653+002	1.653+002	1.653+002	1.653+002	1.653+002	1.653+002
ND153	1.762+002	1.762+002	1.762+002	1.762+002	1.762+002	1.762+002	1.762+002	1.762+002	1.762+002	1.762+002	1.762+002
SM150	3.101+002	3.101+002	3.101+002	3.101+002	3.101+002	3.101+002	3.101+002	3.101+002	3.101+002	3.101+002	3.101+002
SM152	1.324+002	1.324+002	1.324+002	1.324+002	1.324+002	1.324+002	1.324+002	1.324+002	1.324+002	1.324+002	1.324+002
EU153	1.079+002	1.091+002	1.091+002	1.091+002	1.091+002	1.091+002	1.091+002	1.091+002	1.091+002	1.091+002	1.091+002
SM154	3.798+001	3.843+001	3.843+001	3.843+001	3.843+001	3.843+001	3.843+001	3.843+001	3.843+001	3.843+001	3.843+001
GD154	2.697+000	8.568+000	1.578+001	1.578+001	2.452+001	3.426+001	4.147+001	4.213+001	4.213+001	4.213+001	4.213+001
GD156	6.259+001	6.659+001	6.659+001	6.659+001	6.659+001	6.659+001	6.659+001	6.659+001	6.659+001	6.659+001	6.659+001
SUMTOT	3.288+004	3.329+004	3.331+004	2.746+004	2.747+004	2.748+004	2.748+004	2.749+004	2.749+004	2.749+004	2.749+004
TOTAL	3.369+004	3.369+004	3.369+004	2.781+004	2.781+004	2.781+004	2.781+004	2.781+004	2.781+004	2.781+004	2.781+004

A.11

TABLE A.6. Activity of Fission Products

OUTPUT UNIT = 6

WESTINGHOUSE 1104 MW(E) PWR, 3.1 PER CENT ENRICH., 32,700 MW/MTU
 POWER = 3.04000+001MW, BURNUP = 3.26955+004MWU, FLUX = 3.41+014N/CM^2-SFC

SUMMARY TABLE: RADIOACTIVITY, CURIES

DISCHARGE	1 METRIC TON OF U AT 3.1 PER CENT ENRICHMENT											
	2.OVR	5.CYR	SVIREPROJ	10.CYR	20.OVR	50.OVR	100.OVR	1.0KY	10.0KY	100.0KY	1.0MY	
SE 79	4.027+001	4.027+001	4.027+001	4.027+001	4.027+001	4.026+001	4.026+001	4.023+001	3.984+001	3.619+001	1.385+001	9.353+006
KR 85	9.062+003	7.965+003	6.560+003	.000	.000	.000	.000	.000	.000	.000	.000	.000
SR 90	7.064+004	6.736+004	6.272+004	6.272+004	5.568+004	4.389+004	2.149+004	6.537+003	3.251+006	.000	.000	.000
Y 90	7.465+004	6.738+004	6.273+004	6.273+004	5.569+004	4.390+004	2.149+004	6.538+003	3.252+006	.000	.000	.000
ZR 93	1.767+000	1.768+000	1.768+000	1.768+000	1.768+000	1.768+000	1.768+000	1.768+000	1.768+000	1.768+000	1.690+000	1.124+000
NB 93M	1.290+001	2.793+001	4.779+001	4.779+001	7.483+001	1.120+000	1.559+000	1.670+000	1.679+000	1.672+000	1.606+000	1.069+000
NB 95	1.568+006	1.303+003	9.116+003	9.116+003	2.330+011	.000	.000	.000	.000	.000	.000	.000
TC 99	1.284+001	1.291+001	1.291+001	1.291+001	1.291+001	1.291+001	1.291+001	1.290+001	1.287+001	1.249+001	9.322+000	4.984+001
RU106	5.567+005	1.407+005	1.788+004	1.788+004	5.744+002	5.923+001	6.506+010	7.608+025	.000	.000	.000	.000
RH106	6.377+005	1.407+005	1.788+004	1.788+004	5.744+002	5.926+001	6.506+010	7.608+025	.000	.000	.000	.000
PD107	1.160+001	1.160+001	1.160+001	1.160+001	1.160+001	1.160+001	1.160+001	1.160+001	1.160+001	1.157+001	1.148+001	1.043+001
SB125	1.430+004	8.759+003	4.135+003	4.135+003	1.163+003	9.688+001	5.310+002	1.958+007	.000	.000	.000	.000
TE125M	2.971+003	2.138+003	1.009+003	1.009+003	2.887+002	2.364+001	1.294+002	4.777+008	.000	.000	.000	.000
SA126	7.815+001	7.815+001	7.815+001	7.815+001	7.815+001	7.814+001	7.812+001	7.810+001	7.761+001	7.292+001	3.908+001	7.635+004
SB126	1.266+003	1.094+001	1.094+001	1.094+001	1.094+001	1.094+001	1.094+001	1.093+001	1.087+001	1.021+001	5.471+002	1.070+004
SB126M	5.590+002	7.815+001	7.815+001	7.815+001	7.815+001	7.814+001	7.812+001	7.810+001	7.761+001	7.292+001	3.908+001	7.639+004
CS134	1.516+005	7.742+004	2.824+004	2.824+004	5.759+003	1.824+002	7.607+003	3.815+010	.000	.000	.000	.000
CS135	3.298+001	3.306+001	3.306+001	3.306+001	3.306+001	3.306+001	3.306+001	3.306+001	3.305+001	3.296+001	3.208+001	2.446+001
CS137	1.026+005	9.795+004	9.139+004	9.139+004	8.142+004	6.467+004	3.231+004	1.018+004	9.472+006	.000	.000	.000
BA137M	9.729+004	9.266+004	8.646+004	8.646+004	7.707+004	6.113+004	3.057+004	9.627+003	8.961+006	.000	.000	.000
CE144	1.100+006	1.853+005	1.281+004	1.281+004	1.491+002	2.020+002	5.020+014	.000	.000	.000	.000	.000
PR144	1.112+006	1.853+005	1.281+004	1.281+004	1.491+002	2.020+002	5.020+014	.000	.000	.000	.000	.000
PR144M	1.322+004	2.223+003	1.537+002	1.537+002	1.780+000	2.424+004	6.036+016	.000	.000	.000	.000	.000
PM147	1.230+005	7.711+004	3.490+004	3.490+004	9.314+003	6.633+002	2.795+001	4.386+007	.000	.000	.000	.000
SM151	3.489+002	3.512+002	3.432+002	3.432+002	3.307+002	3.057+002	2.427+002	1.651+002	1.612+001	.000	.000	.000
EU154	1.065+004	9.064+003	7.117+003	7.117+003	4.756+003	2.124+003	1.897+002	3.365+000	.000	.000	.000	.000
EU155	6.578+003	4.974+003	3.270+003	3.270+003	1.626+003	4.019+002	6.066+000	5.597+003	.000	.000	.000	.000
SUMTOT	5.653+006	1.169+006	4.504+005	4.439+005	2.940+005	2.174+005	1.063+005	3.307+004	1.898+001	1.830+001	1.403+001	3.041+000
TOTAL	1.760+008	1.171+006	4.509+005	4.439+005	2.941+005	2.174+005	1.063+005	3.307+004	1.898+001	1.830+001	1.403+001	3.041+000

A.12

TABLE A.7. Decay Heat of Fission Products

OUTPUT UNIT = %

WESTINGHOUSE 1184 MW(E) PWR, 3.1 PER CENT ENRICH., 32,700 MW/D/MIU
 POWER= 3.84000+001PM, BURNUP= 3.26955+004MWD, FLUX= 3.41+014N/CM**2-SEC

SUMMARY TABLE: THERMAL POWER, WATTS
 1 METRIC TON OF U AT 3.1 PER CENT ENRICHMENT

DISCHARGE	2.0YR	5.0YR	SV(REPRO)	10.0YR	20.0YR	50.0YR	100.0YR	1.0KY	10.0KY	100.0KY	1.0MY	
SE 79	1.003-004	1.003-004	1.003-004	1.003-004	1.002-004	1.002-004	1.002-004	1.002-004	9.919-005	9.011-005	3.449-005	2.322-009
KR 85	1.357+001	1.193+001	9.827+000	.000	.000	.000	.000	.000	.000	.000	.000	.000
SR 90	8.199+001	7.818+001	7.279+001	7.279+001	6.462+001	5.394+001	2.494+001	7.587+000	3.773-000	.000	.000	.000
Y 90	4.138+002	3.734+002	3.477+002	3.477+002	3.087+002	2.433+002	1.191+002	3.624+001	1.802-000	.000	.000	.000
ZR 93	2.053-004	2.054-004	2.054-004	2.054-004	2.054-004	2.054-004	2.054-004	2.054-004	2.054-004	2.045-004	1.963-004	1.306-004
NB 93M	2.286+005	4.949+005	8.468+005	8.468+005	1.326+004	1.985+004	2.761+004	2.963+004	2.975+004	2.963+004	2.845+004	1.892+004
NR 95	7.519+003	6.250+000	4.373+005	4.373+005	1.118+013	5.415+013	.000	.000	.000	.000	.000	.000
TC 95	6.438+003	6.473+003	6.473+003	6.473+003	6.473+003	6.472+003	6.472+003	6.471+003	6.457+003	6.266+003	4.675+003	2.499+004
RUI06	3.310+001	8.366+000	1.063+000	1.063+000	3.415+002	3.522+005	3.868+014	4.523+029	.000	.000	.000	.000
RM106	6.117+003	1.350+003	1.715+002	1.715+002	5.509+000	5.684+003	6.240+012	7.297+027	.000	.000	.000	.000
PO107	6.877+006	6.877+006	6.877+006	6.877+006	6.877+006	6.877+006	6.877+006	6.877+006	6.876+006	6.870+006	6.804+006	6.181+006
AG110M	7.434+001	9.799+000	4.690+001	4.690+001	2.959+003	1.178+007	7.427+021	.000	.000	.000	.000	.000
SB125	4.472+001	2.738+001	1.293+001	1.293+001	3.690+000	3.029+001	1.663+004	6.120+010	.000	.000	.000	.000
SN126	9.747+004	9.747+004	9.746+004	9.746+004	9.746+004	9.745+004	9.743+004	9.740+004	9.689+004	9.094+004	4.874+004	9.520+007
SB126	2.340+001	2.022+003	2.021+003	2.021+003	2.021+003	2.021+003	2.021+003	2.020+003	2.008+003	1.886+003	1.011+003	1.976+006
SB126M	7.118+000	9.951+003	9.950+003	9.950+003	9.950+003	9.949+003	9.947+003	9.944+003	9.887+003	9.284+003	4.976+003	9.727+006
CS134	1.543+003	7.880+002	2.874+002	2.874+002	5.353+001	1.856+000	7.747+005	3.983+012	.000	.000	.000	.000
CS135	1.101+004	1.103+004	1.103+004	1.103+004	1.103+004	1.103+004	1.103+004	1.103+004	1.103+004	1.100+004	1.071+004	8.162+005
CS137	1.135+002	1.083+002	1.011+002	1.011+002	9.006+001	7.148+001	3.574+001	1.126+001	1.048+000	.000	.000	.000
BA137M	3.820+002	3.638+002	3.395+002	3.395+002	3.024+002	2.400+002	1.200+002	3.760+001	3.514+000	.000	.000	.000
CE144	7.297+002	1.229+002	8.494+000	8.494+000	9.889+002	1.340+005	3.334+017	1.525+036	.000	.000	.000	.000
FR144	8.174+003	1.362+003	9.413+001	9.413+001	1.096+000	1.485+004	3.696+016	.000	.000	.000	.000	.000
PM147	4.413+001	2.766+001	1.252+001	1.252+001	3.341+000	2.379+001	8.591+005	1.573+010	.000	.000	.000	.000
EU154	9.525+001	8.107+001	6.366+001	6.366+001	4.755+001	1.900+001	1.693+000	3.010+002	.000	.000	.000	.000
EU155	4.784+000	3.618+000	2.379+000	2.379+000	1.183+000	2.923+001	4.417+003	4.071+006	.000	.000	.000	.000
SUMTOT	2.541+004	4.727+003	1.525+003	1.516+003	8.768+002	6.275+002	3.015+002	9.293+001	2.003+002	1.905+002	1.178+002	6.702+004
TOTAL	2.094+006	4.729+003	1.527+003	1.517+003	8.772+002	6.276+002	3.016+002	9.295+001	2.007+002	1.905+002	1.178+002	6.704+004

A.13

DISTRIBUTION

No. of
Copies

No. of
Copies

OFFSITE

A. A. Churm
DOE Chicago Patent Group
9800 South Cass Avenue
Argonne, IL 60439

2 R. Y. Lowrey
DOE Albuquerque Operations
Office
P.O. Box 5400
Albuquerque, NM 87185

A. L. Taboas
DOE Albuquerque Operations
Office
P.O. Box 5400
Albuquerque, NM 87185

S. A. Mann
DOE Chicago Operations and
Region Office
Argonne, IL 60439

J. O. Neff
Department of Energy
Columbus Program Office
505 King Avenue
Columbus, OH 43201

W. E. Mott
DOE Division of Environmental
Control Technology
Washington, DC 20545

J. P. Hamric
DOE Idaho Operations Office
550 2nd St.
Idaho Falls, ID 83401

J. W. Peel
DOE Idaho Operations Office
550 2nd St.
Idaho Falls, ID 83401

J. B. Whitsett
DOE Idaho Operations Office
550 2nd St.
Idaho Falls, ID 83401

C. R. Cooley
DOE Nuclear Waste Management
Programs
NE-331, GTN
Washington, DC 20545

G. H. Daly
DOE Nuclear Waste Management
Programs
NE-322, GTN
Washington, DC 20545

J. E. Dieckhoner
DOE Nuclear Waste Management
Programs
NE-321, GTN
Washington, DC 20545

C. H. George
DOE Nuclear Waste Management
Programs
NE-330, GTN
Washington, DC 20545

C. A. Heath
DOE Nuclear Waste Management
Programs
NE-330, GTN
Washington, DC 20545

No. of
Copies

M. L. Lawrence
DOE Nuclear Waste Management
Programs
NE-340, GTN
Washington, DC 20545

D. J. McGoff
DOE Nuclear Waste Management
Programs
NE-320, GTN
Washington, DC 20545

S. Meyers/R. Romatowski
DOE Nuclear Waste Management
Programs
NE-30, GTN
Washington, DC 20545

G. Oertel
DOE Nuclear Waste Management
Programs
NE-320, GTN
Washington, DC 20545

A. F. Perge
DOE Nuclear Waste Management
Programs
NE-30, GTN
Washington, DC 20545

R. W. Ramsey, Jr.
DOE Nuclear Waste Management
Programs
NE-301, GTN
Washington, DC 20545

R. Romatowski
DOE Nuclear Waste Management
Programs
NE-30, GTN
Washington, DC 20545

V. Trice
DOE Nuclear Waste Management
Program
NE-30, GTN
Washington, DC 20545

No. of
Copies

D. L. Vieth
DOE Nuclear Waste Management
Programs
NE-332, GTN
Washington, DC 20545

2 S. W. Ahrends
DOE Oak Ridge Operations Office
P.O. Box E
Oak Ridge, TN 37830

D. E. Large
DOE Oak Ridge Operations Office
P.O. Box E
Oak Ridge, TN 37830

S. G. Harbinson
DOE San Francisco Operations
Office
1333 Broadway
Oakland, CA 94612

W. B. Wilson
DOE Savannah River Operations
Office
P.O. Box A
Aiken, SC 29801

R. P. Whitfield
DOE Savannah River Operations
Office
P.O. Box A
Aiken, SC 29801

J. B. Martin
Division of Waste Management
Nuclear Regulatory Commission
Washington, DC 20555

D. B. Rohrer
Division of Waste Management
Nuclear Regulatory Commission
Washington, DC 20555

No. of
Copies

No. of
Copies

R. D. Smith
Division of Waste Management
Nuclear Regulatory Commission
Washington, DC 20555

R. E. Cunningham
Office of Nuclear Safety
Materials and Safeguards
Nuclear Regulatory Commission
Room 562, 7915 Eastern Avenue
Silver Springs, MD 20910

27 DOE Technical Information Center

J. A. Buckham
Allied-General Nuclear Services
P.O. Box 847
Barnwell, SC 29812

A. Williams
Allied-General Nuclear Services
P.O. Box 847
Barnwell, SC 29812

J. H. Kittel
Argonne National Laboratory
Office of Waste Management
Programs
9700 South Cass Avenue
Argonne, IL 60439

M. J. Steindler/L. E. Trevorrow
Argonne National Laboratory
9700 South Cass Avenue
Argonne, IL 60439

W. Carbiener
Battelle Memorial Institute
Office of Nuclear Waste
Isolation
505 King Avenue
Columbus, OH 43201

Beverly Rawles
Battelle Memorial Institute
Office of Nuclear Waste
Isolation
505 King Avenue
Columbus, OH 43201

Research Library
Battelle Memorial Institute
505 King Avenue
Columbus, OH 43201

R. Maher, Program Manager
Waste Management Programs
Savannah River Plant
E. I. Du Pont de Nemours & Co.
Aiken, SC 29801

M. D. Boersma
E. I. Du Pont de Nemours & Co.
Savannah River Laboratory
Aiken, SC 29801

R. G. Garvin
E. I. Du Pont de Nemours & Co.
Savannah River Laboratory
Aiken, SC 29801

D. L. McIntosh
E. I. Du Pont de Nemours & Co.
Savannah River Laboratory
Aiken, SC 29801

A. L. Ayers
EG & G Idaho
P.O. Box 1625
Idaho Falls, ID 83415

R. Williams
Electric Power Research
Institute
3412 Hillview Avenue
Palo Alto, CA 94304

No. of
Copies

J. L. Larocca, Chairman
Engineering Research and
Development Authority
Empire State Plaza
Albany, NY 12223

2 Environmental Protection Agency
Technological Assessment
Division (AW-559)
Office of Radiation Programs
U.S. Environmental Protection
Agency
Washington, DC 20460

J. R. Berreth
Exxon Nuclear Idaho
P.O. Box 2800
Idaho Falls, ID 83401

G. L. Ritter
Exxon Nuclear Idaho
P.O. Box 2800
Idaho Falls, ID 83401

File Copy
Exxon Nuclear Idaho
P.O. Box 2800
Idaho Falls, ID 83401

3 J. Campbell
Lawrence Livermore Laboratory
P.O. Box 808
Livermore, CA 94550

R. Roy
202 Materials Research
Laboratory
Pennsylvania State University
University Park, PA 16802

J. P. Duckworth
Plant Manager
Nuclear Fuels Services, Inc.
P.O. Box 124
West Valley, NY 14171

No. of
Copies

R. E. Blanco
Oak Ridge National Laboratory
P.O. Box Y
Oak Ridge, TN 37830

J. O. Blomeke
Oak Ridge National Laboratory
P.O. Box Y
Oak Ridge, TN 37830

3 A. L. Lotts
Oak Ridge National Laboratory
P.O. Box X
Oak Ridge, TN 37830

2 A. B. Martin
Rockwell International
Energy Systems Group
8900 DeSoto Avenue
Canoga Park, CA 91304

Paul Hagen
Chemical Operations
Rockwell International
Rocky Flats Plant
P.O. Box 464
Golden, CO 80401

E. Vejvoda, Director
Chemical Operations
Rockwell International
Rocky Flats Plant
P.O. Box 464
Golden, CO 80401

R. G. Kepler
Organic and Electronic
Dept. 5810
Sandia Laboratories
Albuquerque, NM 87185

W. Weart
Sandia Laboratories
Albuquerque, NM 87185

No. of
Copies

No. of
Copies

P. B. Macedo
Keane Hall
Vitreous State Laboratory
The Catholic University of
America
Washington, DC 20017

R. G. Post
College of Engineering
University of Arizona
Tucson, AZ 85721

L. L. Hench
Dept. of Materials Science
and Engineering
University of Florida
Gainesville, FL 32611

Dr. Hayne Palmour III
2140 Burlington Engineering
Laboratories
North Carolina State University
Raleigh, NC 27607

ONSITE

4 DOE Richland Operations Office

P. A. Craig (2)
R. E. Gerton
H. E. Ransom

4 Rockwell Hanford Operations

I. E. Reep
D. D. Wodrich (3)

68 Pacific Northwest Laboratory

S. M. Barnes
W. J. Bjorklund

H. T. Blair
W. F. Bonner
D. W. Brite
R. A. Brouns
J. L. Buelte
R. L. Bunnell
J. R. Carrell
J. G. Carter
L. A. Chick
T. D. Chikalla
R. D. Dierks
G. J. Exarhos
M. S. Hanson
L. K. Holton
J. H. Jarrett
D. E. Knowlton
C. A. Knox
W. L. Kuhn
L. T. Lakey
D. E. Larson
R. O. Lokken
G. B. Long (3)
J. L. McElroy
G. B. Mellinger
J. E. Mendel
R. D. Nelson
J. F. Nesbitt
R. E. Nightingale
R. D. Peters
A. M. Platt
W. A. Ross (5)
J. M. Rusin
D. H. Siemens
S. C. Slate (15)
C. L. Timmerman
R. L. Treat
R. P. Turcotte
H. H. Van Tuyl
J. W. Wald
Technical Information (5)
Publishing Coordination (2)(KC)